Circadian Integration of Hepatic De Novo Lipogenesis and Peripheral Energy Substrates Utilization

Professor Chih-Hao Lee Sihao Liu

Circadian Integration of Hepatic *de novo* Lipogenesis and Peripheral Energy Substrates Utilization

ABSTRACT

The liver maintains energy substrate homeostasis by synchronizing circadian or diurnal expression of metabolic genes with the feeding/fasting state. The activities of hepatic *de novo* lipogenic gene products peak during feeding, converting carbohydrates into fats that provide vital energy sources for peripheral tissues. Conversely, deregulated hepatic lipid synthesis leads to systemic metabolic dysfunction, establishing the importance of temporal regulation of fat synthesis/usage in metabolic homeostasis. Pharmacological activation of peroxisome proliferator-activated receptor δ/β (PPARδ/β) improves glucose handling and systemic insulin sensitivity. However, the mechanisms of hepatic PPARδ actions and the molecular pathways through which it is able to modulate global metabolic homeostasis remain unclear. Here we show that hepatic PPARδ controls the diurnal expression of lipogenic genes in the dark/feeding cycle. Adenovirus mediated liver restricted activation of PPARδ promotes glucose utilization in the liver and fat utilization in the muscle. Liver specific deletion of either PPARδ or the PPARδ-regulated lipogenic gene acetyl-CoA carboxylase 1 (ACC1) reduces muscle fatty acid uptake. Unbiased metabolite profiling identifies 1-stearoyl-2-oleoyl-sn-glycero-

3-phosphocholine (SOPC) as a serum lipid derived from the hepatic PPARδ-ACC1 activity that reduces postprandial lipid levels and increases muscle fatty acid uptake. These findings reveal a regulatory mechanism that coordinates lipid synthesis and utilization in the liver-muscle axis, providing mechanistic insights into the hepatic regulation of systemic energy substrates homeostasis.

Table of Contents

Acknowledgements

I would like to thank all people involved in this thesis work for the help I had along the way.

In particular, Dr. Ben Hatano initiated the hepatic PPARδ overexpression project and generated the PPARδ adenovirus. Dr. Jonathan D. Brown, Dr. Edwin Homan, Mathias Leidl, Dr. Alan Saghatelian and Dr. Jorge Plutzky are instrumental in performing metabolomics profiling experiments. Dr. Karen Inouye, Ariel White, and Dr. Gökhan S. Hotamisligil provided critical assistance in metabolic cages and lipid infusion experiments. Dr. Owen McGuiness carried out the euglycemic-hyperinsulinemic clamp and stable isotope tracer studies. Dr. Christopher Newgard provided ACC1 shRNA adenovirus.

I would also like to thank my advisor Dr. Chih-Hao Lee for his teaching and mentoring, and the current and past members of Lee laboratory: Dr. Kristopher J. Stanya, Dr. Shannon M. Reilly, Dr. Prerna Bhargava, Lingling Dai, Dr. David Jacobi, Dr. Uğur Ünlütürk, Dr. Kyu Yeon Hur, Matthew R. Gangl for their daily support of this thesis work.

Finally, I would like to thank my preliminary qualifying examination committee and dissertation advisory committee members: Dr. Jorge Plutzky, Dr. David E. Cohen, Dr. James R. Mitchell, Dr. Marianne Wessling-Resnick, and Dr. Brendan D. Manning for their advices and for setting a high standard to Ph.D candidates like me.

My professional achievements would not be possible without the support of my family members. I am extremely fortunate to be born in a family that maintains unwavering trust in me. They always believed what I chose to do was in the best interest of myself. When I had difficult times, my parents always encouraged me to face the challenge and never back down from it. At the same time, they provided moral and financial support that is pivotal to my achievements. Yet every time I spoke to them, they always attributed to my success to my own efforts. At this moment, when I am about to hold this doctorial degree, I believe that they are the unsung heroes behind my achievements and I sincerely thank them for years' support and sacrifice.

I am also extremely lucky to have found my life's companion early in the college and have her support throughout my pursuit of this degree. My fiancée, Yang always understands the challenge and commitment required to be a Ph.D. student. Therefore, she quietly handled the challenges in her own life and always left a comforting feeling to me. I am thankful for her belief in me, and all the things she did in the past a few years.

Chapter 1:

INTRODUCTION

Metabolic Flexibility and Metabolic Syndrome

Metabolic flexibility describes the capacity of human body to switch between carbohydrates and lipids as the predominant source of energy substrates [1]. Following a meal, the rapid rise in blood glucose is detected by β-cells in the pancreas, which then release insulin to promote glucose oxidation in the skeletal muscle and reduce glucose production in the liver. At the same time, insulin suppresses free fatty acid release from the adipose tissue, making glucose the predominant source of energy substrates during feeding. As the action of insulin continues, additional glucose can also be converted to glycogen in the liver and skeletal muscle for storage. However, due to the limited capacity of glycogen storage, glucose eventually is synthesized into more energy dense fatty acids by the liver. These newly synthesized fatty acids, together with the dietary lipids are converted into triglycerides and exported in the form of very low density lipoproteins (VLDL). VLDL derived fatty acids are taken up by the skeletal muscle as the energy source or by the adipose tissue for storage in the post-absorptive phase (Figure 1.1). Conversely, at the fasted state fatty acids are released from the adipose tissue for energy production. In the meantime, partly promoted by the release of glucagon from the pancreas, the liver converts stored glycogen, glycerol from lipolysis and amino acids into glucose to maintain normal blood glucose level (Figure 1.2).

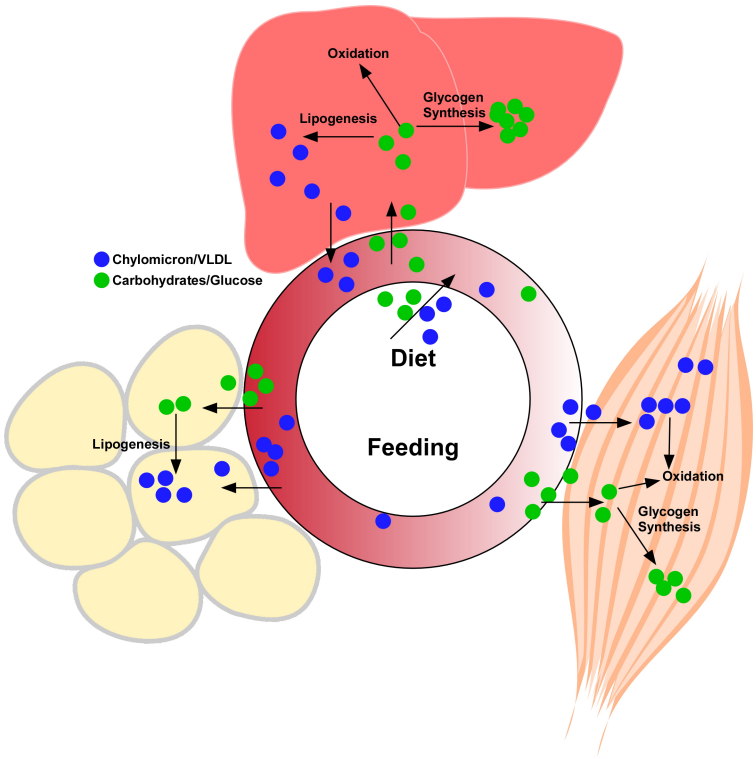

Figure 1.1. Energy substrates utilization under the feeding condition. The dietary source of lipids and carbohydrates enter into the circulation following a meal. Liver, muscle and adipose tissue coordinately utilize these energy substrates mainly under the control of insulin.

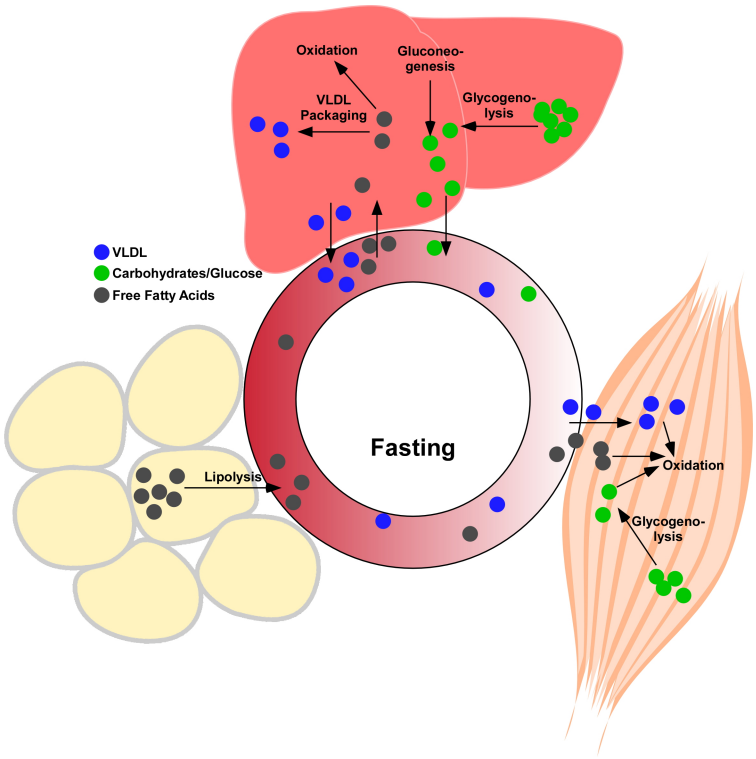

Figure 1.2. Energy substrates utilization under the fasting condition. At the fasting state, diminished blood glucose level reduces circulating insulin concentration. This leads to increased lipolysis in the adipose tissue and increased glycogen breakdown in the liver and muscle. Additional glucose is generated via gluconeogenesis in the liver to maintain blood glucose level. Liver and muscle rely on fatty acids released from the adipose tissue as the major substrate for energy production.

Metabolic syndrome is a collection of metabolic disorders that increase the risk of developing type II diabetes, cardiovascular diseases and certain types of cancer [2]. At the core of metabolic syndrome is the disruption of insulin action, which leads to deregulated glucose metabolism in major insulin responsive tissues described above. Paradoxically, insulin continues to act on lipid synthesis pathways in the liver while failing to curtail the activity of gluconeogenic and lipolytic pathways in the liver and adipose tissue, respectively, exacerbating hyperglycemic and hyperlipidemic conditions. How insulin action is impeded under obese and diabetic conditions remain a major scientific challenge. Recent discoveries have linked insulin resistance with chronic low grade inflammation [3], endoplasmic reticulum (ER) stress [4], mitochondria dysfunction [5], and oxidative stress [6, 7], likely as a result of over-nutrition.

Much of the interest in studying metabolic flexibility stems from the observation that obese and/or diabetic human subjects fails to switch to glucose utilization and continue to oxidize lipids under a glucose tolerance test or euglycemic insulin clamp [8]. Thus the identification of pathways that control metabolic flexibility is key to combating the epidemic of metabolic syndrome.

Lipid Signaling and Metabolic Homeostasis

The seminal work by Randle et al. [9] demonstrated that perfusion of isolated rat muscle with free fatty acids was sufficient to suppress glucose uptake and impair insulin action in muscle cells, suggesting that fatty acids or their derivatives are able to directly influence cellular fuel preference. Later human studies with lipid infusion have confirmed the direct role of fatty acids in mediating insulin resistance [10, 11].

Western lifestyle imposes significant pressure on the metabolic system. Over-nutrition causes ectopic accumulation of lipids in metabolic tissues, and is associated with the development of insulin resistance [12]. This observation is supported by several genetic models in rodents. Overexpression of lipoprotein lipase in the skeletal muscle promotes lipid accumulation and muscle insulin resistance [13]. Similarly, adenoviral overexpression of CD36, a major fatty acid transporter protein in the liver, increases hepatic lipid content and is sufficient to cause hepatic insulin resistance [14]. Conversely, genetic ablation [15-18] or pharmacological inhibition [19] of factors involved in fatty acid transport protects mice from high fat diet (HFD) induced insulin resistance. However, fat deposition alone is not sufficient to explain the impaired insulin action in these tissues. Human can be obese but free from insulin resistance. Endurance training athletes have increased intramuscular lipids but are insulin sensitive [20, 21]. Genetic mouse models with enhanced hepatic lipogenesis [22] are protected from diet induced insulin resistance at least in the short term. Nevertheless, these observations suggest that lipid metabolism is closely involved in the development of

insulin resistance and the resulting loss of metabolic flexibility.

From early examples of luekotrienes and prostaglandins, to the recent identification of bioactive fatty acids [23] and phosphocholines (PCs) [24-26], lipids are well-known signal transducers involved in immune regulation [27, 28], oncogenesis [29], and neurological processes [30]. When fatty acids are taken up by cells, long chain acyl-CoA synthetases (ACSLs) immediately attach a CoA moiety to fatty acids [31]. Fatty acyl-CoAs serve as the substrate for the synthesis of diacylglycerol (DAG) and ceramide, or are used for oxidation in the form of fatty acyl-carnitines. It is thought that when lipid load exceeds the metabolic capacity of the body, these lipid metabolites accumulate and exert inhibitory effects on insulin actions (Figure 1.3).

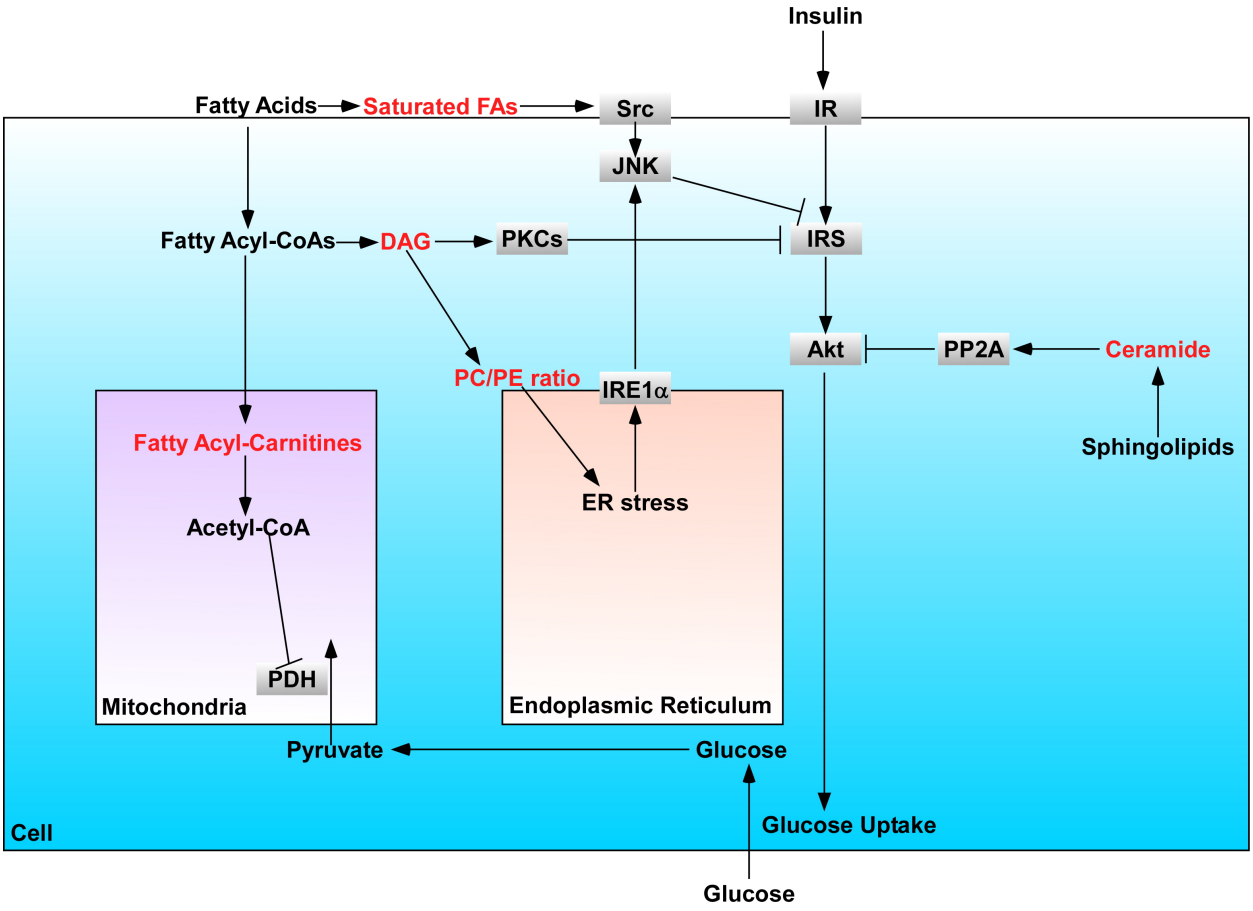

Figure 1.3. Overview of the lipid signaling pathways that interact with the insulin signaling pathway. Key signaling molecules are highlighted in red.

DAG

DAG is an intermediate metabolite that can be synthesized *de novo* from fatty acids. It can also be generated from the hydrolysis of triglycerides and phospholipids by adipocyte-triglyceride lipase (ATGL) and phospholipases, respectively [32]. It has long been known to serve as a secondary messenger for the activation of protein kinase C (PKC) [33]. A particular group of PKCs, known as novel PKCs requires only DAG for its activation [34]. PKC activation highly correlates with insulin resistance in obese animal models and is implicated in suppressing insulin action via serine phosphorylation of insulin receptor substrate 1 (IRS1) in both muscle and liver [35]. While this molecular mechanism has been demonstrated in cell culture models, genetic models of novel PKC knockouts give complex phenotypes. For example, PKCθ knockout mice are protected from lipid infusion induced muscle insulin resistance [36], but fail to prevent long term HFD induced muscle insulin resistance [37]. Additional isoforms of novel PKCs are also implicated in promoting metabolic dysfunction under diet induced obesity. However, improvements in PKCδ and ε knockout mice are confounded by diminished lipid accumulation in the liver [38] or enhanced insulin secretion from the pancreas [39]. Collectively, although DAG level is tightly associated with the insulin resistant state, whether PKC is the obligatory downstream factor in mediating insulin desensitizing effects of DAG is not clear.

Ceramide

Ceramide is a membrane lipid derived from sphingolipid metabolism [40]. It activates protein phosphatase 2A (PP2A) and subsequently inactivates Akt to attenuate insulin signaling [41]. In obesity, ceramide concentrations are increased in muscle and liver [42]. Blockade of ceramide synthesis by a inhibitor of serine palmitoyl transferases 1 leads to improved muscle insulin sensitivity in rats infused with saturated fatty acids or in Zucker rats, a genetic obese model [42].

Fatty acyl-Carnitines

Fatty acids oxidation is initiated by fatty acyl-CoAs import into mitochondria via carnitine palmitoyltransferases [43]. This step converts fatty acyl-CoAs into fatty acyl-carnitines. Muscle and serum levels of medium and long chain fatty acyl-carnitines are indicators of mitochondria fuel selection under normal physiological conditions [43]. High levels of fatty acyl-carnitines in the fasting state correspond to high fatty acid oxidation rate. Obese animals have higher fatty acyl-carnitine levels at the fed state, suggesting the lack of metabolic switch to glucose oxidation. It also raises the possibility that fatty acyl-carnitines antagonize glucose utilization. Although the detailed mechanism is still missing, excessive accumulation of fatty acyl-carnitines in the muscle impairs glucose oxidation by preventing pyruvate channeling into mitochondria. On the contrary, limiting fatty acid entry into mitochondria by deleting malonyl-CoA decarboxylase restores

glucose oxidation in obese animals [44].

Membrane Properties

The concept of lipotoxicity is largely viewed as the consequence of precise signaling mechanisms initiated by specific metabolites [45]. What should not be overlooked, though, is the impact of lipid loading on very fundamental cellular characteristics, such as membrane fluidity and integrity. Saturated fatty acids such as palmitate promote insulin resistance in the muscle through c-jun N-terminal kinase (JNK) followed by serine phosphorylation of IRS1, whereas monounsaturated fatty acids are devoid of such effects [46]. Plasma membrane is partitioned into lipid rafts, within which reside signaling proteins. Lipid rafts are poor in detergent solubility due to high concentrations of saturated fatty acids, sphingolipids and cholesterol. Incubation of cells with saturated fatty acids promotes the aggregation and activation of Src family kinase in the lipid rafts, and the induction of JNK phosphorylation [47].

Lipidomics profiling of ER membrane comparing lean and obese mice revealed significantly increased phosphocholine (PC) to phosphoethanolamine (PE) ratio. Maintaining the normal ratio between PC and PE is essential for the integrity of ER membrane. In obese conditions, the high PC to PE ratio creates a leaky membrane that results in disrupted calcium homeostasis and ER stress, each of which are known to impair insulin signaling. Reverting the PC to PE ratio via ablation of phosphatidylethanolamine N-methyltransferase (PEMT), a key enzyme in converting PE

to PC, restores insulin sensitivity in these mice [48].

Regulation of Lipid Synthesis

The regulation of lipid synthesis is part of the program to maintain metabolic flexibility. The rate of lipid synthesis from carbohydrates (*de novo* lipogenesis) is critically controlled at several steps by acetyl-CoA carboxylase 1 (ACC1), fatty acid synthase (FAS) and stearyl-CoA desaturase 1 (SCD1). Together, these enzymes sequentially utilize the acetyl-CoA derived from the glycolytic pathway to synthesize saturated or monounsaturated fatty acids [49]. These newly synthesized fatty acids are added to the glycerol backbone to form triglycerides (TG), phospholipids and other intermediate metabolites. The availability of energy substrates during fasting and feeding is a major driving force to regulate lipid synthesis. Circadian clock also modulates this process as an additional mechanism to couple lipid synthesis with the fasting and feeding cycle.

In mammalian cells, the ATP/AMP and NAD+/NADH ratios are major forms of energy indicators. Fluctuations of these small molecules are detected by a number of highly conserved energy sensors, which in turn dictate a plethora of signaling and transcriptional events necessary to maintain the balance between energy supply and demand. The AMP-activated protein kinase (AMPK) and NAD+ dependent deacetylase Sirtuins [50], such as SIRT1, have emerged as key energy sensors that elicit adaptive responses to energy deficit in metabolic tissues under conditions such as caloric

restriction (CR), fasting and exercise. Conceivably, these energy-sensing mechanisms are actively modulating lipogenesis. A low ATP/AMP ratio triggers the activation of AMPK. A number of cellular targets have been identified that mediate the immediate effects of AMPK activation. In liver, both acetyl-CoA carboxylase 1 and 2 (ACC1 and ACC2), are targets of AMPK [51]. Phosphorylation of ACC1/2 inactivates their enzymatic activity shifting hepatic metabolism from biosynthetic pathways to fatty acid oxidation. AMPK also regulates the mammalian target of rapamycin complex 1 (mTORC1) via direct phosphorylation at the regulatory subunit Raptor or at the upstream regulatory protein tuberous sclerosis complex protein 2 [52, 53]. In either case, AMPK activation turns off the mTORC1 signaling pathway that is involved in protein and lipid synthesis. In adipocytes, AMPK phosphorylates hormone sensitive lipase (HSL) [54] and adipose triglyceride lipase (ATGL) [55] for the liberation of free fatty acids as energy substrates. In adipose tissue, glucose is the source for fatty acid synthesis and glycerol-3-phosphate, the building block for triglyceride synthesis. In contrast to skeletal muscle, where AMPK promotes glucose uptake, some reports suggest that AMPK activation in the adipocytes inhibits glucose uptake [56], consistent with its role in preventing energy consuming biosynthesis.

The aforementioned nutrient sensing pathways converge at the transcriptional level to regulate lipogenic genes. In liver and adipocytes, several transcription factors have been identified as key regulators of *de novo* lipogenesis that are intimately linked to hormonal signals, energy sensors, and nutrient flux (Figure 1.4).

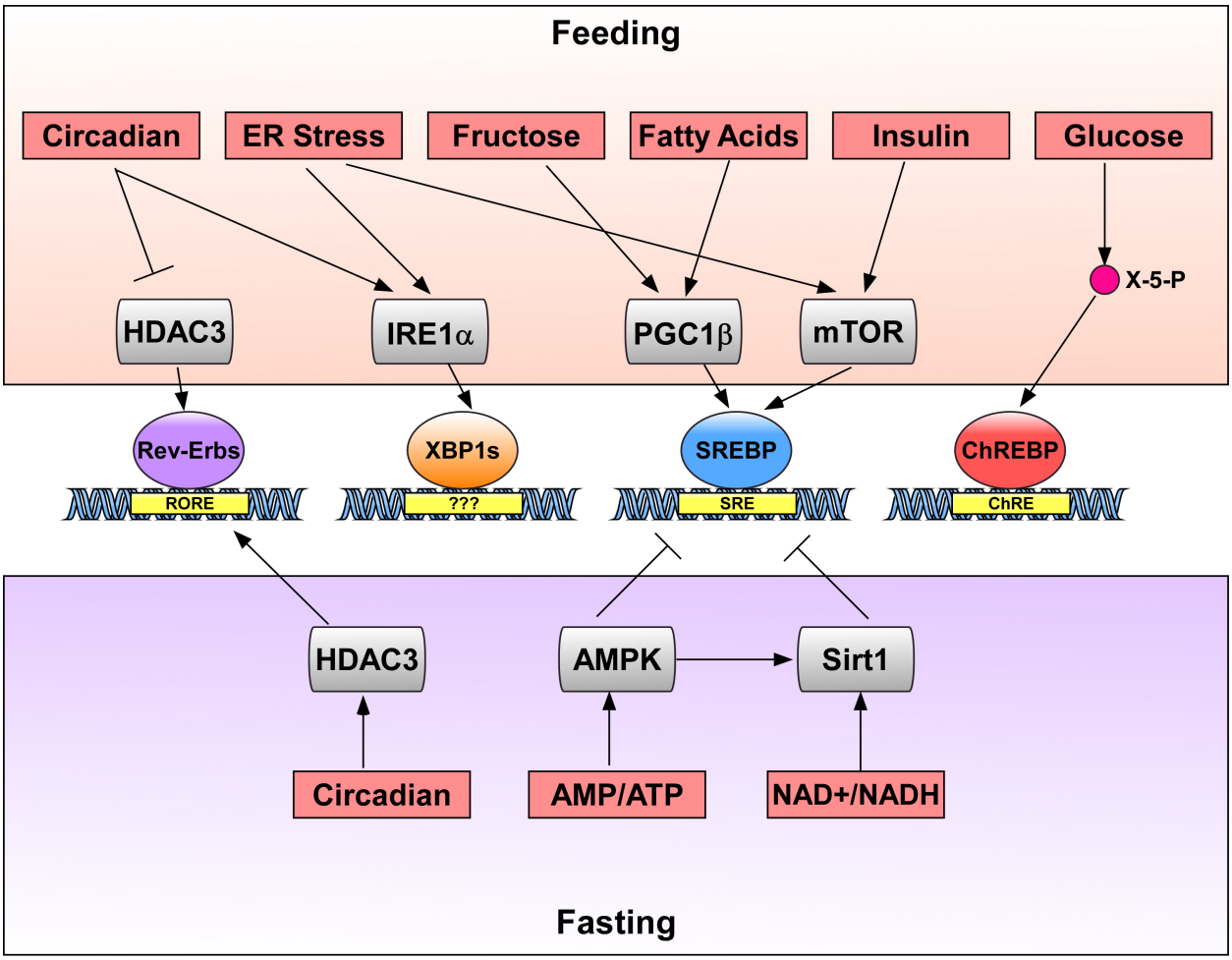

Figure 1.4. Overview of the regulation of lipid synthesis. During feeding or fasting, changes in nutrient flux, hormonal signals, physiological stress and intracellular small molecules are sensed by several signaling pathways that converge at key transcription factors to control lipid synthesis. Each of these transcription factors detects a subset of physiological signals to coordinately modulate the activity of lipogenic pathway.

SREBP

The sterol regulatory element binding protein 1c (SREBP1c) is recognized as the master regulator of *de novo* lipogenesis. It is capable of activating the entire repertoire of lipogenic gene expression in the liver [57]. SREBP1c is mainly thought to be responsible for the insulin induced lipogenic program in the liver, especially under the condition of diet induced or genetic models of obesity [58]. Insulin activates SREBP1c by enhancing its transcription or by promoting the processing of the inactive ER membrane bound form to the active nuclear form [59, 60]. However, the detailed mechanism through which insulin is able to activate SREBP1c is not clear. A plausible link is the mTOR complexes (mTORC1/2) [61]. Constitutive activation of mTOR signaling via genetic ablation of its upstream suppressor TSC1/2 complex induces SREBP1c processing and induces lipogenic gene expression [62]. SREBP1c integrates additional upstream signals to regulate *de novo* lipogenesis. The SREBP1 promoter contains a nuclear receptor LXR response element and the LXR ligand is able to induce SREBP1c expression [63]. It has recently been shown that the nuclear receptor co-activator PGC1β is able to form a complex with SREBP1c and mediate either saturated fat or fructose induced lipogenesis [64, 65]. Reduced cellular PC levels resulting from choline deficient diet also trigger the processing of SREBP1c and promote nuclear translocation of SREBP1c to activate genes involved in PC synthesis and one-carbon cycle metabolism [66]. On the other hand, fasting inhibits SREBP1c activity. This is in part due to the fall of circulating insulin concentration. In addition, the conserved nutrient

sensors Sirt1 and AMPK all have been shown to directly suppress SREBP1c activity by deacetylation [67] or phosphorylation [68], respectively. Consumption of a polyunsaturated fatty acid (PUFA) rich diet inhibits SREBP1c activity, potentially via inhibition of its processing [69]. PUFA are essential fatty acids and it is thought that the dampening of *de novo* lipogenesis by PUFA is necessary to ensure proper composition of membrane lipids that are rich in PUFA [70].

ChREBP

Feeding rodents with a high carbohydrate diet induces hepatic lipogenesis. The carbohydrate response element binding protein (ChREBP) was later shown to be responsible for this effect [71]. It has been shown that the ChREBP activity is regulated, in part, via nuclear translocation. Fasting induced PKA and AMPK activities are able to phosphorylate several serine/threonine sites located on the nuclear localization sequence, and hence retaining ChREBP in the cytosol during fasting [72, 73]. The mechanisms through which glucose is able to regulate ChREBP activity is still lacking. One potential mechanism is the pentose shunt intermediate metabolite xylulose-5-phosphate [72], which activates the protein phosphatase PP2A to remove the serine/threonine phosphorylation induced by PKA, permitting ChREBP translocation into the nucleus during high carbohydrate feeding in the liver. In addition, a second regulatory mechanism, unique to the adipose tissue, was recently uncovered: An N-terminal truncated isoform of ChREBP (ChREBPβ) is a much more potent activator of

lipogenic gene expression. ChREBPβ expression is regulated by the conventional isoform of ChREBP (ChREBPα), which is not subject to glucose regulation but is thought to directly sense glucose or glucose metabolites [74]. The rationale of this two-tiered regulation has not been demonstrated experimentally. Perhaps, it allows additional signals to prime the lipogenic response to glucose without directly activating it in the absence of glucose.

ER Stress and IRE1α-XBP1

The ER is a major site for protein folding and lipid synthesis. Because of its ability to control the synthesis of nutrients in response to external stimuli, ER is considered a nutrient sensing organelle. As mentioned above, the PC composition of the ER may be critical to activate SREBP1c, linking ER function to lipogenesis [66]. Upon feeding or chronic over-nutrition, the elevated biosynthetic requirements for the ER trigger ER stress, or the unfolded protein response (UPR). To date, the three branches of UPR pathways have all been implicated in the regulation of lipogenesis (Reviewed in [4]). In particular, the X-box binding protein 1 (XBP1), downstream of the ER stress sensor IRE1α, has been shown to transcriptionally activate genes involved in *de novo* lipogensis such as SCD1 and ACC2 [75]. Recently, IRE1α has been shown to degrade lipogenesis and sterol biosynthesis gene mRNA through regulated IRE1-dependent decay (RIDD), adding another layer of regulation [76].

Circadian Regulators

The adipose and hepatic lipogenesis programs exhibit a diurnal fluctuation corresponding to the feeding behavior in mice. Although the aforementioned mechanisms are capable of inducing lipogenic programs as an adaptive response, the coupling of cellular circadian clock machinery to lipogenesis may provide benefits to maximize cellular responses when substrates are made available. The nuclear receptor Rev-erb α and β are core components of mammalian circadian clock [77-79]. The expression of Rev-erbα/β maintains a 24-hour cycle and peaks during the day, corresponding to the fasting state in mice. Rev-erbα has also been shown as a heme sensor [80]. Upon heme or other endogenous ligands binding, a co-repressor complex consisting of nuclear receptor co-repressor 1 (NcoR) and histone deacetylase 3 (HDAC3) is recruited to turn off target gene expression. Genome-wide chromatin-immunoprecipitation-sequencing (ChIP-seq) of rev-erbα/β, as well as its co-repressors NcoR and HDAC3, revealed extensive co-occupancy around lipogenic genes, including the master regulator SREBP1c. They were functionally important to suppress the hepatic lipogenic program in the day.

Lipid products appear to play a role in the feedback regulation of *de novo* lipogenic pathway activities. For example, the lack of endogenous monounsaturated fatty acid (MUFA) synthesis via SCD1 deletion in the liver is able to prevent the transcriptional activation of the lipogenic program under high carbohydrate diet

conditions [81]. The alteration of the ER membrane composition [66] and/or the activation of ER stress [82] are likely mechanisms. However, it also raises the possibility that additional transcription factors exist to sense the MUFA level in the cell and regulate *de novo* lipogenesis.

Lipogenesis and Metabolic Diseases

The importance of *de novo* lipogenesis in maintaining normal cellular functions is highlighted by the fact that whole body knockout of ACC1 or FAS is incompatible with life [83, 84]. Although *de novo* lipogenesis is increasingly recognized to play an important role in many cell types, such as immune cells and cancer cells, the adipocytes and liver are the two predominant sites of *de novo* lipogenesis in the context of global metabolic regulation.

I. Lipid Synthesis in the Adipose Tissue

De novo lipogenesis in the adipocytes is relatively less studied. It is quantitively less important in *ad libitum* feeding conditions in mice, but is significantly increased during caloric restriction [85]. On the contrary, obese mice have reduced lipogenic gene expressions [23]. These observations suggest a potentially beneficial role of adipose *de novo* lipogenesis in metabolic homeostasis. This notion is supported by genetic models with increased adipose lipogenesis. For example, adipose tissue specific glucose

transporter Glut4 overexpression increases the entire *de novo* lipogenic program activity through the transcription factor ChREBP and improves systemic insulin sensitivity of mice with diet induced obesity [74]. Similarly, the fatty acid binding protein FABP4 (aP2) knockout mice have increased *de novo* lipogenic gene expressions in the adipose tissue and are protected from diet induced insulin resistance [17, 18, 23]. The reduced adipose inflammation and adipocytokine production, increased adipokine and lipokine secretion and decreased free fatty acid release are all proposed to explain the beneficial effects of an enhanced adipose lipogenesis program. However, several lines of evidence also present a contradicting view that lipogenesis in the adipose tissue is deleterious to global metabolic homeostasis. The adipose specific SREBP1c overexpression mice developes insulin resistance and lipodystrophy [86]. FAS knockout in the adipose tissue is beneficial by promoting a brown fat like phenotype [87]. Similarly, SCD1 adipose knockout is protective, in part, by reducing adipose inflammation [88]. These data reinforce the idea that intermediate metabolites generated through manipulating lipogenic pathways are likely the direct link between lipid metabolism and insulin resistance.

II. Lipid Synthesis in the Liver

In humans, stable isotope tracer studies have estimated the contribution of *de novo* lipogenesis to overall VLDL TG quantities amounts to approximately 5% at the fasting state and 18% at the postprandial state [89, 90], whereas in patients with fatty

liver diseases, *de novo* lipogenesis contributes to roughly 30% of overall VLDL TG quantities [91]. Thus hepatic *de novo* lipogenesis is an importance source contributing to dyslipidemia in patients with fatty liver diseases [92]. Indeed, suppression of hepatic *de novo* lipogenesis via genetic knockouts protects mice from a range of deleterious outcomes by diet induced or genetic obesity [93, 94]. As mentioned earlier, the accumulation of triglyceride *per se* is not sufficient to cause systemic insulin resistance, but rather the intermediate metabolites are likely detrimental. Indeed, a number of models with reduced hepatic lipogenesis show a concurrent reduction in hepatic DAG level [94, 95]. Paradoxically, short term adenoviral overexpression of key lipogenic genes such as ChREBP [96] or acute ablation of repressors of lipogenesis, such as HDAC3 [97], improves overall metabolic functions in obese animals. A likely explanation is the formation of small lipid droplets, drastically different from HFD induced large lipid droplets. These lipid droplets are sequestered from cytosolic kinases, despite containing increased DAG [97]. Alternatively, it was shown in drosophila S2 cells that small lipid droplets are more readily utilized for oxidation, thereby decreasing the likelihood of generating deleterious intermediate metabolites [98]. Of note, the intrinsic short duration of gain of function studies makes it difficult to evaluate the long-term outcome of a constitutively active lipogenic program. One study shows that liver specific DGAT2 transgenic mice do not develop insulin resistance despite severe hepatic steatosis under standard chow diet [22], while the other study using the same animals observes the existence of severe insulin resistance [99]. Recently, liver specific overexpression of SREBP1c has also been shown to induce insulin resistance [100]. Taken together, the

dissociation of hepatic steatosis from insulin resistance demonstrates the importance of lipid sequestration in preventing insulin resistance. These seemingly contradictory results strengthen the notion that intermediate signaling molecules from either lipid synthesis or breakdown are likely the direct link between lipid metabolism and tissue insulin resistance.

Regardless of the site, manipulation of the lipogenic program elicits a global change in metabolic homeostasis. As evidenced in the adipose tissue, the systemic effects are likely mediated through secreted factors. Notably, a product of lipogenesis, palmitoleate was identified as a lipokine, capable of improving muscle insulin sensitivity and suppressing hepatic lipogenesis [23]. Metabolomics profiling among adipose tissue, liver and serum has revealed a greater extent of similarities between liver and serum profiles than between adipose tissue and serum ones [101]. It was found that hepatic FAS is required to produce nuclear receptor PPARα ligands in the context of fat free diet [26]. Given the minimal contribution of *de novo* lipogenesis to overall energy substrates, this raises the question whether hepatic *de novo* lipogenesis regulates systemic metabolic homeostasis through lipid factors.

Circadian Regulation and Metabolic Flexibility

The 24 hour cycle of day and night as the earth evolving around its axis provides predictability to organisms living on it: the optimal time for photosynthesis and food availability. Although metabolic processes can be regulated solely based on adaptive

mechanisms, it would likely require all potential biochemical pathways to be primed for activation. Thus such scenario is energetically costly. This leads to the development of the circadian clock machinery that incorporates environmental cues, such as the light/dark and feeding/fasting cycle, to proactively regulate behavior and physiological functions [102, 103].

I. Molecular Architecture of the Circadian Clock

The hierarchical architecture of the circadian clock maintains a master regulator in the suprachiasmatic nucleus (SCN) located below the optical nerve in the hypothalamus [102]. It receives photonic signals from the retina and synchronizes daily activities and feeding behavior with the light and dark cycle. It also sets the molecular timing, or phase of the peripheral clock via neuronal or hormonal signals.

At the molecular level, the circadian clock machinery is comprised of several feedback loops (Figure 1.5). The core clock consists of a transcriptional activator complex formed by the transcription factor Bmal1 and Clock, and a repressor complex of Per and Cry genes. The activator complex binds to the E-box elements on Per and Cry gene promoters to mediate their transcription, whose protein products together with a number of chromatin modifying enzymes negatively regulate Bmal1 and Clock activities via direct protein-protein interactions. Upon exceeding a critical threshold, the repressor complex prevents further accumulation of Per and Cry proteins. Bmal1 and Clock also induce the expression of the nuclear receptor Rev-erbα and β. These two

genes recognize the ROR response elements (RORE) on the Bmal1 promoter and compete with transcriptional activator RORs to repress Bmal1 gene expression. Thus diminished Bmal1 and Clock activities at the peak of Per and Cry actions remove the negative regulation of Bmal1 transcription by Rev-erbα and β. This regulatory logic permits the reactivation of the activator complex once Per and Cry proteins are degraded (Reviewed in [102, 103]). Post-transcriptional modifications are prevalent in the circadian clock system. The degradation of Per proteins is actively regulated by caesin kinases. Cry proteins are phosphorylated by AMPK and subsequently targeted by E3 ligase FBXL3 [104]. Bmal1 can be SUMOylated [105], phosphorylated [106, 107], deacetylated [108] and ADP-ribosylated [109]. Each of these modifications perturbs the Bmal1 transcriptional activity. The design of such a system with complex feedback loops not only ensures the robustness of the circadian oscillation, but also generates multiple expression patterns of circadian clock genes [103]. The latter is important to achieve optimized behavioral and physiological outputs at different time of the day.

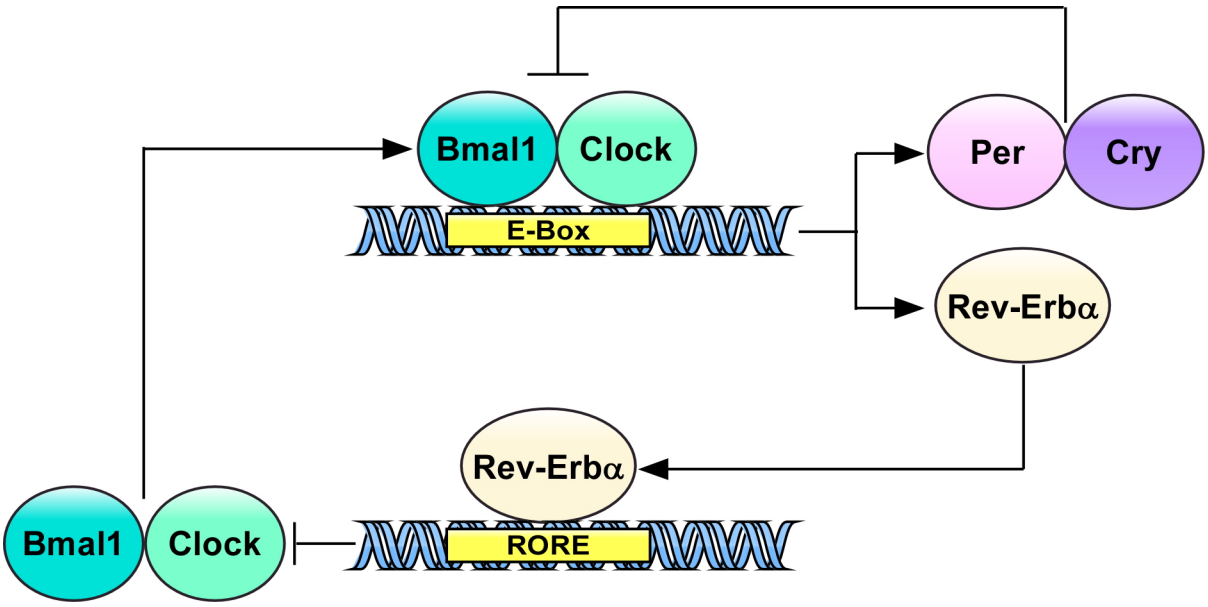

Figure 1.5. The molecular architecture of core circadian clock. The feedback loops

(**Figure 1.5. Continued**) constituted by core clock proteins ensure a self-sustained expression cycle over the course of the day. In addition, these core clock proteins control a number of metabolic processes so that the metabolic processes are coupled with environmental cues such as light/dark and feeding/fasting cycles.

II. Circadian Regulation of Metabolism

Transcriptional profiling of liver over the course of 48 hours has identified that 2% to 15% of the mammalian transcriptome is rhythmically expressed [110-113]. Among these rhythmic transcripts are transcription factors and critical enzymes regulating cellular energy sensor levels. The expression or activity of roughly 20 nuclear receptors [114], transcription factors involved in xenobiotic detoxification pathways [115], UPR components [116], the NAD+ salvage pathway [117, 118] and MicroRNAs [119-121] are directly under the control of the core clock machinery. Hence the hierarchical architecture of the molecular clock makes possible the regulation of a large quantity of transcripts, many of which are involved in carbohydrate, lipid and cholesterol metabolism.

There are long standing interests in understanding the metabolic consequences of altered circadian clock due to public health concerns of shift work. The impact of disrupted circadian clock on metabolism was first revealed from the Clock mutant mice [122]. These mice lack behavioral circadian rhythm and developed insulin resistance on HFD. Although the altered neuroendocrine signals and the hyperphagic phenotype in

these mice contribute to the metabolic deterioration, perturbed metabolic pathways in metabolic tissues are also likely factors. Disrupted circadian clock has been postulated to cause metabolic disorders in two ways: (1) The reduced expression of metabolic genes at all time, (2) The shift of metabolic gene expression so that biochemical reactions happen at the wrong time. Mouse genetic models so far support the latter scenario. Liver specific deletion of Bmal1 results in a hypoglycemic phenotype only during the day when the Bmal1 activity is the greatest [123]. In mouse liver, the repressor Cry1 and Cry2 protein levels peak around the night to day transition time and diminish at day to night transition. They are found to suppress gluconeogenesis at the post-absorptive phase (night to day transition). Disruption of Cry1/2 genes leads to a hyperglycemic phenotype at night to day transition upon fasting [124, 125]. The effects of circadian proteins on glucose metabolism are further validated in human genome-wide association studies, in which polymorphisms around the Cry2 protein are associated with hyperglycemia and type II diabetes [126].

Circadian clock genes also play significant roles in lipid metabolism. The role of the aforementioned Rev-erbs-NcoR-HDAC3 axis in mediating hepatic *de novo* lipogenesis is a prime example [79]. In addition, Clock mutant mice develop hypertriglyceridemia particularly during the day time as a result of abnormal lipoprotein production [127]. Both Bmal1 and Per2 are shown to promote the transcription and activity of nuclear receptor PPARα [128, 129], although the functional outcomes of these pathways have not been examined. Loss of core clock components Cry or Clock impairs the rhythm of XBP1 and the response to ER stress induced by tunicamycin in a time

dependent manner [116], resulting in altered lipid metabolism.

The coordinated regulation of both glucose and lipid metabolism by peripheral circadian clock highlights a fundamental role of circadian clock in modulating metabolic flexibility.

III. Reciprocal Control of Circadian Clock through Metabolic Signals

Despite the important role of SCN clock in setting overall timing, the peripheral clock has also developed the ability to sense food derived signals, especially in the liver. These local signals play a dominant role in setting the peripheral clock when feeding time is in conflict with the light and dark cycle. We have just begun to uncover the metabolic signals feeding into the peripheral circadian clock. The AMPK/SIRT1-PGC-1α-PPARs nutrient sensing pathway has been shown to impose extensive controls over circadian clock machinery. SIRT1 and PARP1 deacetylates [108] and acetylates [109] the core clock transcription factor Bmal1, respectively, leading to its degradation or stabilization. AMPK phosphorylates Cry1, which promotes its degradation in response to low glucose or a synthetic activator AICAR [104]. PGC-1α co-activates the ROR family of orphan nuclear receptors to stimulate the expression of Bmal1 and Rev-erbs [130]. Both PPARα and PPARγ regulate the expression of Bmal1 in the liver [128] and vasculature [131], respectively. A large scale RNAi screen of cellular circadian clock modulators identified an integral role of the folate synthesis pathway in setting cellular clock, although the direct metabolites and genes within the pathway remain elusive.

Besides the nutrient sensing pathways, insulin signaling pathway components were also enriched in the RNAi screen [132]. A potential mechanistic link is Glycogen Synthease Kinase 3 (GSK3). It phosphorylates Bmal1 and alters its protein stability [106]. Immunoprecipitation of Bmal1 in fibroblast identified PKCα as a component of the activator complex, linking stress signaling directly to circadian clock [133]. The importance of metabolic feedback to the circadian clock is revealed by examining the circadian rhythm of mice fed a high fat diet [134]. These animals developed aberrant feeding behavior, underscoring the interplay between metabolism and circadian rhythm in the development of metabolic syndrome.

It is worth noting that it takes days for the food derived signals to alter circadian clock and hence the metabolic programs associated with it. However, once the new time is set, it persists even without food derived signals. The resilience of the peripheral clock to change likely offsets the metabolic fluctuation in the events of unexpected food availability, while the self-sustained cycling preserves metabolic capacity in anticipation of food.

Preview of Thesis Work

In single cell organisms, nutrient influx and energy sensing mechanisms convey the availability of energy substrates and regulate substrates utilization. Multicellular organisms have evolved to acquire specializations in cellular functions. The fact that in mice and humans, the energy production or biosynthesis organ (liver) is separated from

the energy consumption organ (skeletal muscle) and the energy storage organ (white adipose tissue) dictates a system for inter-organ communication in order to achieve metabolic flexibility. So far, we know that the coordinated utilization of glucose is communicated via Insulin and counter-regulatory hormones, and the information about the adipose tissue metabolic state is conveyed through lipokine [23] and adipokines. Yet no direct evidence exists linking lipid production in the liver with lipid utilization in the muscle. As has been discussed extensively in the previous sections, lipid synthesis in the liver produces lipophilic signaling intermediates, suggesting a potential role of lipid signaling molecules in inter-organ communication. The circadian clock control of lipid metabolism in the liver may provide an additional layer of regulation in muscle fuel selection.

The overarching goal of the thesis work has been to understand the liver's role in determining metabolic flexibility, specifically with regard to hepatic *de novo* lipogenesis in this process. As discussed above, elevated lipid synthesis in the liver is a hallmark of insulin resistance state. However, our understanding of hepatic lipogenesis is incomplete and key questions remain to be addressed. In this thesis work, we have identified PPARδ as an additional regulator of the hepatic *de novo* lipogenic pathway and defined its role in the circadian regulation of muscle fatty acids utilization.

References

1. Galgani, J.E., C. Moro, and E. Ravussin, *Metabolic flexibility and insulin resistance.* Am J Physiol Endocrinol Metab, 2008. **295**(5): p. E1009-17.

2. Alberti, K.G., et al., *Harmonizing the metabolic syndrome: a joint interim statement of the International Diabetes Federation Task Force on Epidemiology and Prevention; National Heart, Lung, and Blood Institute; American Heart Association; World Heart Federation; International Atherosclerosis Society; and International Association for the Study of Obesity.* Circulation, 2009. **120**(16): p. 1640-5.

3. Donath, M.Y. and S.E. Shoelson, *Type 2 diabetes as an inflammatory disease.* Nat Rev Immunol, 2011. **11**(2): p. 98-107.

4. Hotamisligil, G.S., *Endoplasmic reticulum stress and the inflammatory basis of metabolic disease.* Cell, 2010. **140**(6): p. 900-17.

5. Muoio, D.M. and P.D. Neufer, *Lipid-induced mitochondrial stress and insulin action in muscle.* Cell Metab, 2012. **15**(5): p. 595-605.

6. Houstis, N., E.D. Rosen, and E.S. Lander, *Reactive oxygen species have a causal role in multiple forms of insulin resistance.* Nature, 2006. **440**(7086): p. 944-8.

7. Evans, J.L., et al., *Oxidative stress and stress-activated signaling pathways: a unifying hypothesis of type 2 diabetes.* Endocr Rev, 2002. **23**(5): p. 599-622.

8. Kelley, D.E. and L.J. Mandarino, *Fuel selection in human skeletal muscle in insulin resistance: a reexamination.* Diabetes, 2000. **49**(5): p. 677-83.

9. Randle, P.J., et al., *The glucose fatty-acid cycle. Its role in insulin sensitivity and the metabolic disturbances of diabetes mellitus.* Lancet, 1963. **1**(7285): p. 785-9.

10. Roden, M., et al., *Mechanism of free fatty acid-induced insulin resistance in humans.* J Clin Invest, 1996. **97**(12): p. 2859-65.

11. Dresner, A., et al., *Effects of free fatty acids on glucose transport and IRS-1-associated phosphatidylinositol 3-kinase activity.* J Clin Invest, 1999. **103**(2): p. 253-9.

12. Goodpaster, B.H. and D.E. Kelley, *Skeletal muscle triglyceride: marker or mediator of obesity-induced insulin resistance in type 2 diabetes mellitus?* Curr Diab Rep, 2002. **2**(3): p. 216-22.

13. Kim, J.K., et al., *Tissue-specific overexpression of lipoprotein lipase causes tissue-specific insulin resistance.* Proc Natl Acad Sci U S A, 2001. **98**(13): p. 7522-7.

14. Koonen, D.P., et al., *Increased hepatic CD36 expression contributes to dyslipidemia associated with diet-induced obesity.* Diabetes, 2007. **56**(12): p. 2863-71.

15. Doege, H., et al., *Silencing of hepatic fatty acid transporter protein 5 in vivo reverses diet-induced non-alcoholic fatty liver disease and improves hyperglycemia.* J Biol Chem, 2008. **283**(32): p. 22186-92.

16. Kim, J.K., et al., *Inactivation of fatty acid transport protein 1 prevents fat-induced insulin resistance in skeletal muscle.* J Clin Invest, 2004. **113**(5): p. 756-63.

17. Cao, H., et al., *Regulation of metabolic responses by adipocyte/macrophage Fatty Acid-binding proteins in leptin-deficient mice.* Diabetes, 2006. **55**(7): p. 1915-22.

18. Maeda, K., et al., *Adipocyte/macrophage fatty acid binding proteins control integrated metabolic responses in obesity and diabetes.* Cell Metab, 2005. **1**(2): p. 107-19.

19. Furuhashi, M., et al., *Treatment of diabetes and atherosclerosis by inhibiting fatty-acid-binding protein aP2.* Nature, 2007. **447**(7147): p. 959-65.

20. van Loon, L.J. and B.H. Goodpaster, *Increased intramuscular lipid storage in the insulin-resistant and endurance-trained state.* Pflugers Arch, 2006. **451**(5): p. 606-16.

21. Goodpaster, B.H., et al., *Skeletal muscle lipid content and insulin resistance: evidence for a paradox in endurance-trained athletes.* J Clin Endocrinol Metab, 2001. **86**(12): p. 5755-61.

22. Monetti, M., et al., *Dissociation of hepatic steatosis and insulin resistance in mice overexpressing DGAT in the liver.* Cell Metab, 2007. **6**(1): p. 69-78.

23. Cao, H., et al., *Identification of a lipokine, a lipid hormone linking adipose tissue to systemic metabolism.* Cell, 2008. **134**(6): p. 933-44.

24. Lee, J.M., et al., *A nuclear-receptor-dependent phosphatidylcholine pathway with antidiabetic effects.* Nature, 2011. **474**(7352): p. 506-10.

25. Ortlund, E.A., et al., *Modulation of human nuclear receptor LRH-1 activity by phospholipids and SHP.* Nat Struct Mol Biol, 2005. **12**(4): p. 357-63.

26. Chakravarthy, M.V., et al., *Identification of a physiologically relevant endogenous ligand for PPARalpha in liver.* Cell, 2009. **138**(3): p. 476-88.

27. Aoki, T. and S. Narumiya, *Prostaglandins and chronic inflammation.* Trends Pharmacol Sci, 2012. **33**(6): p. 304-11.

28. Uderhardt, S., et al., *12/15-lipoxygenase orchestrates the clearance of apoptotic cells and maintains immunologic tolerance.* Immunity, 2012. **36**(5): p. 834-46.

29. Flavin, R., et al., *Fatty acid synthase as a potential therapeutic target in cancer.* Future Oncol, 2010. **6**(4): p. 551-62.

30. Frisca, F., et al., *Biological effects of lysophosphatidic acid in the nervous system.* Int Rev Cell Mol Biol, 2012. **296**: p. 273-322.

31. Li, L.O., E.L. Klett, and R.A. Coleman, *Acyl-CoA synthesis, lipid metabolism and lipotoxicity.* Biochim Biophys Acta, 2010. **1801**(3): p. 246-51.

32. Zechner, R., et al., *FAT SIGNALS--lipases and lipolysis in lipid metabolism and signaling.* Cell Metab, 2012. **15**(3): p. 279-91.

33. Nishizuka, Y., *The role of protein kinase C in cell surface signal transduction and tumour promotion.* Nature, 1984. **308**(5961): p. 693-8.

34. Moscat, J. and M.T. Diaz-Meco, *The atypical protein kinase Cs. Functional specificity mediated by specific protein adapters.* EMBO Rep, 2000. **1**(5): p. 399-403.

35. Li, Y., et al., *Protein kinase C Theta inhibits insulin signaling by phosphorylating IRS1 at Ser(1101).* J Biol Chem, 2004. **279**(44): p. 45304-7.

36. Kim, J.K., et al., *PKC-theta knockout mice are protected from fat-induced insulin resistance.* J Clin Invest, 2004. **114**(6): p. 823-7.

37. Gao, Z., et al., *Inactivation of PKCtheta leads to increased susceptibility to obesity and dietary insulin resistance in mice.* Am J Physiol Endocrinol Metab, 2007. **292**(1): p. E84-91.

38. Bezy, O., et al., *PKCdelta regulates hepatic insulin sensitivity and hepatosteatosis in mice and humans.* J Clin Invest, 2011. **121**(6): p. 2504-17.

39. Frangioudakis, G., et al., *Diverse roles for protein kinase C delta and protein kinase C epsilon in the generation of high-fat-diet-induced glucose intolerance in mice: regulation of lipogenesis by protein kinase C delta.* Diabetologia, 2009. **52**(12): p. 2616-20.

40. Wymann, M.P. and R. Schneiter, *Lipid signalling in disease.* Nat Rev Mol Cell Biol, 2008. **9**(2): p. 162-76.

41. Summers, S.A., *Ceramides in insulin resistance and lipotoxicity.* Prog Lipid Res, 2006. **45**(1): p. 42-72.

42. Holland, W.L., et al., *Inhibition of ceramide synthesis ameliorates glucocorticoid-, saturated-fat-, and obesity-induced insulin resistance.* Cell Metab, 2007. **5**(3): p. 167-79.

43. Koves, T.R., et al., *Mitochondrial overload and incomplete fatty acid oxidation contribute to skeletal muscle insulin resistance.* Cell Metab, 2008. **7**(1): p. 45-56.

44. Muoio, D.M., et al., *Muscle-specific deletion of carnitine acetyltransferase compromises glucose tolerance and metabolic flexibility.* Cell Metab, 2012. **15**(5): p. 764-77.

45. Erion, D.M. and G.I. Shulman, *Diacylglycerol-mediated insulin resistance.* Nat Med, 2010. **16**(4): p. 400-2.

46. Solinas, G., et al., *Saturated fatty acids inhibit induction of insulin gene transcription by JNK-mediated phosphorylation of insulin-receptor substrates.* Proc Natl Acad Sci U S A, 2006. **103**(44): p. 16454-9.

47. Holzer, R.G., et al., *Saturated fatty acids induce c-Src clustering within membrane subdomains, leading to JNK activation.* Cell, 2011. **147**(1): p. 173-84.

48. Fu, S., et al., *Aberrant lipid metabolism disrupts calcium homeostasis causing liver endoplasmic reticulum stress in obesity.* Nature, 2011. **473**(7348): p. 528-31.

49. Lodhi, I.J., X. Wei, and C.F. Semenkovich, *Lipoexpediency: de novo lipogenesis as a metabolic signal transmitter.* Trends Endocrinol Metab, 2011. **22**(1): p. 1-8.

50. Guarente, L., *Sirtuins as potential targets for metabolic syndrome.* Nature, 2006. **444**(7121): p. 868-74.

51. Carling, D., V.A. Zammit, and D.G. Hardie, *A common bicyclic protein kinase cascade inactivates the regulatory enzymes of fatty acid and cholesterol biosynthesis.* FEBS Lett, 1987. **223**(2): p. 217-22.

52. Gwinn, D.M., et al., *AMPK phosphorylation of raptor mediates a metabolic checkpoint.* Mol Cell, 2008. **30**(2): p. 214-26.

53. Inoki, K., T. Zhu, and K.L. Guan, *TSC2 mediates cellular energy response to control cell growth and survival.* Cell, 2003. **115**(5): p. 577-90.

54. Watt, M.J., et al., *Regulation of HSL serine phosphorylation in skeletal muscle and adipose tissue.* Am J Physiol Endocrinol Metab, 2006. **290**(3): p. E500-8.

55. Ahmadian, M., et al., *Desnutrin/ATGL is regulated by AMPK and is required for a brown adipose phenotype.* Cell Metab, 2011. **13**(6): p. 739-48.

56. Salt, I.P., J.M. Connell, and G.W. Gould, *5-aminoimidazole-4-carboxamide ribonucleoside (AICAR) inhibits insulin-stimulated glucose transport in 3T3-L1 adipocytes.* Diabetes, 2000. **49**(10): p. 1649-56.

57. Horton, J.D., et al., *Regulation of sterol regulatory element binding proteins in livers of fasted and refed mice.* Proc Natl Acad Sci U S A, 1998. **95**(11): p. 5987-92.

58. Haas, J.T., et al., *Hepatic insulin signaling is required for obesity-dependent expression of SREBP-1c mRNA but not for feeding-dependent expression.* Cell Metab, 2012. **15**(6): p. 873-84.

59. Shimomura, I., et al., *Insulin selectively increases SREBP-1c mRNA in the livers of rats with streptozotocin-induced diabetes.* Proc Natl Acad Sci U S A, 1999. **96**(24): p. 13656-61.

60. Shimomura, I., Y. Bashmakov, and J.D. Horton, *Increased levels of nuclear SREBP-1c associated with fatty livers in two mouse models of diabetes mellitus.* J Biol Chem, 1999. **274**(42): p. 30028-32.

61. Li, S., M.S. Brown, and J.L. Goldstein, *Bifurcation of insulin signaling pathway in rat liver: mTORC1 required for stimulation of lipogenesis, but not inhibition of gluconeogenesis.* Proc Natl Acad Sci U S A, 2010. **107**(8): p. 3441-6.

62. Yecies, J.L., et al., *Akt stimulates hepatic SREBP1c and lipogenesis through parallel mTORC1-dependent and independent pathways.* Cell Metab, 2011. **14**(1): p. 21-32.

63. Joseph, S.B., et al., *Direct and indirect mechanisms for regulation of fatty acid synthase gene expression by liver X receptors.* J Biol Chem, 2002. **277**(13): p. 11019-25.

64. Lin, J., et al., *Hyperlipidemic effects of dietary saturated fats mediated through PGC-1beta coactivation of SREBP.* Cell, 2005. **120**(2): p. 261-73.

65. Nagai, Y., et al., *The role of peroxisome proliferator-activated receptor gamma coactivator-1 beta in the pathogenesis of fructose-induced insulin resistance.* Cell Metab, 2009. **9**(3): p. 252-64.

66. Walker, A.K., et al., *A conserved SREBP-1/phosphatidylcholine feedback circuit regulates lipogenesis in metazoans.* Cell, 2011. **147**(4): p. 840-52.

67. Walker, A.K., et al., *Conserved role of SIRT1 orthologs in fasting-dependent inhibition of the lipid/cholesterol regulator SREBP.* Genes Dev, 2010. **24**(13): p. 1403-17.

68. Li, Y., et al., *AMPK phosphorylates and inhibits SREBP activity to attenuate hepatic steatosis and atherosclerosis in diet-induced insulin-resistant mice.* Cell Metab, 2011. **13**(4): p. 376-88.

69. Takeuchi, Y., et al., *Polyunsaturated fatty acids selectively suppress sterol regulatory element-binding protein-1 through proteolytic processing and autoloop regulatory circuit.* J Biol Chem, 2010. **285**(15): p. 11681-91.

70. Clarke, S.D. and D.B. Jump, *Dietary polyunsaturated fatty acid regulation of gene transcription.* Annu Rev Nutr, 1994. **14**: p. 83-98.

71. Hasegawa, J., et al., *A novel factor binding to the glucose response elements of liver pyruvate kinase and fatty acid synthase genes.* J Biol Chem, 1999. **274**(2): p. 1100-7.

72. Kabashima, T., et al., *Xylulose 5-phosphate mediates glucose-induced lipogenesis by xylulose 5-phosphate-activated protein phosphatase in rat liver.* Proc Natl Acad Sci U S A, 2003. **100**(9): p. 5107-12.

73. Kawaguchi, T., et al., *Mechanism for fatty acid "sparing" effect on glucose-induced transcription: regulation of carbohydrate-responsive element-binding protein by AMP-activated protein kinase.* J Biol Chem, 2002. **277**(6): p. 3829-35.

74. Herman, M.A., et al., *A novel ChREBP isoform in adipose tissue regulates systemic glucose metabolism.* Nature, 2012. **484**(7394): p. 333-8.

75. Lee, A.H., et al., *Regulation of hepatic lipogenesis by the transcription factor XBP1.* Science, 2008. **320**(5882): p. 1492-6.

76. So, J.S., et al., *Silencing of Lipid Metabolism Genes through IRE1alpha-Mediated mRNA Decay Lowers Plasma Lipids in Mice.* Cell Metab, 2012. **16**(4): p. 487-99.

77. Cho, H., et al., *Regulation of circadian behaviour and metabolism by REV-ERB-alpha and REV-ERB-beta.* Nature, 2012. **485**(7396): p. 123-7.

78. Bugge, A., et al., *Rev-erbalpha and Rev-erbbeta coordinately protect the circadian clock and normal metabolic function.* Genes Dev, 2012. **26**(7): p. 657-67.

79. Feng, D., et al., *A circadian rhythm orchestrated by histone deacetylase 3 controls hepatic lipid metabolism.* Science, 2011. **331**(6022): p. 1315-9.

80. Yin, L., et al., *Rev-erbalpha, a heme sensor that coordinates metabolic and circadian pathways.* Science, 2007. **318**(5857): p. 1786-9.

81. Miyazaki, M., et al., *Hepatic stearoyl-CoA desaturase-1 deficiency protects mice from carbohydrate-induced adiposity and hepatic steatosis.* Cell Metab, 2007. **6**(6): p. 484-96.

82. Flowers, M.T., et al., *Liver gene expression analysis reveals endoplasmic reticulum stress and metabolic dysfunction in SCD1-deficient mice fed a very low-fat diet.* Physiol Genomics, 2008. **33**(3): p. 361-72.

83. Abu-Elheiga, L., et al., *Mutant mice lacking acetyl-CoA carboxylase 1 are embryonically lethal.* Proc Natl Acad Sci U S A, 2005. **102**(34): p. 12011-6.

84. Chirala, S.S., et al., *Fatty acid synthesis is essential in embryonic development: fatty acid synthase null mutants and most of the heterozygotes die in utero.* Proc Natl Acad Sci U S A, 2003. **100**(11): p. 6358-63.

85. Bruss, M.D., et al., *Calorie restriction increases fatty acid synthesis and whole body fat oxidation rates.* Am J Physiol Endocrinol Metab, 2010. **298**(1): p. E108-16.

86. Shimomura, I., et al., *Insulin resistance and diabetes mellitus in transgenic mice expressing nuclear SREBP-1c in adipose tissue: model for congenital generalized lipodystrophy.* Genes Dev, 1998. **12**(20): p. 3182-94.

87. Lodhi, I.J., et al., *Inhibiting adipose tissue lipogenesis reprograms thermogenesis and PPARgamma activation to decrease diet-induced obesity.* Cell Metab, 2012. **16**(2): p. 189-201.

88. Liu, X., et al., *Loss of Stearoyl-CoA desaturase-1 attenuates adipocyte inflammation: effects of adipocyte-derived oleate.* Arterioscler Thromb Vasc Biol, 2010. **30**(1): p. 31-8.

89. Barrows, B.R. and E.J. Parks, *Contributions of different fatty acid sources to very low-density lipoprotein-triacylglycerol in the fasted and fed states.* J Clin Endocrinol Metab, 2006. **91**(4): p. 1446-52.

90. Timlin, M.T. and E.J. Parks, *Temporal pattern of de novo lipogenesis in the postprandial state in healthy men.* Am J Clin Nutr, 2005. **81**(1): p. 35-42.

91. Donnelly, K.L., et al., *Sources of fatty acids stored in liver and secreted via lipoproteins in patients with nonalcoholic fatty liver disease.* J Clin Invest, 2005. **115**(5): p. 1343-51.

92. Sorensen, L.P., et al., *Basal and insulin mediated VLDL-triglyceride kinetics in type 2 diabetic men.* Diabetes, 2011. **60**(1): p. 88-96.

93. Moon, Y.A., et al., *The Scap/SREBP pathway is essential for developing diabetic fatty liver and carbohydrate-induced hypertriglyceridemia in animals.* Cell Metab, 2012. **15**(2): p. 240-6.

94. Jurczak, M.J., et al., *Dissociation of inositol-requiring enzyme (IRE1alpha)-mediated c-Jun N-terminal kinase activation from hepatic insulin resistance in conditional X-box-binding protein-1 (XBP1) knock-out mice.* J Biol Chem, 2012. **287**(4): p. 2558-67.

95. Choi, C.S., et al., *Continuous fat oxidation in acetyl-CoA carboxylase 2 knockout mice increases total energy expenditure, reduces fat mass, and improves insulin sensitivity.* Proc Natl Acad Sci U S A, 2007. **104**(42): p. 16480-5.

96. Benhamed, F., et al., *The lipogenic transcription factor ChREBP dissociates hepatic steatosis from insulin resistance in mice and humans.* J Clin Invest, 2012. **122**(6): p. 2176-94.

97. Sun, Z., et al., *Hepatic Hdac3 promotes gluconeogenesis by repressing lipid synthesis and sequestration.* Nat Med, 2012. **18**(6): p. 934-42.

98. Krahmer, N., et al., *Phosphatidylcholine synthesis for lipid droplet expansion is mediated by localized activation of CTP:phosphocholine cytidylyltransferase.* Cell Metab, 2011. **14**(4): p. 504-15.

99. Jornayvaz, F.R., et al., *Hepatic insulin resistance in mice with hepatic overexpression of diacylglycerol acyltransferase 2.* Proc Natl Acad Sci U S A, 2011. **108**(14): p. 5748-52.

100. Knebel, B., et al., *Liver-specific expression of transcriptionally active SREBP-1c is associated with fatty liver and increased visceral fat mass.* PLoS One, 2012. **7**(2): p. e31812.

101. Kotronen, A., et al., *Comparison of lipid and fatty acid composition of the liver, subcutaneous and intra-abdominal adipose tissue, and serum.* Obesity (Silver Spring), 2010. **18**(5): p. 937-44.

102. Bass, J. and J.S. Takahashi, *Circadian integration of metabolism and energetics.* Science, 2010. **330**(6009): p. 1349-54.

103. Asher, G. and U. Schibler, *Crosstalk between components of circadian and metabolic cycles in mammals.* Cell Metab, 2011. **13**(2): p. 125-37.

104. Lamia, K.A., et al., *AMPK regulates the circadian clock by cryptochrome phosphorylation and degradation.* Science, 2009. **326**(5951): p. 437-40.

105. Cardone, L., et al., *Circadian clock control by SUMOylation of BMAL1.* Science, 2005. **309**(5739): p. 1390-4.

106. Sahar, S., et al., *Regulation of BMAL1 protein stability and circadian function by GSK3beta-mediated phosphorylation.* PLoS One, 2010. **5**(1): p. e8561.

107. Tamaru, T., et al., *CK2alpha phosphorylates BMAL1 to regulate the mammalian clock.* Nat Struct Mol Biol, 2009. **16**(4): p. 446-8.

108. Asher, G., et al., *SIRT1 regulates circadian clock gene expression through PER2 deacetylation.* Cell, 2008. **134**(2): p. 317-28.

109. Asher, G., et al., *Poly(ADP-ribose) polymerase 1 participates in the phase entrainment of circadian clocks to feeding.* Cell, 2010. **142**(6): p. 943-53.

110. Miller, B.H., et al., *Circadian and CLOCK-controlled regulation of the mouse transcriptome and cell proliferation.* Proc Natl Acad Sci U S A, 2007. **104**(9): p. 3342-7.

111. Panda, S., et al., *Coordinated transcription of key pathways in the mouse by the circadian clock.* Cell, 2002. **109**(3): p. 307-20.

112. Hughes, M.E., et al., *Harmonics of circadian gene transcription in mammals.* PLoS Genet, 2009. **5**(4): p. e1000442.

113. Atwood, A., et al., *Cell-autonomous circadian clock of hepatocytes drives rhythms in transcription and polyamine synthesis.* Proc Natl Acad Sci U S A, 2011. **108**(45): p. 18560-5.

114. Yang, X., et al., *Nuclear receptor expression links the circadian clock to metabolism.* Cell, 2006. **126**(4): p. 801-10.

115. Gachon, F., et al., *The circadian PAR-domain basic leucine zipper transcription factors DBP, TEF, and HLF modulate basal and inducible xenobiotic detoxification.* Cell Metab, 2006. **4**(1): p. 25-36.

116. Cretenet, G., M. Le Clech, and F. Gachon, *Circadian clock-coordinated 12 Hr period rhythmic activation of the IRE1alpha pathway controls lipid metabolism in mouse liver.* Cell Metab, 2010. **11**(1): p. 47-57.

117. Ramsey, K.M., et al., *Circadian clock feedback cycle through NAMPT-mediated NAD+ biosynthesis.* Science, 2009. **324**(5927): p. 651-4.

118. Nakahata, Y., et al., *Circadian control of the NAD+ salvage pathway by CLOCK-SIRT1.* Science, 2009. **324**(5927): p. 654-7.

119. Gatfield, D., et al., *Integration of microRNA miR-122 in hepatic circadian gene expression.* Genes Dev, 2009. **23**(11): p. 1313-26.

120. Vodala, S., et al., *The Oscillating miRNA 959-964 Cluster Impacts Drosophila Feeding Time and Other Circadian Outputs.* Cell Metab, 2012. **16**(5): p. 601-12.

121. Shende, V.R., et al., *Expression and rhythmic modulation of circulating microRNAs targeting the clock gene Bmal1 in mice.* PLoS One, 2011. **6**(7): p. e22586.

122. Turek, F.W., et al., *Obesity and metabolic syndrome in circadian Clock mutant mice.* Science, 2005. **308**(5724): p. 1043-5.

123. Lamia, K.A., K.F. Storch, and C.J. Weitz, *Physiological significance of a peripheral tissue circadian clock.* Proc Natl Acad Sci U S A, 2008. **105**(39): p. 15172-7.

124. Lamia, K.A., et al., *Cryptochromes mediate rhythmic repression of the glucocorticoid receptor.* Nature, 2011. **480**(7378): p. 552-6.

125. Zhang, E.E., et al., *Cryptochrome mediates circadian regulation of cAMP signaling and hepatic gluconeogenesis.* Nat Med, 2010. **16**(10): p. 1152-6.

126. Dupuis, J., et al., *New genetic loci implicated in fasting glucose homeostasis and their impact on type 2 diabetes risk.* Nat Genet, 2010. **42**(2): p. 105-16.

127. Pan, X., et al., *Diurnal regulation of MTP and plasma triglyceride by CLOCK is mediated by SHP.* Cell Metab, 2010. **12**(2): p. 174-86.

128. Canaple, L., et al., *Reciprocal regulation of brain and muscle Arnt-like protein 1 and peroxisome proliferator-activated receptor alpha defines a novel positive feedback loop in the rodent liver circadian clock.* Mol Endocrinol, 2006. **20**(8): p. 1715-27.

129. Schmutz, I., et al., *The mammalian clock component PERIOD2 coordinates circadian output by interaction with nuclear receptors.* Genes Dev, 2010. **24**(4): p. 345-57.

130. Li, S., et al., *Circadian metabolic regulation through crosstalk between casein kinase 1delta and transcriptional coactivator PGC-1alpha.* Mol Endocrinol, 2011. **25**(12): p. 2084-93.

131. Wang, N., et al., *Vascular PPARgamma controls circadian variation in blood pressure and heart rate through Bmal1.* Cell Metab, 2008. **8**(6): p. 482-91.

132. Zhang, E.E., et al., *A genome-wide RNAi screen for modifiers of the circadian clock in human cells.* Cell, 2009. **139**(1): p. 199-210.

133. Robles, M.S., et al., *Identification of RACK1 and protein kinase Calpha as integral components of the mammalian circadian clock.* Science, 2010. **327**(5964): p. 463-6.

134. Kohsaka, A., et al., *High-fat diet disrupts behavioral and molecular circadian rhythms in mice.* Cell Metab, 2007. **6**(5): p. 414-21.

Chapter 2:

ROLE OF PEROXISOME PROLIFERATOR-ACTIVATED RECEPTOR DELTA/BETA IN HEPATIC METABOLIC REGULATION

(Published in J Biol Chem. 2011 Jan 14;286(2):1237-47.)

Introduction

The prevalence of metabolic diseases has increased substantially, partly due to rising obesity caused by sedentary life styles and energy surplus. Insulin resistance is at the core of these disorders. Excess energy substrates beyond the catabolic or storage capacity of the body are believed to cause organelle dysfunction [1]. Elevated non-esterified free fatty acid has been shown to activate inflammatory response through JNK, which suppresses insulin signaling [2-4], while partitioning fatty acid substrates for catabolism or triglyceride synthesis prevents high fat diet induced insulin resistance [5, 6]. Conversely, de novo synthesis of beneficial MUFAs alleviates cellular stress and protects against detrimental effects of saturated fatty acids [7]. Therefore, a key step towards the development of drugs to treat metabolic diseases is to understand mechanisms controlling energy substrate metabolism. In this regard, the liver is one of the most important tissues for energy homeostasis known for its role in sustaining energy availability through anabolic and catabolic pathways. Hepatic insulin resistance results in over-production of glucose and very low-density lipoproteins (VLDL), worsening the extent of glucotoxicity and lipotoxicity [1]. Metformin is one of the commonly prescribed anti-diabetic drugs that target hepatic glucose output [8]. This drug increases the activity of AMPK, an energy sensor that is activated by elevated intracellular AMP or AMP/ATP ratio. In the liver, AMPK reduces glucose production by suppressing the expression of gluconeogenic enzymes, such as phosphoenolpyruvate

carboxykinase (PEPCK) [9]. AMPK also mediates the beneficial effects of adiponectin on glucose and lipid metabolism through adiponectin receptors [10, 11].

While not a major site for glucose deposition, the liver also plays a role in compartmentalizing glucose during feeding [12]. Postprandial hyperglycemia triggers insulin secretion, which in turn suppresses gluconeogenesis and at the same time, induces hepatic glucokinase (GK) expression [13-15]. Glucose transported into the liver through glucose transporter 2 (GLUT2) is phosphorylated by GK to generate glucose-6-phosphate, which enters metabolic pathways for glycogen synthesis, glycolysis and lipogenesis. Genetic manipulations that sustain GK protein levels in the liver have been shown to lower blood glucose and improve insulin sensitivity [16-18]. This pathway appears to be an alternative approach to control hyperglycemia. However, it is unclear whether this process can be pharmacologically activated.

The three peroxisome proliferator-activated receptors, PPARα, δ/β and γ, belong to the nuclear receptor family. They are activated by dietary fats and are important metabolic regulators [19, 20]. PPARα and PPARγ mediate the lipid lowering and insulin sensitizing effects of fenofibrates and thiazolidinediones, respectively [21, 22]. PPARα reduces circulating triglycerides by up-regulation of fatty acid catabolism in the liver, whereas PPARγ increases insulin sensitivity, in part, through directing fatty acid flux into storage in adipocytes. PPARδ also shows promise as a drug target to treat metabolic diseases [23]. The reported effects of PPARδ activation by systemic ligand administration or by transgenic approaches in animal models include correction of dyslipidemia and hyperglycemia, prevention of diet-induced obesity, enhancement of

insulin sensitivity and modulation of muscle fiber type switching [24-29]. Most of the observed beneficial effects are believed to be mediated by increasing fatty acid catabolism and mitochondria function in muscle and adipocytes. It is proposed that in muscle AMPK activates PPARδ to increase oxidative metabolism and running endurance [30]. We and others have recently shown that PPARδ also plays an important role in macrophage alternative activation, which exhibits anti-inflammatory properties and as such, counteracts the inhibitory effect of inflammatory signaling on insulin sensitivity [31, 32].

A previous study demonstrated that administration of a synthetic PPARδ agonist, GW501516, lowered hyperglycemia in db/db mice by reducing hepatic glucose production and increasing glucose disposal [28]. Expression profiling analyses suggested that fatty acid oxidation genes were up-regulated in muscle, whereas several lipogenic genes were induced in the liver. While the function of PPARδ in muscle fat burning is well documented, whether alteration in hepatic gene expression observed in systemic drug treatment is a primary or secondary effect has not been addressed. In this study, we sought to determine whether PPARδ has a direct role in hepatic metabolic regulation. Our results demonstrated that PPARδ regulates energy substrate utilization and limits lipotoxicity in the liver.

Results

Liver-restricted PPARδ expression improves glucose homeostasis

To assess potential roles of hepatic PPARδ in the regulation of glucose homeostasis, we utilized adenoviral mediated gene delivery to increase PPARδ expression/activity in the liver. Previous studies have demonstrated that the over-expressed PPARδ is active *in vivo* [33]. A cohort of wild type C57BL/6 male mice were fed a high fat diet for 10 weeks to induce insulin resistance, followed by injection with adenoviral GFP (control) or PPARδ (adPPARδ) through the tail vein. Adenovirus delivered through tail vein is known to concentrate in the liver, which is used commonly to achieve liver-restricted expression. Examination of liver sections showed that approximately 70% of hepatocytes were infected as determined by GFP expression, resulting in a 4- to 5- fold increase in the PPARδ protein level (Figure 2.2A). A series of metabolic studies were conducted within a week following the injection. These mice were first placed in metabolic cages and the respiratory exchange ratio (RER) was examined to determine whether increased hepatic PPARδ altered fuel substrate usage. We found a moderate but significant increase in the RER at the resting period in adPPARδ mice (Figure 2.1A and Figure 2.3), indicating that PPARδ may increase glucose utilization in the liver. In line with this, adPPARδ mice had a lower fasting glucose level compared to control animals at the basal state (GFP: 131±7.13; PPARδ: 109.5±3.15, $P<0.05$) and throughout the course of glucose tolerance test (GTT) (Figure 2.1B). Insulin levels measured during GTT showed no significant difference between the two groups (data not shown). Insulin tolerance test demonstrated that adPPARδ mice had improved insulin sensitivity, supporting the notion that hepatic PPARδ over-expression enhances glucose handling (Figure 2.1C). To determine how hepatic

PPARδ regulates glucose metabolism, liver samples were collected for histological and gene expression studies. Interestingly, H & E staining of liver sections revealed signs of glycogen and lipids deposition in adenoviral PPARδ infected livers (Figure 2.1D). Glycogen and lipids accumulation were further determined by periodic acid-schiff (PAS) staining and oil red O staining. After an overnight fast, livers of control mice contained minimal glycogen. In contrast, adenoviral PPARδ infected livers showed a substantial increase in glycogen positive staining (Figure 2.1D). Similarly, adPPARδ infected livers had elevated neutral lipids stains (Figure 2.1D). Quantitative analyses demonstrated increased glycogen and triglyceride content in livers of adPPARδ mice, whereas fatty acid and cholesterol concentrations remained similar (Figure 2.1D). We did not observe significant differences in white adipose tissue (WAT) histology, body weight, the ratio of liver or WAT weight to body weight and levels of fasting free fatty acid, triglyceride and cholesterol between the two groups, indicating the effects of hepatic PPARδ activation on glucose homeostasis were not secondary to changes in other metabolic parameters (Table 2.1). Gene expression analysis determined by RT quantitative PCR (qPCR) demonstrated that genes involved in glucose uptake and utilization, such as GLUT2, GK and pyruvate kinase (PK), were increased in livers of adPPARδ mice compared to control animals (Figure 2.1E). Lipogenic genes, including fatty acid synthase (FAS), acetyl-CoA carboxylase 1 (ACC1), ACC2 and stearoyl-CoA desaturase 1 (SCD1) were up-regulated, most of which have been shown to be induced by systemic ligand treatment in livers of db/db mice [28]. Sterol responsive element binding protein 1c (SREBP-1c) and PPARγ co-activator-1β (PGC-1β), which has been shown to regulate

FAS through co-activation of SREBP-1c, were also induced [34]. In contrast, gluconeogenic genes, including PEPCK and HNF4α, were suppressed in PPARδ virus infected livers (Figure 2.1E). Levels of PPARα and its targets genes, acyl-CoA oxidase (AOX) and carnitine palmitoyl-coA transferase 1 (CPT1) and medium chain acyl-CoA dehydrogenase (MCAD) were unaffected, implicating that PPARδ over-expression did not cause non-specific, cross-regulation of PPARα pathways. In addition, the expression of PPARδ and its target genes was unchanged in other tissues such as muscle and WAT (Figure 2.2B). These data suggest that increased hepatic PPARδ activity lowers glucose levels in high fat fed mice and implicate a role for PPARδ in hepatic metabolic regulation.

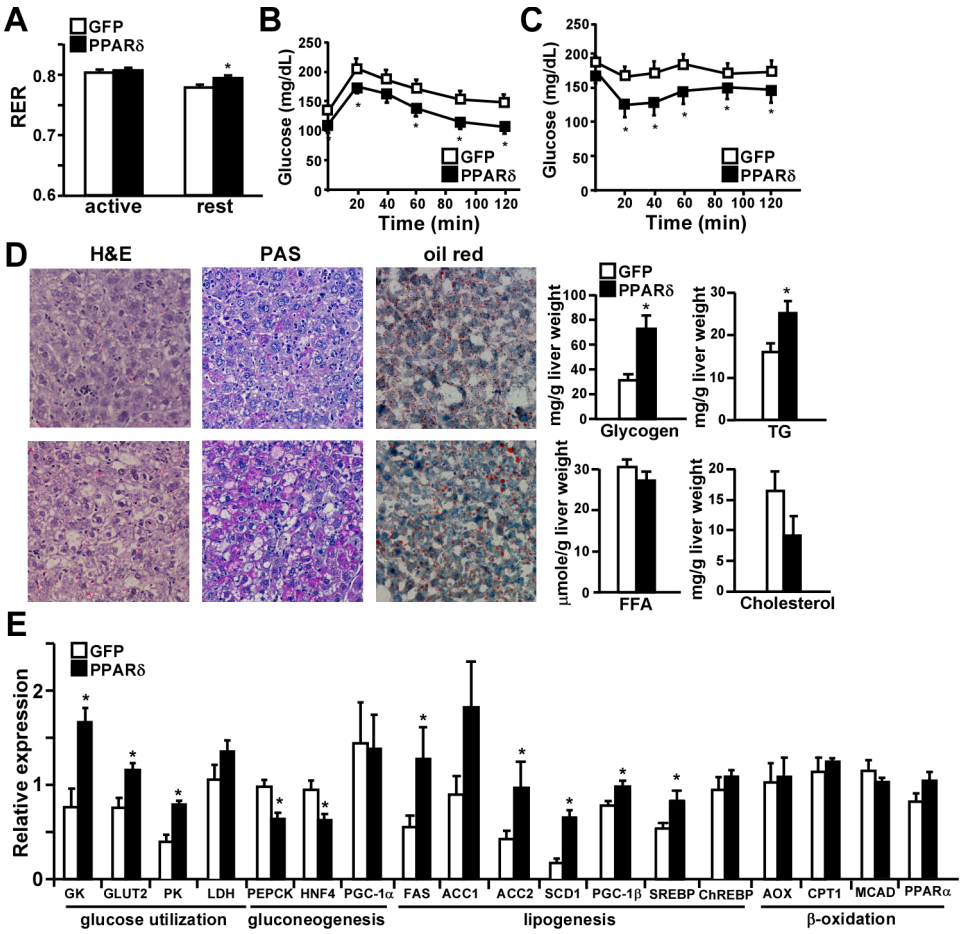

Figure 2.1. Liver-restricted PPARδ expression improves glucose homeostasis in mice fed a high fat diet. **A**, Adenoviral mediated hepatic PPARδ expression increases the respiratory exchange ratio at the resting state. High fat fed C57BL/6 male mice were injected with adenoviral GFP or PPARδ through the tail vein. 3 days after viral injection, mice (n=5) were placed in metabolic cages to determine the respiratory exchange ratio (RER). Mice were 20 weeks old and had been on high fat diet for 10 weeks. Active: average RER during the dark cycle; Rest: average RER during the light cycle. **B**, Glucose tolerance test (GTT) and **C**, insulin tolerance test (ITT) showing improved glucose handling and insulin sensitivity in adenoviral PPARδ infected mice compared to

(**Figure 2.1. continued**) control animals (n=7). GTT (overnight fasted) and ITT (6 hours fasted) were performed 4 and 5 days after virus injection, respectively. GFP and PPARδ indicate mice receiving adenoviral GFP and PPARδ, respectively. **D**, Histological analyses of liver sections (200X) from GFP and PPARδ adenovirus injected mice. Liver samples were collected 7 days following virus injection after overnight fast. H&E staining was conducted for morphological assessment and PAS staining (counter stained with hematoxylin) was performed to identify glycogen, which stained purple. Hepatic glycogen and lipid contents were quantified by enzymatic assays. TG: triglyceride; FFA: free fatty acid. **E**, PPARδ regulates the expression of genes in glucose and lipid metabolism. Liver samples were harvested from control (GFP) or adPPARδ (PPARδ) mice after overnight fast and gene expression was determined by RT qPCR. LDH: lactate dehydrogenase; SREBP: SREBP-1c; ChREBP: carbohydrate response element binding protein; AOX: acyl-CoA oxidase; CPT1: carnitine palmitoyl-coA transferase 1; MCAD: medium chain Acyl-CoA dehydrogenase. *$p<0.05$.

Table 2.1. Metabolic parameters of adenoviral injected C57BL/6 mice

	Normal Chow		High Fat Diet	
Adenovirus	**GFP**	**PPARδ**	**GFP**	**PPARδ**
Weight (g)	29.38±0.51	30.45±0.82	27.65±1.25	26.91±1.08
Liver/body weight	0.0856±0.0022	0.0819±0.0016	0.0548±0.0020	0.0555±0.0026
Fat/body weight	N/D	N/D	0.0287±0.0047	0.0285±0.0055
Triglycerides (mg/dL)	53.96±5.42	56.00±3.45	123.55±34.06	115.68±33.41
Free fatty acid (mmol/L)	N/D	N/D	0.8779±0.2219	0.9130±0.2680
Cholesterol (mg/dL)	N/D	N/D	71.156±5.048	68.448±6.164
Glucose (mg/dL)	117±3.34	91.75±9.39*	131±7.13	109.5±3.15*
Insulin (ng/ml)	N/D	N/D	2.42±0.88	2.34±0.53

* $P<0.05$. The normal chow (NC) cohort was 3 months old, while the high fat fed (HF) cohort was 18 weeks old (10-week high fat diet challenge, starting at 8 weeks of age). The HF cohort lost more weight as mice were put through 3 overnight fasts during the one-week experiment period following virus injection. For this reason, the experiments for the NC cohort were conducted in 2 weeks. N/D: not determined.

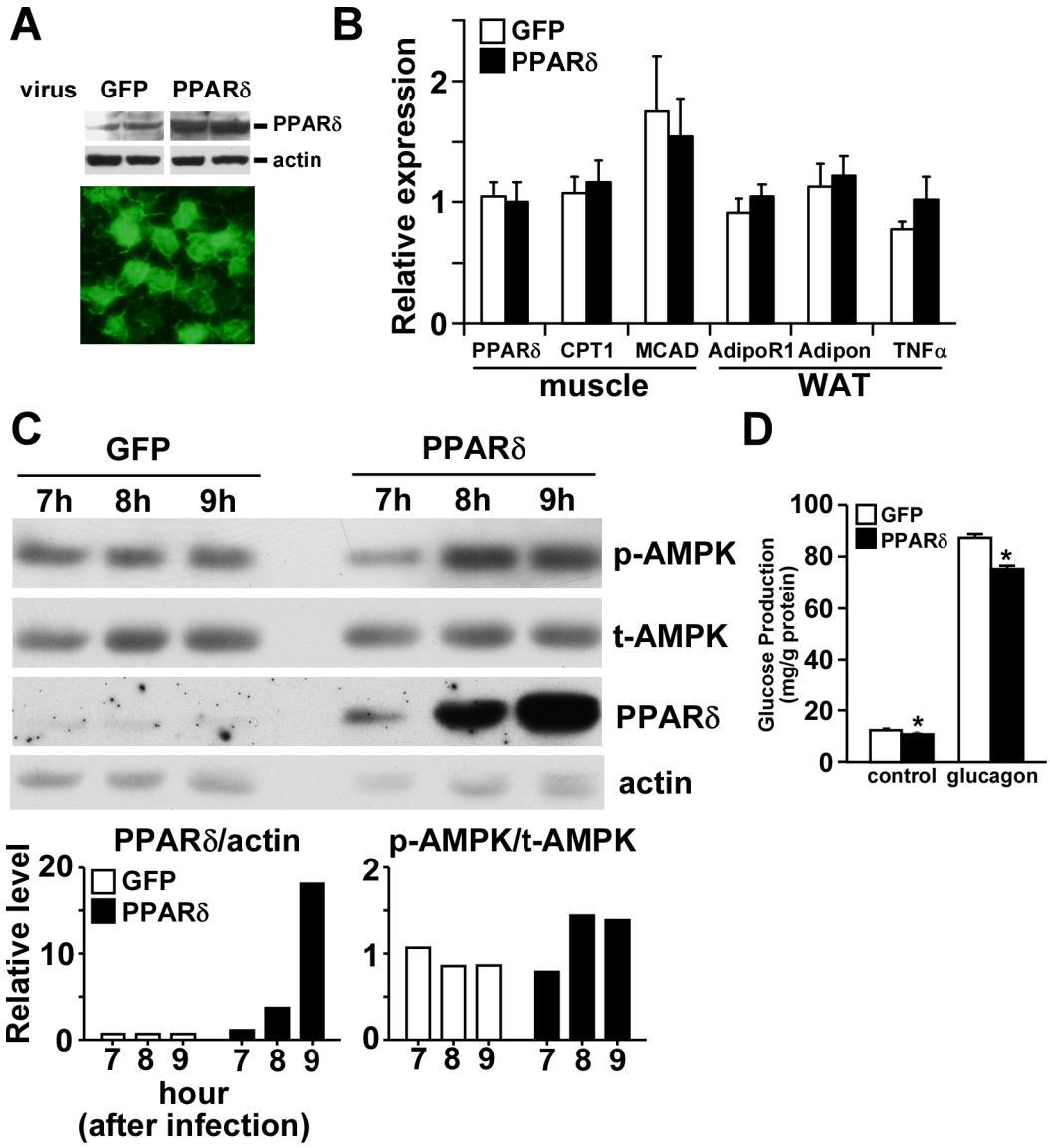

Figure 2.2. Liver-specific PPAR expression through adenoviral gene delivery. **A**, Adenoviral mediated PPARδ expression in the liver. High fat fed C57BL/6 male mice were injected with adenoviral GFP or PPARδ through the tail vein. Liver samples were harvested 3 days later to determine infection efficiency by GFP signal (lower panel) or expression levels by Western blotting (upper panel). **B**, Gene expression analyses of muscle and white adipose tissue (WAT) samples from control (GFP) or PPARδ virus injected mice (n=7) by Q-PCR. CPT1: carnitine palmitoyl-coA transferase 1; MCAD:

(**Figure 2.2. Continued**) medium chain acyl-CoA dehydrogenase.Adipon: adiponectin; AdipoR1: adiponectin receptor 1. **C**. Assessment of adenoviral mediated PPARδ expression in primary hepatocytes by Western blotting. adPPARδ protein could be detected 7 hours after infection and reached the maximal level by 9 hours (26-fold over endogenous protein). The effect of AMPK activation could be observed with a 6-fold increase in PPARδ protein (8 hours). Lower panel: quantification of Western blot signal using ImageJ. **D**. PPARδ over-expression in primary hepatocytes reduces both basal (control) and glucagon-induced glucose production. adGFP or adPPARδ infected hepatocytes were incubated ± 10 μg/ml glucagon for 5 hr, followed by the glucose production assay for 2 hr. *$p<0.05$.

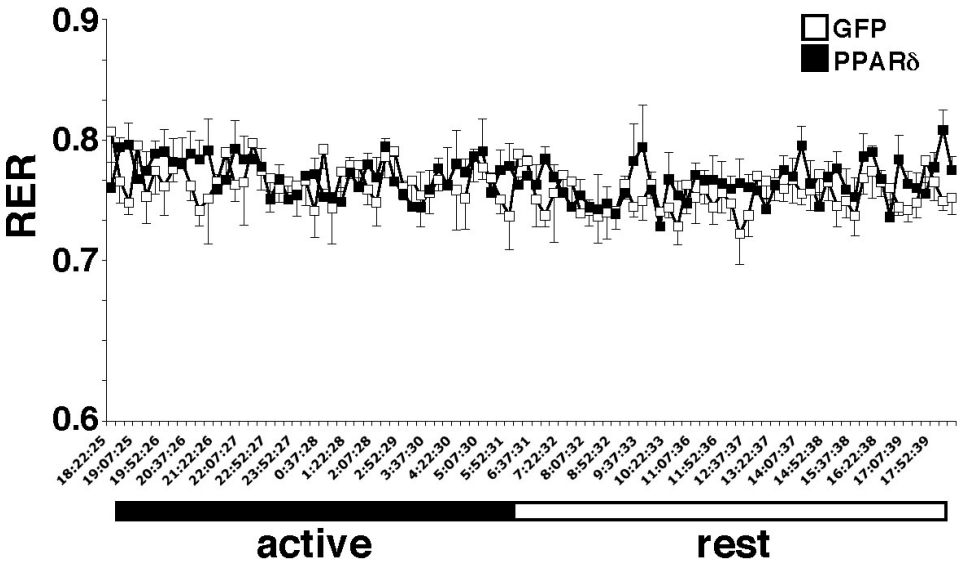

Figure 2.3. Metabolic cage study and respiratory exchange ratio (RER). High fat fed C57BL/6 male mice were injected with adenoviral GFP or PPARδ through the tail vein. 3 days after viral injection, mice (n=5) were placed in metabolic cages for 2 days. Data were collected for the second day over a period of 24 hours to determine the respiratory exchange ratio (RER=VCO_2/VO_2). Active: RER during the dark cycle; Rest: RER during the light cycle.

PPARδ regulates hepatic glucose utilization

The liver utilizes excess glucose for glycogen and lipid synthesis during feeding. To further probe the function of PPARδ activation in the liver at the fed state without the effects contributed by the high fat diet, adenoviral mediated PPARδ expression was conducted in a cohort of 3 months old, lean C57BL/6 mice and liver samples were collected under ad libitum feeding condition. Histological and quantitative studies demonstrated that increased glycogen and triglyceride contents were also evident in livers of chow fed adPPARδ mice (Figure 2.4A and 2.4B). In concert, we found elevated protein levels of glycogen synthase (GS) and ACC (Figure 2.4C). Under *ad libitum* feeding, only PK, ACC1 and SCD1 were significantly induced in adPPARδ livers (Figure 2.4D), which was not unexpected, as genes such as GK and PEPCK are also regulated by insulin at the fed state. Hepatic PPARδ expression also reduced fasting glucose levels in these animals (GFP: 117±3.34; PPARδ: 91.75±9.39, $P<0.05$, Table 2.1). However, chow fed control and adPPARδ mice performed similarly in GTT and ITT and there was no statistical difference in feeding glucose or triglyceride concentrations (data not shown). To determine whether the modulation of hepatic glucose metabolism is cell autonomous, we performed metabolic tracer studies in isolated primary hepatocytes. GFP or PPARδ virus infected hepatocytes were labeled with ^{14}C-glucose to trace glucose utilization for glycogen synthesis and oxidation as well as lipogenesis without or with insulin stimulation. Insulin-stimulated ^{14}C-glucose incorporation into glycogen (Figure 2.5A) and fatty acids (Figure 2.5B) were increased in adenoviral PPARδ

infected hepatocytes. In addition, insulin stimulated glucose oxidation determined by $^{14}CO_2$ production was also enhanced in these cells (Figure 2.5C), whereas basal fatty acid β-oxidation was reduced (Figure 2.5D). The increased glucose oxidation and decreased fatty acid catabolism is consistent with the RER result (Figure 2.1A). PPARδ over-expression in hepatocytes increased the expression of GK, GLUT2, FAS, ACC1 and PGC-1β (Figure 2.5E). To validate gene regulation by endogenous PPARδ and determine immediate targets, we treated primary hepatocytes from wild type or PPARδ-/- livers with a PPARδ ligand, GW501516, for 6 hours and found that ACC1, SCD1 and PGC-1β were up-regulated in a PPARδ-dependent manner, while GK, GLUT2 and FAS were unchanged (Figure 2.5F and data not shown). These data suggest that PPARδ over-expression is sufficient to drive target gene expression, likely due to the presence of endogenous ligands. In addition, PPARδ activation enhances hepatic glucose utilization through direct and indirect transcription regulation.

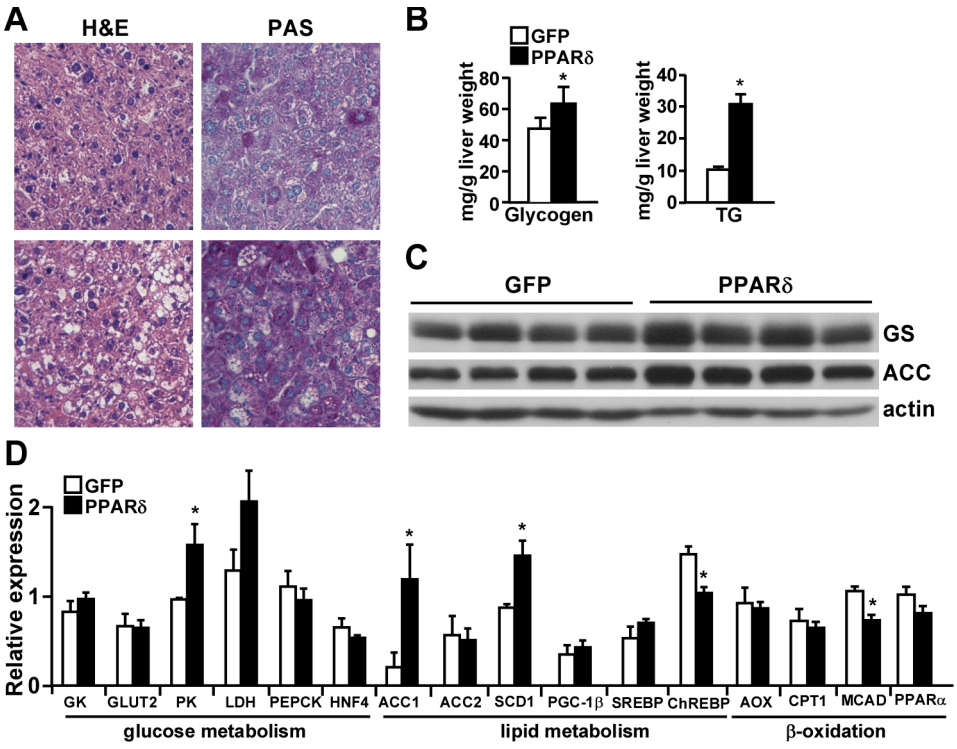

Figure 2.4. Assessment of the effect of hepatic PPARδ expression on glycogen synthesis and lipogenesis in chow fed mice. **A** and **B**, Histological, glycogen and lipid analyses of liver samples from GFP and PPARδ adenovirus injected mice on a chow diet. Liver samples were collected from ad libitum fed animals 2 weeks following virus injection. H&E and PAS (counter stained with hematoxylin) staining (**A**) as well as enzymatic assays (**B**) were conducted to determine glycogen and triglyceride (TG) content. **C**, Levels of liver glycogen synthase (GS) and acetyl co-A carboxylase (ACC) determined by Western blotting. Samples were collected from 4 individual animals from GFP and PPARδ adenovirus injected mice. Actin was included as the loading control. **D**, Hepatic gene expression determined by RT qPCR. Liver samples were harvested from control (GFP) or adPPARδ (PPARδ) mice under *ad libitum* feeding condition.*p<0.05.

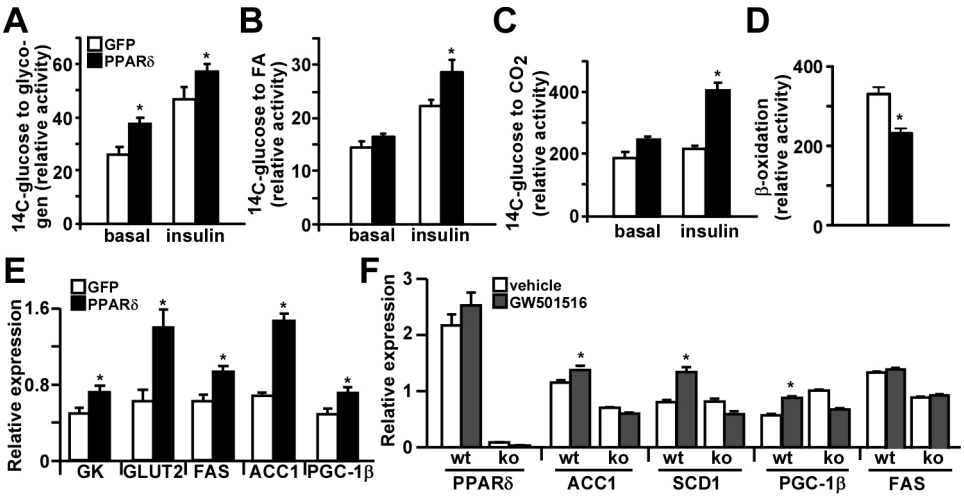

Figure 2.5. PPARδ increases glucose utilization in primary hepatocytes. **A**-**C**, PPARδ increases glucose flux to glycogen synthesis, lipogenesis and glycolysis determined by radioactive tracers. Hepatocytes infected with GFP or PPARδ virus were labeled with ^{14}C-glucose without or with 100 nM insulin. The conversion of radioactive glucose to glycogen, fatty acid and CO_2 (to estimate glycolysis) was determined and normalized to protein content. **D**, Fatty acid β-oxidation assay determined by ^{3}H-palmitate. **E**, The expression of glucokinase (GK), GLUT2 and and lipogenic genes is up-regulated in hepatocytes infected with adenoviral PPARδ. Gene expression was determined by RT qPCR 48 hours post-infection. **F**, Assessment of target gene regulation by endogenous PPARδ. Primary hepatocytes from wild type (wt) and liver-specific PPARδ-/- (ko) mice were given 0.1 μM GW501516 for 6 hours and gene expression was examined by RT qPCR. *p<0.05.

PPARδ increases monounsaturated fatty acid pools

Fatty acids have been shown to serve as signaling molecules, which could exert beneficial (e.g., lipokines) or detrimental (e.g., lipotoxicity) metabolic outcomes [1, 7]. To examine the effect of PPARδ regulated lipogenic program on lipid compositions, hepatic fatty acids/triglycerides were analyzed. adPPARδ livers contained less saturated fatty acids, notably C16:0, in both normal chow and high fat fed cohorts (Figure 2.6A and 2.6B). In contrast, the concentration of C18:1 (oleic acid) was increased. In addition, the ratios of MUFAs to saturated fatty acids were increased in livers expressing PPARδ. Previous work has demonstrated that C18 MUFAs are strong activators of PPARδ [35]. Indeed, lipid extracts from adPPARδ livers exerted a stronger PPARδ-activating activity than control lipids (Figure 2.7A). SCD1 catalyzes the conversion of saturated fatty acids to unsaturated fatty acids. We found that the activity of a 5.3 kb mouse SCD1 promoter could be induced by PPARδ activation and this effect was lost in the proximal 1.5 kb promoter region (Figure 2.6C). This result was consistent with the up-regulation of SCD1 in adPPARδ livers. To determine whether the enhanced lipogenesis led to an increase in VLDL production, circulating triglyceride concentrations were determined after administration of a lipoprotein lipase inhibitor, Triton WR1339, in control and adPPARδ mice. There was no difference in the rate of TG release by the liver between the two groups (Figure 2.6D), indicating that PPARδ does not affect the steady state VLDL-triglyceride production.

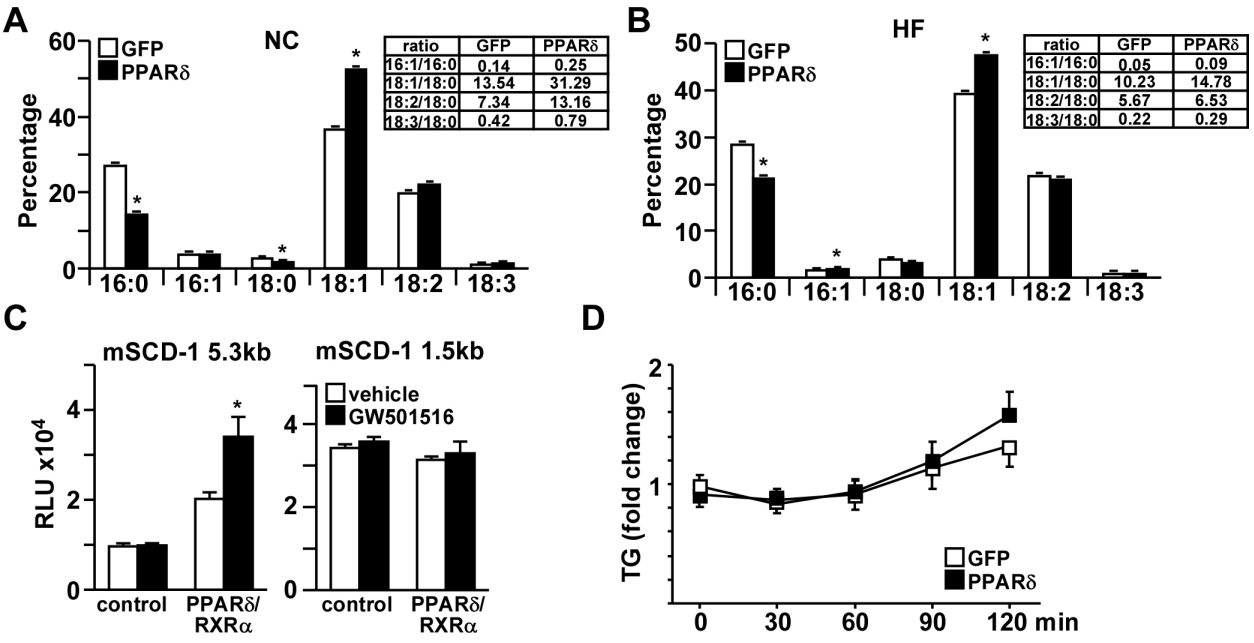

Figure 2.6. Increased monounsaturated to saturated fatty acid ratios in adPPARδ livers. **A** and **B**, Triglycderides were isolated from GFP or PPARδ adenovirus infected livers of normal chow (NC) or high fat diet (HF) fed mice. Fatty acid compositions in triglycerides were determined by gas-liquid chromatography. The ratios of monounsaturated to saturated fatty acids were shown in the tables. **C**, PPARδ regulates SCD1 promoter. Luciferase reporters driven by 5.3 kb or 1.5kb mouse SCD1 promoter were co-transfected with expression vectors for PPARδ/RXRα into HepG2 cells, together with a β-galactosidase reporter internal control ± GW501516 (0.1 μM, PPARδ agonist) for 24 hours. The reporter luciferase activity was normalized to β-galactosidase activity to obtain relative luciferase unit (RLU). **D**. Triglyceride (TG) production determined by administration of a lipoprotein lipase inhibitor, Triton WR1339. Serum TG concentrations were measured at the indicated time course after Triton injection. *$p<0.05$.

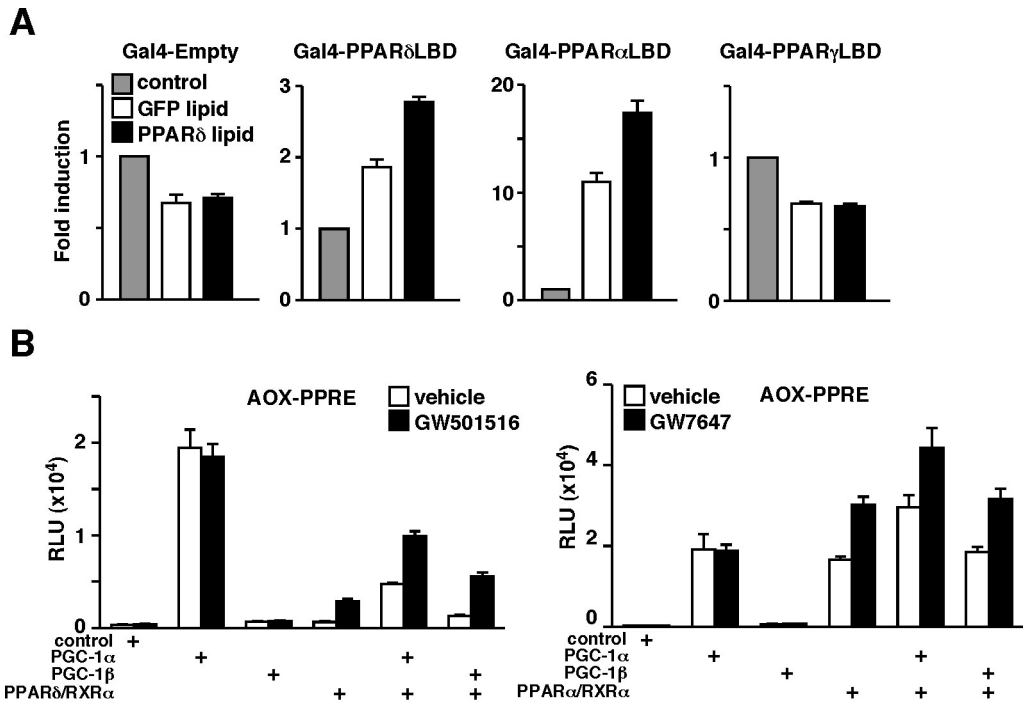

Figure 2.7. Differential PPARδ and PPARα activities in the liver. **A**, PPARδ facilitates the production of lipid ligands. Primary hepatocytes were transfected with a luciferase reporter driven by sv40 promoter containing Gal4 binding sites (4 copies), expression vectors for Gal4 (Gal4 DNA binding domain), Gal4-PPARδLBD (Gal4DBD-PPARδ ligand binding domain), Gal4-PPARαLBD (ligand binding domain) or Gal4-PPARα LBD, together with a renilla luciferase internal control. Lipids were extracted from GFP (empty bars) or PPARδ (black bars) adenovirus infected livers from the normal chow cohort. ~50 μM triglycerides (BSA bound) were given to transfected primary hepatocytes cultured in lipoprotein deficient FBS + 4 μg/ml lipoprotein lipase (to release fatty acids) for 24 hours. **B**, Functional interaction between PPARδ/PGC-1β and PPARα/PGC-1α on a PPRE-containing heterologous promoter. A luciferase report driven by tk promoter with 3-copy PPREs was co-transfected with combinations of expression vectors for

(**Figure 2.7. Continued**) PPARδ/RXRα, PGC-1β and PGC-1α into HepG2 cells, together with a β- galactosidase reporter internal control ± GW501516 (0.1 μM, PPARδ agonist) or GW7647 (0.1 μM, PPARα agonist) for 24 hours. The luciferase activity was normalized to β-galactosidase activity to obtain relative luciferase unit (RLU).

Transcriptional regulation of hepatic gene expression by PPARδ

PGC-1β has been shown to be induced by fatty acids and regulate certain lipogenic genes by serving as a co-activator for SREBP-1c [34]. Up-regulation of PGC-1β in adPPARδ livers is expected to increase lipid synthesis. To investigate the molecular mechanism through which PPARδ regulates hepatic gene expression and the potential involvement of PGC-1β in this process, reporters driven by promoters of potential target genes were constructed and their activities were examined in HepG2 cells by transient transfection assays. The activities of both 2 kb and 0.3 kb mouse GK promoters could be induced by PPARδ and RXRα co-transfection, which were further enhanced by PGC-1β (Figure 2.8A and 2.8B). Ligand activation had additional effects only in the presence of PGC-1β. PPARδ/RXRα up-regulated human ACC2 promoter I in a ligand-dependent manner, as described previously [28] (Figure 2.8E). Similarly, this ligand activity was substantially amplified by PGC-1β co-activation. In contrast, PPARδ had no effect on 1.3 kb human ACC2 promoter II and 3kb mouse FAS promoter, both of which are known SREBP-1c targets [36]. PGC-1β was able to increase SREBP-1c activities on these gene promoters (Figure 2.8C and 2.8D). PGC-1α has also been shown to co-activate PPARδ, particularly in muscle. Unexpectedly, PGC-1α co-transfection reduced PPARδ effects on ACC2 promoter I (Figure 2.8E, left panel). In contrast, it strongly potentiated PPARα activation of MCAD promoter (Figure 2.8E, right panel). The preferential functional interaction of PPARδ/PGC-1β and PPARα/PGC-1α could also be observed using a reporter containing 3 copies of AOX PPRE (Figure

2.7B). Collectively, these data suggest that PGC-1β is a co-activator of PPARδ in the liver and support the notion that PPARδ regulates hepatic gene expression through direct and indirect mechanisms.

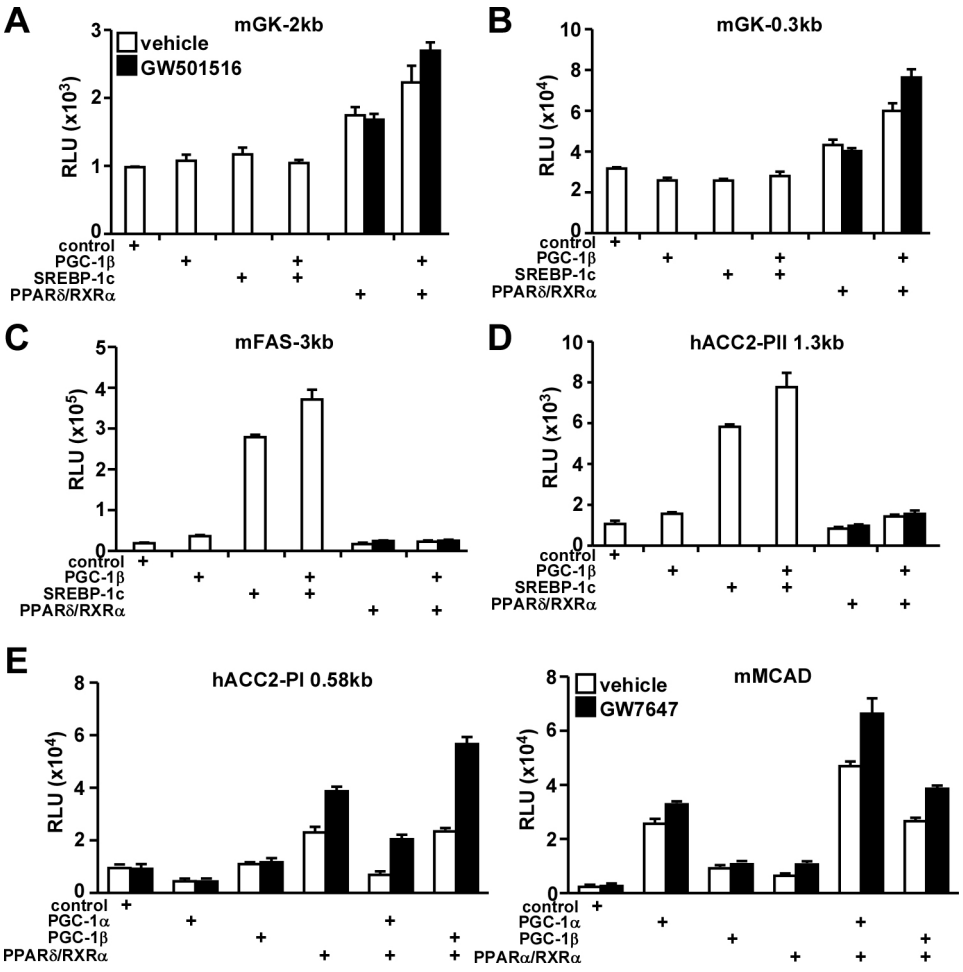

Figure 2.8. Direct and indirect transcriptional mechanisms by PPARδ in the control of hepatic gene expression. **A**-**E**, promoter analyses to determine PPARδ direct target genes. Promoter regions of potential target genes were cloned into a luciferase reporter. The resulting constructs were co-transfected with combinations of expression vectors for PPARδ/RXRα, SREBP-1c, PGC-1β and PGC-1α (for **E** only) into HepG2 cells, together with a β-galactosidase reporter internal control. PPARδ/RXRα transfected cells were cultured in the presence or absence of GW501516 (0.1 μM, PPARδ agonist) for 24 hours. The reporter luciferase activity was normalized to β-galactosidase activity to obtain relative luciferase unit (RLU). mGK-2kb: mouse GK 2 kb promoter; hACC2-PI

(**Figure 2.8. Continued**) and PII: human ACC2 promoter I and II; mFAS: mouse FAS promoter; mMCAD: mouse MCAD promoter.

adPPARδ mice are protected from lipotoxicity

The induced lipogenic program in adPPARδ mice raised the concern whether increased lipid deposition caused hepatic pathology. Liver damage was assessed by serum levels of liver alanine aminotransferase (ALT) and aspartate aminotransferase (AST), which leak out to the circulation with liver injury. Intriguingly, both ALT and AST were reduced in adPPARδ mice (Figure 2.9A). Consistent with this finding, the activity of the stress signaling JNK, determined by the level of phospho-JNK, was reduced in adPPARδ livers, whereas that of phospho-Erk, another member of the mitogen-activated protein kinase, was not affected (Figure 2.9B). These results indicate that PPARδ may reduce lipotoxicity thereby improving metabolic homeostasis. In fact, when treated with albumin-bound palmitic acid (C16:0), PPARδ adenovirus infected hepatocytes had lower JNK phosphorylation and higher insulin-stimulated Akt phosphorylation, compared to control cells (Figure 2.9C). There was an increase in triglyceride accumulation in adPPARδ hepatocytes (Figure 2.9C). Free fatty acids have also been shown to induce chronic inflammation [2]. We therefore examined the expression of genes in inflammatory response and found that pro-inflammatory cytokines/chemokines, including IL-1β, TNFα, IFNγ and MCP-1 were all down-regulated in adPPARδ livers, compared to GFP infected livers from chow fed mice (Figure 2.9D). The expression of F4/80, a pan-macrophage marker, was also reduced. In contrast, markers for anti-inflammatory, alternative macrophage activation [37], such as Mgl1 and MRC1, were up-regulated in adPPARδ livers. The difference in inflammatory gene

expression was less evident in the high fat fed cohort, although there was a trend toward a reduction in TNFα ($p=0.08$) and IFNγ in adPPARδ livers. These results indicate that PPARδ-controlled lipogenic program may protect the liver against lipotoxicity.

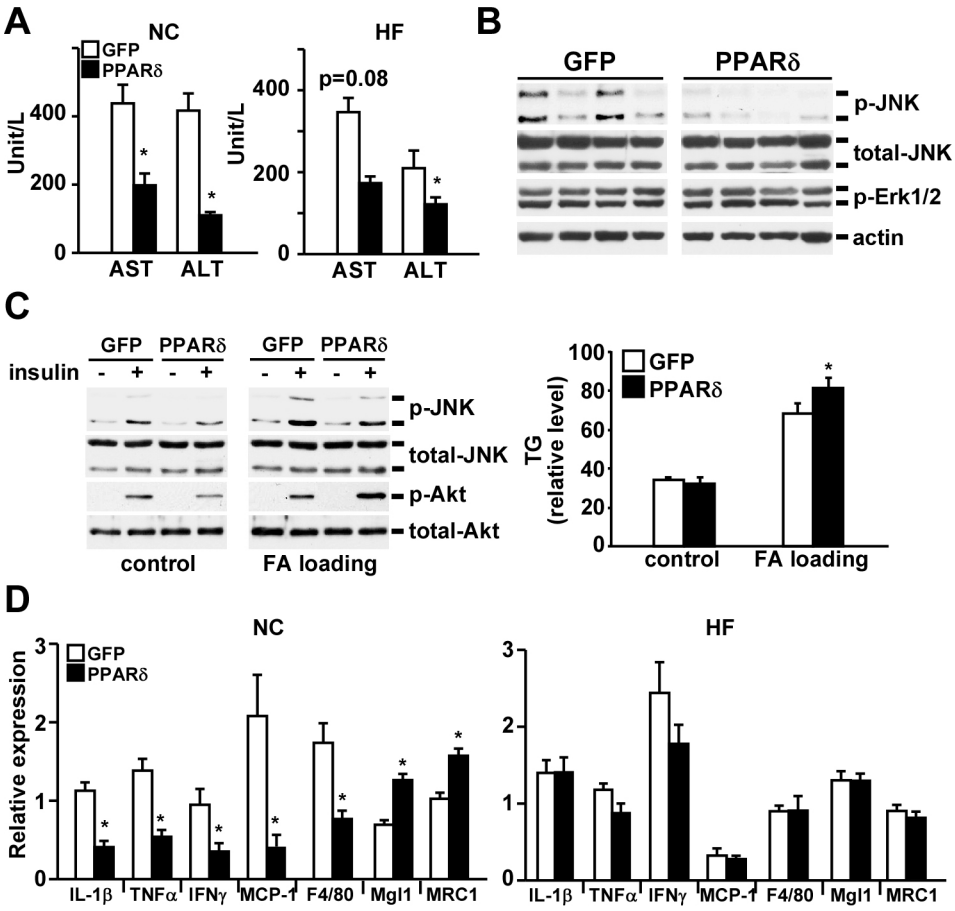

Figure 2.9. Reduced stress signaling and inflammatory gene expression in the liver of adPPARδ mice. **A**, Assessment of liver damage in GFP or PPARδ adenovirus infected mice on normal chow (NC) or high fat diet (HF) diets by serum AST and ALT activities. **B**, Western blot analyses demonstrating decreased JNK activity in livers of adPPARδ mice. Liver lysates were harvested from 4 individual mice/group of the high fat fed cohort. p-JNK: phospho-JNK; t-JNK: total JNK; p-Erk1/2: phospho-Erk1/2. **C**, PPARδ inhibits phospho-JNK and increases insulin-stimulated phospho-Akt in primary hepatocytes. Hepatocytes were infected with GFP or PPARδ virus for 24 hours in William's E, 5% FBS. Cells were washed and maintained in the same medium ± 100 μM palmitate (albumin-bound) overnight. Hepatocytes were serum starved for 2 hours,

(**Figure 2.9. Continued**) followed by insulin stimulation (100 nM) for 30 min. Left panel: JNK and Akt signaling was determined by Western blotting in GFP or PPARδ adenovirus infected heaptocytes without (control) or with fatty acid treatment (FA loading). Right panel: normalized cellular triglyceride content. **D**, PPARδ suppresses the expression of pro-inflammatory genes. Liver samples were harvested from control (GFP) or adPPARδ (PPARδ) mice on normal chow (NC) or high fat (HF) diets and gene expression was determined by RT qPCR. *$p<0.05$.

PPARδ activates AMPK in the liver

As mentioned earlier, AMPK plays a major role in reducing glucose production and has been linked to PPARδ activity [30]. Expression analyses showed that PPARδ suppressed genes encoding gluconeogenesis (Figure 2.1E). We sought to determine whether the activity of PPARδ in increasing glycogen storage (which decreases energy substrate availability) and lipogenesis (which consumes energy) might alter the energetic status thereby exerting a secondary effect on AMPK activation. Western blot analyses demonstrated that levels of phospho-AMPK, which is indicative of AMPK activity, were higher in liver lysates of adPPARδ mice (Figure 2.10A). It is known that AMPK can be activated by raising AMP coupled with falling ATP or by adiponectin signaling. To determine whether the increased AMPK activation was accompanied by changes in AMP and/or ATP levels, liver adenine nucleotide concentrations were measured by HPLC (Figure 2.10B). Consistent with the increase in AMPK activity, levels of ATP were decreased ($p<0.05$) and AMP were increased ($p=0.08$) in livers of adPPARδ mice compared to those of control animals. ADP and total adenine nucleotide remained unchanged. Interestingly, we also found that adPPARδ livers expressed higher levels of adiponectin receptor 2 (adipoR2), which activates AMPK through the adiponectin signaling pathway [10, 11] (Figure 2.10C). We did not detect any difference in circulating adiponectin concentrations (Figure 2.10D), suggesting that PPARδ may increase the response to adiponectin through up-regulation of adipoR2 in the liver. To further demonstrate the increased AMPK activity was mediated by hepatic PPARδ

expression, AMPK phosphorylation was examined in primary hepatocytes infected with GFP or PPARδ adenovirus. The level of phospho-AMPK was higher in adenoviral PPARδ infected hepatocytes (Figure 2.10E). Furthermore, metformin-induced AMPK activation was further enhanced in these cells, compared to GFP infected hepatocytes (Figure 2.10F). To probe whether PPARδ-mediated AMPK activation modulates glucose metabolism, glucose production was assessed in isolated hepatocytes. The basal glucose production rate was lower in adenoviral PPARδ infected hepatocytes compared to GFP infected cells (Figure 2.10G). A similar suppressive effect of adPPARδ was observed in glucagon-stimulated gluconeogenesis (Figure 2.2D). The ability of adPPARδ to inhibit basal glucose production was abolished by addition of compound C, an AMPK inhibitor (Figure 2.10G), supporting the hypothesis that PPARδ could indirectly activate AMPK through limiting substrate availability, which contributes to the glucose lowering effect of PPARδ.

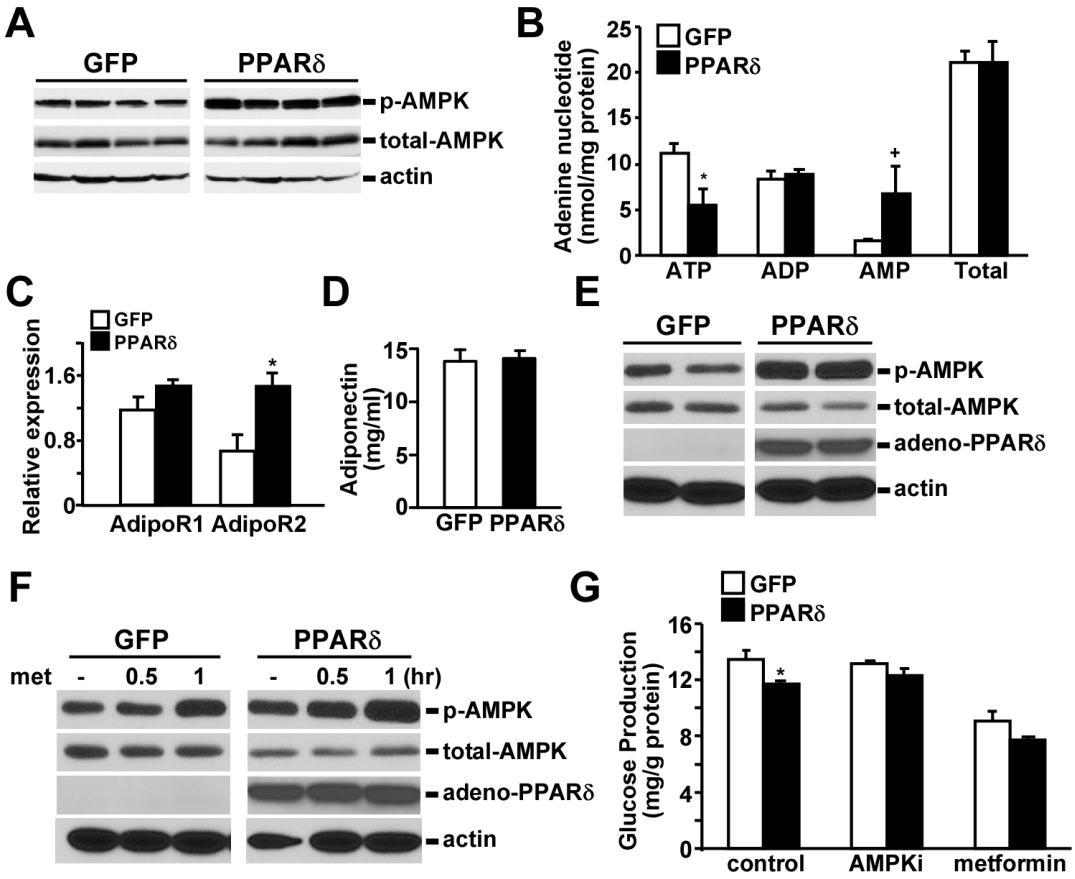

Figure 2.10. Increased hepatic AMPK activity in adPPARδ mice. **A**, Western blot analyses showing increased phospho-AMPK (p-AMPK, Thr-172) in adPPARδ livers. Liver lysates were collected from 4 individual GFP or adPPARδ mice. **B**, Adenine nucleotide concentrations of liver lysates from control or adPPARδ mice (n=4) determined by HPLC assays. $^{*}p<0.05$; $^{\dagger}p=0.08$. **C**, RT qPCR analyses demonstrating up-regulation of adiponectin receptor 2 (AdipoR2) in adPPARδ livers. The difference in adiponectin receptor 1 (AdipoR1) expression was not significant. **D**, Circulating adiponectin concentrations in control (GFP) and adPPARδ mice determined by ELISA. **E** and **F**, PPARδ expression increases AMPK phosphorylation. Hepatocytes were infected with GFP or PPARδ virus for 24 hours in William's E, 5% FBS. Cells were washed and cultured in DMEM for 2 hours. In **E**, hepatocytes were incubated in DMEM

(**Figure 2.10. Continued**) for 4 more hours before harvesting. Results from two representative samples were shown. In **F**, hepatocytes were treated with metformin (met, 2 mM) and harvested at different time points. The basal phospho-AMPK was higher at 6-hour (**E**) than 3-hour (**F**, minus metformin) after replacing medium to DMEM in PPARδ expressing hepatocytes. **G**, PPARδ reduces glucose production through AMPK activation in primary hepatocytes. Hepatocytes were treated as described above. Cells were then cultured in glucose free DMEM containing 1 mM pyruvate and 10 mM lactate, without or with 20 μM compound C (AMPKi: AMPK inhibitor) or 2 mM metformin (AMPK activator) for 2 hours. Supernatant was collected to determine glucose concentration. Metformin was included as a control for AMPK mediated suppression of glucose production. *$p<0.05$.

Discussion

PPARδ is known for its role in regulating oxidative metabolism, particularly in the muscle [27, 30]. Previous studies have demonstrated that pharmacological activation of PPARδ lowered glucose level and reduced hepatic glucose production [25, 28]. However, whether the liver is a major site of PPARδ action has not been explored. In this study, we employ adenoviral mediated gene delivery to target PPARδ to the liver and show that PPARδ regulates glucose utilization for glycogen synthesis and lipogenesis, resulting in a secondary effect of AMPK activation. The combined actions effectively lower glucose levels in both chow and high fat fed mice. The lipogenic activity of PPARδ increases the production of MUFAs, which are activators of PPARδ, and may protect the liver from free fatty acid-mediated lipotoxicity and inflammatory response. The current work unveils a function for PPARδ in the control of hepatic energy substrate homeostasis.

In response to substrate abundance, such as at the fed state, glucose is stored as glycogen and to a lesser extent, used for fatty acid synthesis in the liver. GK plays an important role in this process, since glucose entering the liver through GLUT2 is first phosphorylated by GK. The resulting product, glucose 6-phosphate, can then be utilized for glycogen synthesis, glycolysis and lipogenesis [13]. The level of GK is normally low during fasting and induced by feeding. Previous studies showed that hepatic GK over-expression increased glucose flux into glycogen synthesis, glucose oxidation and

lipogenesis, resulting in lowered glucose levels [16-18]. This suggests that in addition to regulating glucose production, the liver has the capacity to modulate glycemia through glucose utilization mechanisms. Interestingly, many of the effects observed in adPPARδ mice mimic adenoviral GK over-expression [18], including reduced fasting glucose concentrations and increased hepatic glucose utilization (glycogen storage, glycolysis and lipogenesis). Therefore, the glucose lowering effect of adPPARδ is in part driven by increased glucose usage through GK up-regulation and *de novo* lipogenesis independent of insulin concentrations, although the insulin action on glucose utilization is likely amplified in adPPARδ mice. Our data show that increased hepatic PPARδ expression sustains GK levels leading to glycogen accumulation even after overnight fast. PPARδ also up-regulates fatty acid synthesis program as well as the lipogenic transcription factor and co-activator, SREBP-1c and PGC-1β, resulting in increased lipid content. There is no significant difference in the expression of GK and some lipogenic genes between ad libitum fed adPPARδ and control mice. Of note, the gene expression pattern at the fed state could be confounded by the timing of eating of individual animals before tissue collection. Nevertheless, glucose tracer experiments in primary hepatocytes support the hypothesis that PPARδ regulates glucose utilization, as evident from increased radioactive tracers in glycogen, fatty acid and CO_2, the product of glycolysis. This functional outcome is mediated by direct and indirect transcriptional mechanisms. Promoter analyses suggest that PGC-1β co-activates PPARδ to increase ACC2 promoter I activity, while PGC-1β/SREBP-1c up-regulate the activities of reports driven by FAS and ACC promoter II. The regulation of GK is more complex. PPARδ

expression up-regulated GK in a ligand-independent manner. However, PGC-1β is able to increase PPARδ-controlled GK promoter activity in the absence and presence of ligand. It is unclear how PPARδ induces PGC-1β and SREBP-1c. The increased fatty acid production may lead to PGC-1β up-regulation [34]. Although PGC-1α has also been shown to co-activate PPARδ, our data suggest a preferential interaction between PPARδ/PGC-1β and PPARα/PGC-1α in the liver, which may explain the functional difference in fatty acid synthesis and oxidation, respectively. Previous work has demonstrated that the expression of PPARδ is up-regulation at the dark cycle, whereas PPARα is induced at the light cycle [38]. It appears that the specificity of these two closely related receptors is determined by their temporal expression and co-factor interaction.

The lipogenic activity of PPARδ raises the concern whether PPARδ activation is associated with steatosis or steatohepatitis. Interestingly, adPPARδ mice either on normal chow or high fat diet seem to have improved liver integrity determined by serum ALT and AST assays. The stress signaling JNK and inflammatory markers are also suppressed in adPPARδ livers. Free fatty acids are known to cause lipotoxicity, including induction of inflammatory response [2]. It is possible that by partitioning fatty acids for triglyceride synthesis, PPARδ activation protects the liver from free fatty acid-mediated damage. In fact, adenoviral mediated PPARδ expression in primary hepatocytes suppresses fatty acid-induced JNK activation and at the same time, increases insulin stimulated Akt phosphorylation, which is consistent with the improved ITT in high fat fed adPPARδ mice. In addition, certain MUFAs, such as C16:1n7

(palmitoleate) and C18:1n7 (oleic acid), have been shown to alleviate endoplasmic reticulum (ER) stress induced by saturated fatty acids and improve metabolic homeostasis [7, 39]. These MUFAs are immediate products of SCD1 [40, 41]. We find that adPPARδ livers contain more MUFAs and less saturated fatty acids on both chow and high fat diets, which is accompanied by increased SCD1 expression. Therefore, PPARδ may function to direct free fatty acid for storage and/or to convert toxic lipids to less toxic or even beneficial lipid species, thereby protecting livers from lipotoxicity. Additional work will be required to determine the role of SCD1 in mediating the protective effect.

PPARδ has been linked to AMPK activation [30]. The underlying mechanism remains elusive. AMPK has been shown to suppress lipogenesis and glycogen synthesis [10, 42]. At the first glance, it seems paradoxical that PPARδ-expressing livers have more glycogen and lipid accumulation and at the same time show increased AMPK activity. Our data suggest that PPARδ limits substrate availability through the control of glucose utilization for glycogen store and lipogenesis, which consumes energy. Together with reduced β-oxidation, these changes lead to lowered ATP/increased AMP and a secondary effect of AMPK activation, which further contributes to the glucose lowering effect observed in adPPARδ mice. In support of this notion, PPARδ expression in primary hepatocytes increases the level of phospho-AMPK. Inhibition of AMPK activity reverts the effect of reduced basal glucose production in adenoviral PPARδ infected hepatocytes. In addition, we observed increased AdipoR2 expression in adPPARδ livers, which could mediate adiponectin signaling thereby

increasing AMPK activity. Therefore, AMPK activation may serve as a feedback mechanism and explain why long-term PPARδ ligand treatment does not cause severe hepatic lipid accumulation [25, 27]. Of note, although adenoviral mediated over-expression has been useful for identifying hepatic functions for several metabolic regulators [43, 44], whether pharmacological activation of PPARδ could activate AMPK to the same extent as acute activation described in the current study remains to be determined.

Immune cells and inflammatory response have emerged as integral components of metabolic diseases [45]. JNK, a major pro-inflammatory signaling molecule, phosphorylates insulin receptor substrate-1 (IRS-1) and prevents insulin-mediated activation of phosphatidylinositol 3-kinase and its downstream effector Akt [2, 4]. The current work demonstrates that PPARδ suppresses inflammation in the liver. It has been demonstrated that oleic acid (C18:1) or synthetic ligands activate macrophage PPARδ to turn on anti-inflammatory, alternative activation [31, 32]. It is possible that hepatic PPARδ produces lipid lignads (MUFAs), which in turn activate macrophage (or Kupffer cells in the liver) PPARδ to modulate immune response. In fact, the expression of pro-inflammatory markers, such as TNFα and IFNγ, is down-regulated, while alternative activation markers, such as Mgl1 and MRC1, are induced in chow fed adPPARδ livers. The reduction in pro-inflammatory gene expression is less evident on high fat diet, likely due to the fact that high fat feeding also induces a strong inflammatory response in non-hepatic cells (e.g., immune cells) [44, 46]. These observations indicate that PPARδ functions as a nuclear sensor of dietary fats capable of modulating immune response

through regulation of metabolic programs. Despite the potential beneficial effects identified in this work, since fatty liver is often associated with type 2 diabetes, the use of PPARδ agonists to improve glucose handling may worsen the condition of steatosis. Nevertheless, results from the current study provide valuable information for designing drugs that target PPARδ for treating metabolic diseases.

Materials and Methods

Animal experiments

C57BL/6 mice (14 age matched, 8 weeks old males from the Jackson Laboratory) were challenged with a high-fat, high-carbohydrate diet (F3282, Bio-Serv, Frenchtown, NJ) for 10 weeks. They were then transduced with purified adenovirus via tail vein injection (n=7 for both GFP and PPARδ adenovirus). Adenoviral expression cassettes were constructed in the pShuttle-IRES-hrGFP vector and amplified in AD293 cells (Stratagene, La Jolla, CA). 100 μl of 5 x 10^{10} pfu/ml virus was injected into each mouse. Liver-specific PPARδ-/- mice (in C57BL/6 background) was generated by crossing PPARδ f/f mice to albumin-Cre transgenic mice. Mice were fasted overnight for serum collection, tissue harvesting and glucose tolerance test (GTT). Insulin tolerance test (ITT) was performed after a 6 hour fast. A similar metabolic phenotype was observed in two additional cohorts (n=5), which were used for metabolic cage studies and to determine adenine nucleotide concentrations. The experiment was repeated in 3 months old chow fed mice to evaluate gene expression at the fed state (n=4/group).

Statistics analyses were performed using Student's t-Test (2-tailed), unless otherwise indicated. Values were presented as means±SEM. Significance was established at $p<0.05$. Animal studies were approved by the Harvard Medical Area Standing Committee on Animals.

Metabolic studies

Metabolic cage studies were conducted in a Comprehensive Lab Animal Monitoring System (Columbus Instruments, Columbus, OH). Mice were placed in metabolic cages for 2 days and data were collected at the beginning of the second dark (active) cycle for 24 hours. The respiratory exchange ratio was determined by the ratio of CO_2 produced (VCO_2) over O_2 consumed (VO_2). The values of RER during the dark (active) and light (rest) cycle were averaged (Figure 2.3). As mice were on high fat diet, RER was close to 0.7 throughout the day (RER=0.7 for fatty acid usage; RER=1 for glucose usage). For GTT 1.5 mg glucose/g body weight was injected into the peritoneum. Blood glucose was measured before and after injection at the indicated time points using the OneTouch glucose monitoring system (Lifescan, Milpitas, CA). ITT was conducted similarly (0.5 u insulin/kg body weight). To determine triglyceride production, mice were injected with Triton WR1339 (500 μg/g body weight) and blood was drawn via tail bleeding at different time points for triglyceride concentration measurement. Serum and hepatic triglyceride, non-esterified fatty acid, total cholesterol as well as serum ALT and AST were measured using commercial kits (Wako Chemicals

and ThermoDMA). Hepatic glycogen was determined as described [47]. Insulin and adiponectin were measured using ELISA kits (Linco, St. Charles, MO). Adenine nucleotides (ATP, ADP and AMP) were determined in perchloric acid extracts of freeze clamped tissues and normalized by protein concentration as described previously [48]. Hepatic fatty acid/triglyceride composition was determined by gas-liquid chromatography as described [40].

Histology, gene expression and signaling analysis

Liver samples were either cryo-preserved for GFP detection or fixed in formalin for H&E or PAS staining. All of the histology work was performed in the Dana Farber Research Pathology Cores, which provided preliminary histological assessment by a pathologist. SYBR green-based real-time quantitative PCR (RT qPCR) reactions were conducted as described [28], using 36B4 levels as loading controls to obtain relative expression levels. For Western blot analyses, tissue or cell lysates were prepared in a buffer containing protease and phosphatase inhibitors. Antibodies against AMPK, Akt, Erk and JNK were purchased from Cell Signaling and PPARδ and actin antibodies were from Santa Cruz. For reporter assays, the 2kb and 0.3kb mouse GK (liver-specific) as well as the 3 kb mouse FAS promoter fragment were cloned in the pGL3-basic vector (Promega). Human ACC2 promoters I and II (all in pGL3-basic) were as described previously [28]. The resulting reporter was co-transfected with expression vectors for PPARδ/RXRα, SREBP-1c, PGC-1α and PGC-1β, all under the control of a CMV

promoter, together with a β-galactosidase internal control in HepG2 cells. Cells were harvested 40-48 hours after transfection and GW501516 (0.1 μM) was treated for 24 hours. For endogenous gene regulation by PPARδ, primary hepatocytes were cultured in Williams' E medium with 5% lipoprotein deficient, dialyzed FBS supplemented with 100 nM insulin and treated with 0.1 μM GW501516 for 6 hours.

In vitro functional assays

Primary hepatocytes were isolated from 2-3-month old male C57BL/6 mice through portal vein perfusion with Blenzyme 3 (Roche, Indianapolis, IN) and cultured in Williams' E medium with 5% regular FBS. Hepatocytes were infected with GFP or PPARδ virus for 24 hours. Cells were washed and incubated with DMEM (low glucose) for two hours. To measure glucose flux to glycogen synthesis, lipogenesis and oxidation, hepatocytes transduced with GFP or PPARδ virus were labeled with 1 μCi/ml D-[^{14}C (U)]-glucose overnight with or without 100 nM insulin. Media was collected and cells lysed. For measuring glucose oxidation to CO_2, the medium was transferred to a 15 ml conical tube and 100 μl of 70% perchloric acid added. Filter paper pre-soaked in 1 M NaOH was then placed on the top of the tube to capture CO_2. Samples were incubated at 37°C overnight and the filters placed in scintillation vials to count radioactivity. Fatty acid oxidation was conducted by loading cells with ^{3}H-palmitate (albumin bound). The rate of β-oxidation was determined by measuring $^{3}H_2O$ produced in the supernatant. For glycogen synthesis from labeled glucose, cellular glycogen was

isolated and the radioactivity determined. Glucose conversion to extractable lipids (fatty acid/triglyceride) was measured as described [28]. For glucose production, hepatocytes were incubated for 2 hours in glucose free DMEM, containing 1 mM pyruvate and 10 mM lactate. Compound C (Calbiochem) and metformin (Sigma), an inhibitor and activator of AMPK, respectively, were added at the final concentration of 20 μM and 2 mM. The glucose content in the supernatant was measured using a glucose oxidase kit (Trinity Biotech). All values were normalized by protein contents. Statistical analysis for glucose production was performed using one-way ANOVA.

References

1. Qatanani, M. and M.A. Lazar, *Mechanisms of obesity-associated insulin resistance: many choices on the menu.* Genes Dev, 2007. **21**(12): p. 1443-55.

2. Song, M.J., et al., *Activation of Toll-like receptor 4 is associated with insulin resistance in adipocytes.* Biochem Biophys Res Commun, 2006. **346**(3): p. 739-45.

3. Haber, E.P., et al., *Pleiotropic effects of fatty acids on pancreatic beta-cells.* J Cell Physiol, 2003. **194**(1): p. 1-12.

4. Hirosumi, J., et al., *A central role for JNK in obesity and insulin resistance.* Nature, 2002. **420**(6913): p. 333-6.

5. Liu, L., et al., *Upregulation of myocellular DGAT1 augments triglyceride synthesis in skeletal muscle and protects against fat-induced insulin resistance.* J Clin Invest, 2007. **117**(6): p. 1679-89.

6. Schenk, S. and J.F. Horowitz, *Acute exercise increases triglyceride synthesis in skeletal muscle and prevents fatty acid-induced insulin resistance.* J Clin Invest, 2007. **117**(6): p. 1690-8.

7. Cao, H., et al., *Identification of a lipokine, a lipid hormone linking adipose tissue to systemic metabolism.* Cell, 2008. **134**(6): p. 933-44.

8. Staels, B., *Metformin and pioglitazone: Effectively treating insulin resistance.* Curr Med Res Opin, 2006. **22 Suppl 2**: p. S27-37.

9. Kahn, B.B., et al., *AMP-activated protein kinase: Ancient energy gauge provides clues to modern understanding of metabolism.* Cell metabolism, 2005. **1**(1): p. 15-25.

10. Yamauchi, T., et al., *Targeted disruption of AdipoR1 and AdipoR2 causes abrogation of adiponectin binding and metabolic actions.* Nat Med, 2007. **13**(3): p. 332-9.

11. Yamauchi, T., et al., *Adiponectin stimulates glucose utilization and fatty-acid oxidation by activating AMP-activated protein kinase.* Nat Med, 2002. **8**(11): p. 1288-95.

12. Pagliassotti, M.J. and A.D. Cherrington, *Regulation of net hepatic glucose uptake in vivo.* Annu Rev Physiol, 1992. **54**: p. 847-60.

13. Girard, J., P. Ferre, and F. Foufelle, *Mechanisms by which carbohydrates regulate expression of genes for glycolytic and lipogenic enzymes.* Annu Rev Nutr, 1997. **17**: p. 325-52.

14. Postic, C., M. Shiota, and M.A. Magnuson, *Cell-specific roles of glucokinase in glucose homeostasis.* Recent Prog Horm Res, 2001. **56**: p. 195-217.

15. Postic, C., et al., *Dual roles for glucokinase in glucose homeostasis as determined by liver and pancreatic beta cell-specific gene knock-outs using Cre recombinase.* J Biol Chem, 1999. **274**(1): p. 305-15.

16. Shiota, M., et al., *Glucokinase gene locus transgenic mice are resistant to the development of obesity-induced type 2 diabetes.* Diabetes, 2001. **50**(3): p. 622-9.

17. Niswender, K.D., et al., *Effects of increased glucokinase gene copy number on glucose homeostasis and hepatic glucose metabolism.* J Biol Chem, 1997. **272**(36): p. 22570-5.

18. Wu, C., et al., *Enhancing hepatic glycolysis reduces obesity: differential effects on lipogenesis depend on site of glycolytic modulation.* Cell Metab, 2005. **2**(2): p. 131-40.

19. Desvergne, B. and W. Wahli, *Peroxisome proliferator-activated receptors: nuclear control of metabolism.* Endocr Rev, 1999. **20**(5): p. 649-88.

20. Lee, C.H., P. Olson, and R.M. Evans, *Minireview: lipid metabolism, metabolic diseases, and peroxisome proliferator-activated receptors.* Endocrinology, 2003. **144**(6): p. 2201-7.

21. Lee, S.S., et al., *Targeted disruption of the alpha isoform of the peroxisome proliferator-activated receptor gene in mice results in abolishment of the pleiotropic effects of peroxisome proliferators.* Mol Cell Biol, 1995. **15**(6): p. 3012-22.

22. Lehmann, J.M., et al., *An antidiabetic thiazolidinedione is a high affinity ligand for peroxisome proliferator-activated receptor gamma (PPAR gamma).* J Biol Chem, 1995. **270**(22): p. 12953-6.

23. Reilly, S.M. and C.H. Lee, *PPAR delta as a therapeutic target in metabolic disease.* FEBS Lett, 2008. **582**(1): p. 26-31.

24. Oliver, W.R., Jr., et al., *A selective peroxisome proliferator-activated receptor delta agonist promotes reverse cholesterol transport.* Proc Natl Acad Sci U S A, 2001. **98**(9): p. 5306-11.

25. Tanaka, T., et al., *Activation of peroxisome proliferator-activated receptor delta induces fatty acid beta-oxidation in skeletal muscle and attenuates metabolic syndrome.* Proc Natl Acad Sci U S A, 2003. **100**(26): p. 15924-9.

26. Wang, Y.X., et al., *Peroxisome-proliferator-activated receptor delta activates fat metabolism to prevent obesity.* Cell, 2003. **113**(2): p. 159-70.

27. Wang, Y.X., et al., *Regulation of Muscle Fiber Type and Running Endurance by PPARdelta.* PLoS Biol, 2004. **2**(10): p. E294.

28. Lee, C.H., et al., *PPAR{delta} regulates glucose metabolism and insulin sensitivity.* Proc Natl Acad Sci U S A, 2006.

29. Lee, C.H., et al., *Transcriptional repression of atherogenic inflammation: modulation by PPARdelta.* Science, 2003. **302**(5644): p. 453-7.

30. Narkar, V.A., et al., *AMPK and PPARdelta agonists are exercise mimetics.* Cell, 2008. **134**(3): p. 405-15.

31. Kang, K., et al., *Adipocyte-derived Th2 cytokines and myeloid PPARdelta regulate macrophage polarization and insulin sensitivity.* Cell Metab, 2008. **7**(6): p. 485-95.

32. Odegaard, J.I., et al., *Alternative M2 activation of Kupffer cells by PPARdelta ameliorates obesity-induced insulin resistance.* Cell Metab, 2008. **7**(6): p. 496-507.

33. Luquet, S., et al., *Peroxisome proliferator-activated receptor delta controls muscle development and oxidative capability.* Faseb J, 2003. **17**(15): p. 2299-301.

34. Lin, J., et al., *Hyperlipidemic effects of dietary saturated fats mediated through PGC-1beta coactivation of SREBP.* Cell, 2005. **120**(2): p. 261-73.

35. Chawla, A., et al., *PPARdelta is a very low-density lipoprotein sensor in macrophages.* Proc Natl Acad Sci U S A, 2003. **100**(3): p. 1268-73.

36. Brown, M.S. and J.L. Goldstein, *The SREBP pathway: regulation of cholesterol metabolism by proteolysis of a membrane-bound transcription factor.* Cell, 1997. **89**(3): p. 331-40.

37. Gordon, S., *Alternative activation of macrophages.* Nat Rev Immunol, 2003. **3**(1): p. 23-35.

38. Yang, X., et al., *Nuclear Receptor Expression Links the Circadian Clock to Metabolism.* Cell, 2006. **126**(4): p. 801-810.

39. Erbay, E., et al., *Reducing endoplasmic reticulum stress through a macrophage lipid chaperone alleviates atherosclerosis.* Nat Med, 2009. **15**(12): p. 1383-91.

40. Miyazaki, M., et al., *Oleoyl-CoA is the major de novo product of stearoyl-CoA desaturase 1 gene isoform and substrate for the biosynthesis of the Harderian gland 1-alkyl-2,3-diacylglycerol.* J Biol Chem, 2001. **276**(42): p. 39455-61.

41. Miyazaki, M., Y.C. Kim, and J.M. Ntambi, *A lipogenic diet in mice with a disruption of the stearoyl-CoA desaturase 1 gene reveals a stringent requirement of endogenous monounsaturated fatty acids for triglyceride synthesis.* J Lipid Res, 2001. **42**(7): p. 1018-24.

42. Horike, N., et al., *AMP-activated protein kinase activation increases phosphorylation of glycogen synthase kinase 3beta and thereby reduces cAMP-responsive element transcriptional activity and phosphoenolpyruvate carboxykinase C gene expression in the liver.* J Biol Chem, 2008. **283**(49): p. 33902-10.

43. Herzig, S., et al., *CREB regulates hepatic gluconeogenesis through the coactivator PGC-1.* Nature, 2001. **413**(6852): p. 179-83.

44. Arkan, M.C., et al., *IKK-beta links inflammation to obesity-induced insulin resistance.* Nat Med, 2005. **11**(2): p. 191-8.

45. Hotamisligil, G.S., *Inflammation and metabolic disorders.* Nature, 2006. **444**(7121): p. 860-7.

46. Cai, D., et al., *Local and systemic insulin resistance resulting from hepatic activation of IKK-beta and NF-kappaB.* Nat Med, 2005. **11**(2): p. 183-90.

47. Akiyama, T.E., et al., *Peroxisome proliferator-activated receptor beta/delta regulates very low density lipoprotein production and catabolism in mice on a Western diet.* J Biol Chem, 2004. **279**(20): p. 20874-81.

48. Zhang, L., H. He, and J.A. Balschi, *Metformin and phenformin activate AMP-activated protein kinase in the heart by increasing cytosolic AMP concentration.* Am J Physiol Heart Circ Physiol, 2007.

Chapter 3:

A DIURNAL, CIRCULATING LIPID MEDIATOR INTEGRATES HEPATIC LIPOGENESIS AND PERIPHERAL FATTY ACID UTILIZATION

(Manuscript submitted)

Introduction

Food intake increases the activity of hepatic biosynthetic pathways, notably *de novo* lipogenesis, which mediate the conversion of glucose to fats to be stored or oxidized. In mice, the hepatic lipogenic program is under direct control of the circadian rhythm peaking with nocturnal feeding [1, 2]. This temporal regulation is enforced by daytime repression of lipogenic genes by the nuclear receptor Rev-erbα via recruitment of an HDAC3-containing repressor complex [3]. The transcriptional activators of lipid synthesis in the dark cycle have not been well defined. While postprandial liver-derived lipids are important sources of energy production, disturbances in hepatic lipogenesis cause systemic metabolic phenotypes [4-8]. These observations indicate potential communications between liver and peripheral tissues in the control of energy substrate homeostasis. However, the underlying mechanisms remain unclear.

Results

Hepatic *de novo* lipogenesis modulates muscle fatty acid utilization

We have previously shown that the nuclear receptor PPARδ promotes hepatic fatty acid (FA) synthesis [9]. Despite the enhanced lipogenic activity, acute hepatic PPARδ activation through adenoviral PPARδ over-expression (adPPARδ) reduced circulating triglyceride (TG) and free fatty acid (FFA) levels (Figure 3.1A). Interestingly, FA uptake and β-oxidation were increased in isolated soleus muscle, compared to

control mice (adGFP) (Figure 3.1B). These findings raised the possibility of a PPARδ-dependant signal coupling liver lipid metabolism to FA oxidation in muscle. To approach the mechanisms and identify the molecules involved, we performed untargeted liquid chromatography-mass spectrometry (LC-MS) based metabolomics profiling of hepatic lipids with a focus on metabolites of the PPARδ-regulated lipogenic pathway [10, 11]. Metabolite set enrichment analyses revealed the most significantly altered pathway in the adPPARδ/adGFP comparison was that of acetyl-CoA carboxylase (ACC), a rate limiting enzyme in *de novo* lipogenesis (Figure 3.1C). In direct contrast to the effects of hepatic PPARδ activation, acute liver-specific ACC1 knockdown (LACC1KD) reduced hepatic TG content and elevated serum TG and FFA levels (Figure 3.1D). Moreover, FA uptake was decreased in isolated soleus muscle from LACC1KD mice (Figure 3.1E). *In vivo* FA utilization was assessed using ^{3}H-oleic acid tracers through portal vein injection. Taking into account the potential diurnal fluctuations in hepatic lipogenesis and fatty acid fluxes, we have performed this analysis at both the light and dark cycles. The rate of ^{3}H-oleic acid clearance in the circulation was decreased in LACC1KD mice in the dark/feeding cycle, when the lipogenic program is active (ZT18 or 12 am. Zeitgeber time ZT0: lights on at 6 am; ZT12: lights off at 6 pm) (Figure 3.1F). This defect was accompanied by reduced muscle FA uptake (Figure 3.1G). These results suggest that hepatic *de novo* lipogenesis is actively linked to muscle FA utilization, a process that can be experimentally separated from FA availability.

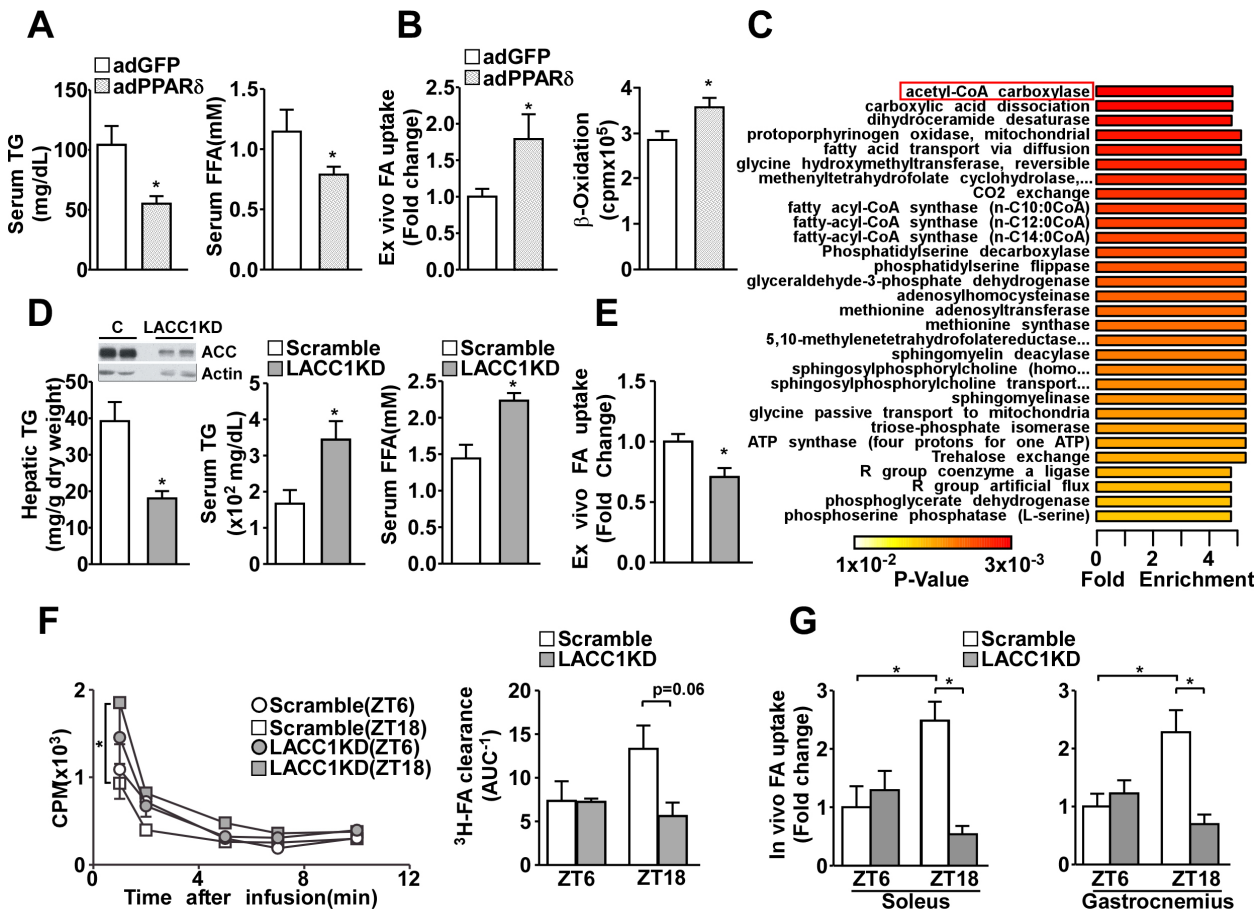

Figure 3.1. Hepatic *de novo* lipogenesis modulates muscle fatty acid utilization. **A.** Serum triglyceride (TG) and free fatty acid (FFA) level in GFP (adGFP) or PPARδ (adPPARδ) adenovirus injected mice fed a normal chow diet. Assays were carried out 4 days after injection. **B.** *Ex vivo* fatty acid uptake (left) and oxidation (right) in isolated soleus muscle of adGFP and adPPARδ mice. **C.** Metabolite set enrichment analysis of lipids from adGFP and adPPARδ liver lysates. Metabolites were identified based on database search of matching mass-charge ratio and retention time. Identified metabolites and their relative quantity were used to calculate the enrichment and statistical significance. Top 30 perturbed enzyme or pathways were shown based on

(**Figure 3.1. Continued**) statistical significance. **D.** Hepatic TG (left) and serum TG (middle) and FFA (right) levels in adenovirus mediated liver specific scrambled (Scramble) or ACC1 (LACC1KD) knockdown mice. Representative immunoblots for ACC protein in Scramble and LACC1KD liver samples were shown. **E.** *Ex vivo* fatty acid uptake in isolated soleus muscle of Scramble and LACC1KD mice. **F.** Serum ^{3}H radioactivity disappearance after portal vein infusion of ^{3}H-oleic acid (left). The rate of ^{3}H FA clearance is represented as the inverse of area under the curve (AUC) of disappearance (right). **G.** *In vivo* fatty acid uptake in soleus (left) and gastrocnemius (right) muscle of Scramble or LACC1KD mice. ^{3}H-oleic acid complexed with 3.5% FA free BSA was infused through portal vein. Blood samples were collected at 1, 2, 5, 7, and 10 minutes. The assay was carried out at two time points: 12pm or zeitgeber time 6 (ZT6), and 12am or ZT18 (ZT0: lights on at 6 am; ZT12: lights off at 6 pm). *$p<0.05$, two-tailed t-test. Data were presented as mean±SEM.

Temporal regulation of hepatic lipogenic gene expression and serum lipidomes by PPARδ

To further explore the mechanism by which hepatic PPARδ controls crosstalk to the peripheral musculature, we examined the lipogenic pathway in liver-conditional PPARδ knockout (LPPARDKO, PPARδ$^{f/f}$ x albumin-cre, C57BL/6) and control (wt, PPARδ$^{f/f}$) mice. Consistent with the PPARδ-ACC1 link in metabolomics analyses, induction of ACC1 in the dark cycle was abolished in the liver of LPPARDKO mice and the diurnal expression of ACC2, fatty acid synthase (FAS) and stearoyl-CoA desaturase 1 (SCD1) was shifted (Figure 3.2A), indicating that PPARδ controls the temporal expression of hepatic lipogenic genes. In fact, PPARδ expression displayed diurnal oscillation that peaked in the dark cycle and coincided with the expression of Bmal1, a clock regulator with peak expression in the dark cycle, in the liver and in dexamethasone-synchronized primary hepatocytes (Figure 3.3A). The expression of diacylglycerol acyltransferase (DGAT1, triglyceride synthesis), choline kinase α (ChKα, phosphocholine synthesis) (Figure 3.2A) and core circadian clock genes (Bmal1, Per1, Cry1, and Rev-erbα) were unchanged in LPPARDKO mice, while the feeding activity, as determined in metabolic cage studies was unaltered (Figure 3.3B, C). Importantly, LPPARDKO resulted in reduced muscle FA uptake in the dark cycle *in vivo*, mirroring the results from LACC1KD mice (Figure 3.2B).

Products of *de novo* lipogenesis can exert diverse regulatory functions [12-14], in

addition to serving as energy substrates. Human and mouse metabolomic and lipidomic studies indicate that the serum lipid composition closely resembles that of the liver [15] . We also observed a 45% overlap between mouse liver and serum lipidomes (Figure 3.4A), suggesting that changes in hepatic *de novo* lipogenesis may have significant effects on peripheral tissue metabolism through liver-derived circulating lipids. We therefore profiled lipidomes of serum samples from wt and LPPARDKO mice collected at 6 ZT points. A total of 735 unique ion features were detected in both positive and negative ionization modes. Hierarchical clustering of metabolites demonstrated a clear alteration in the pattern of serum lipids in LPPARDKO mice, compared to wt controls (Figure 3.2C). A dendrogram based on the clustering analysis revealed the main differences between these two genotypes occurred during the dark cycle (ZT16, 20 and 24, or 10 pm, 2 am and 6am) (Figure 3.2D), when PPARδ-controlled lipogenesis is most active. Furthermore, principal component analysis (PCA) demonstrated similarities between LPPARDKO and LACC1KD serum in the dark cycle (Figure 3.2E), consistent with the reduced muscle FA utilization phenotype in both models. These findings support the notion that the PPARδ-ACC1 axis in the liver may modulate peripheral substrate utilization through serum lipid metabolites.

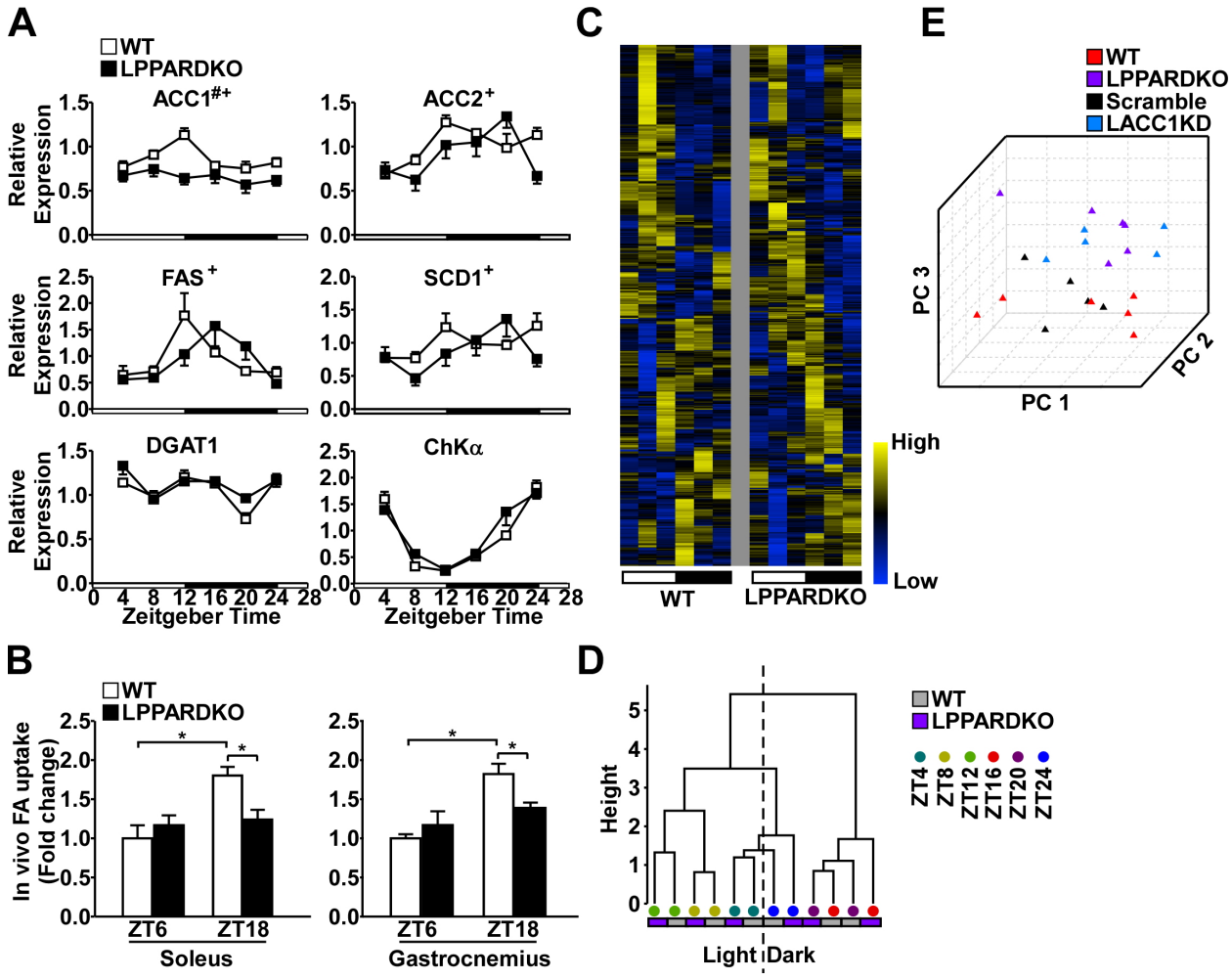

Figure 3.2. Temporal regulation of hepatic lipogenic gene expression and serum lipidomes by PPARδ. **A.** Expression of PPARδ targets in the liver measured by RT-qPCR. Liver samples from wild type (wt) and PPARδ liver specific knockout (LPPARDKO) mice were collected every 4 hours for a 24-hour cycle starting at ZT4. X axis: white bar represents light cycle time points (ZT4, 8, 12) and black bar represents dark cycle time points (ZT16, 20, 24). Statisitical significance was determined by two-way ANOVA. #p<0.05 for significance between wt and LPPARDKO; +p<0.05 for significant differences of the circadian expression pattern. **B.** *In vivo* fatty acid uptake in soleus (left) and gastrocnemius (right) muscle of wt and LPPARDKO mice from two time

(**Figure 3.2. Continued**) points (ZT6 and ZT18). The assay was performed as in Figure 3.1G. **C.** Heat map of all identified positive and negative ionization mode features in LC-MS based untargeted metabolomics. Features were arranged by unsupervised hierarchical clustering. **D.** Dendrogram based on hierarchical clustering of serum samples from wt and LPPARDKO mice. **E.** Principal component analysis of all identified positive mode features among wt, LPPARDKO, Scramble and LACC1KD serum. The score plot of the first three principal components, which represent 53.2% of total variation, was shown. *$p<0.05$, two-tailed t-test. Data were presented as mean±SEM.

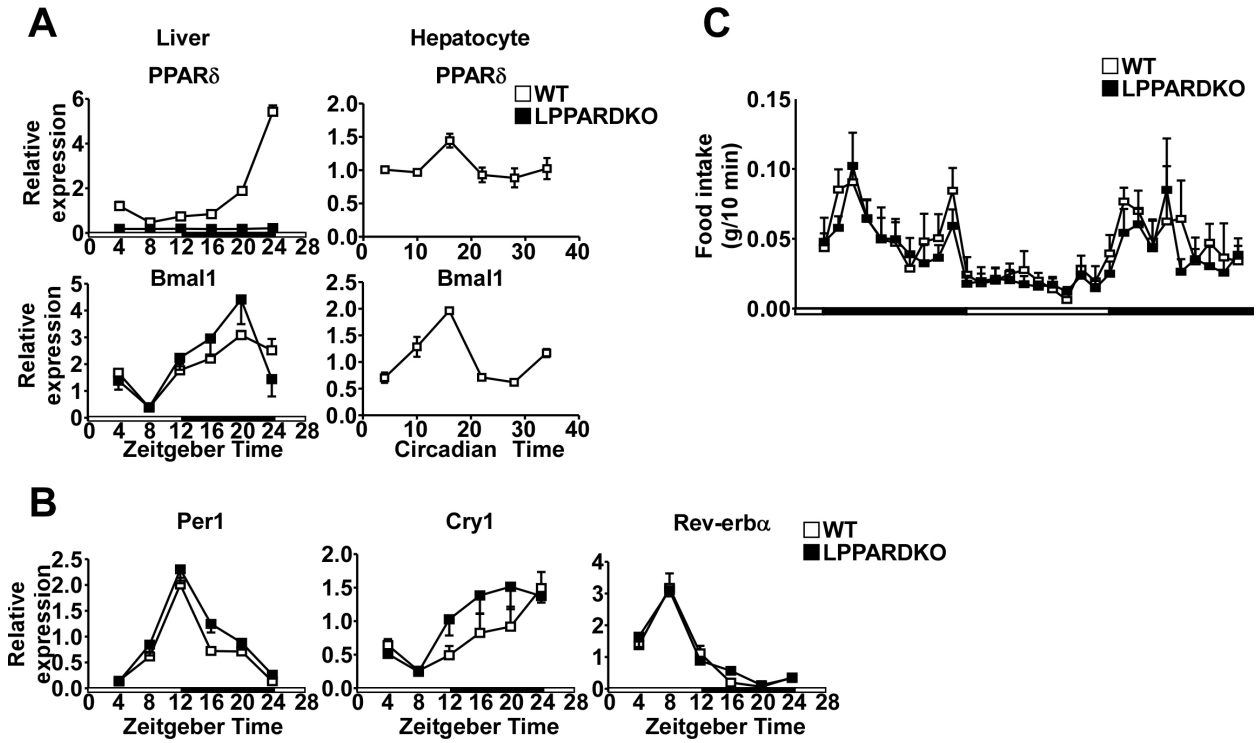

Figure 3.3. A. PPARδ and Bmal1 gene expression in wt and LPPARDKO liver (left), and dexamethasone synchronized wt primary hepatocytes (right). Circadian times refer to hours after dexamethasone treatment. PPARδ expression followed a similar pattern as that of Bmal1. **B.** Core circadian clock gene expression in the liver of wt and LPPARDKO mice. **C.** Food intake in wt and LPPARDKO mice measured by metabolic cages.

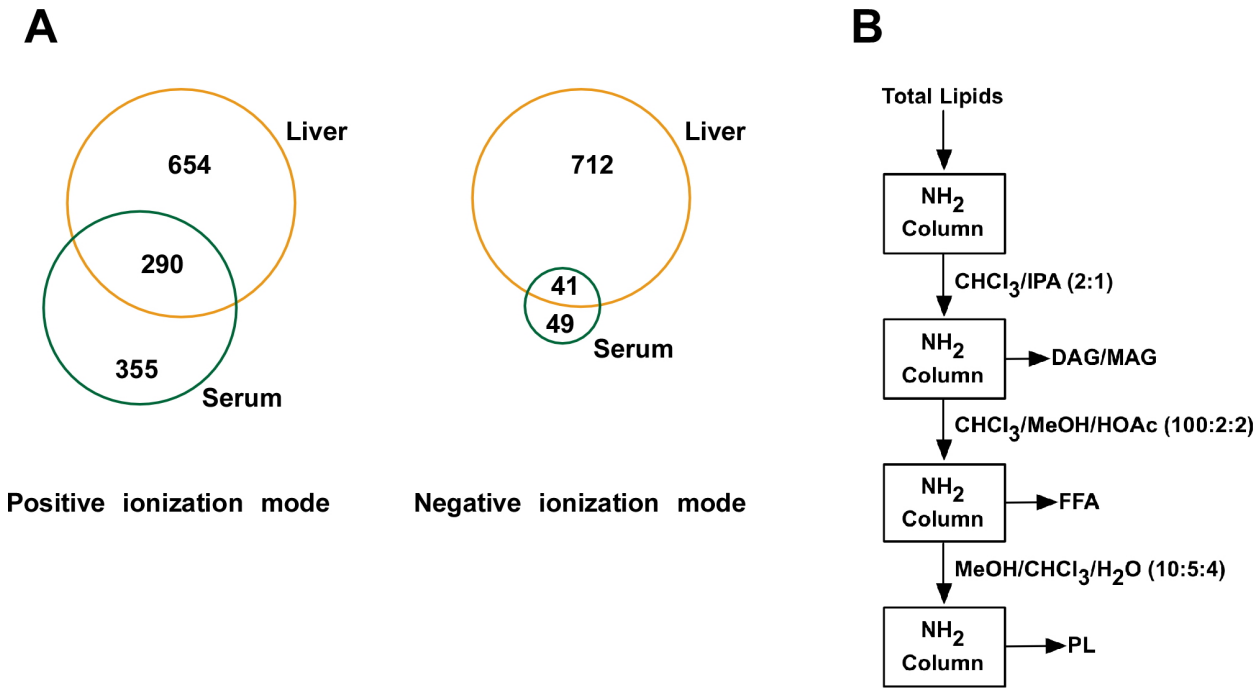

Figure 3.4. A. Comparison of liver and serum lipidomes. Serum and liver features in both positive and negative ionization modes from wt mice were aligned with mass tolerance of m/z=0.01 and retention time tolerance of 60 seconds. Common features were filtered to remove isotopic peaks and peaks with ion intensities less than $5x10^4$. **B.** Column purification of serum lipids scheme (See methods for detail). $CHCl_3$: chloroform; IPA: isopropyl alcohol; MeOH: methanol; HOAc: acetic acid.

Identification of a serum phospholipid associated with hepatic PPARδ-ACC1 activity

To test directly whether the PPARδ-mediated alterations in liver, and consequently, serum lipid composition are responsible for the muscle FA utilization effects, C2C12 myotubes were incubated with serum or serum lipid extracts from LPPARDKO or control animals. Treatment of myotubes with serum or lipid extracted from serum collected in the dark cycle from wt mice increased FA uptake, while serum or lipids derived from LPPARDKO animals had no such effect (Figure 3.5A,B). Delipidated serum also had no differential effects on FA uptake. Fractionation of serum lipids by column purification (Figure 3.5B) revealed that the activity stimulating FA uptake segregated with the phospholipid (PL) fraction (Figure 3.5B). To identify PLs that might mediate the functional interaction between hepatic lipid synthesis and muscle FA utilization, we compared liver or serum metabolomes from our three relevant models LPPARKO, LACC1KD, adPPARδ in positive ionization mode, which detects PLs as well as triacylglycerols (TG), diacyglycerols (DAG) and monoacylglyerols (MAG). A total of 158 features were significantly altered in LPPARKO serum at ZT16/ZT20 compared to wt samples ($p<0.05$, corresponding to 19.6% FDR). 189 were significantly changed in LACC1KD serum compared to scramble controls at ZT16 ($p<0.05$, FDR=17%). Lastly, 418 features were identified in liver lysates from adPPARδ mice compared to adGFP mice ($P<0.05$, FDR=11.3%). Cross-comparison of the metabolomes from these three models yielded 14 commonly changed features, whose putative identities were

assigned based on database search (Figure 3.5C,D). Among these, 4 molecules (PC[36:1], TG[56:7], TG[56:6], TG[58:6]) showed changes in the same direction in LPPARDKO (vs. wt) and ACC1KD (vs. control) but the opposite direction in PPARδ over-expression liver lysates (Figure 3.5D), corresponding to the observed muscle fatty acid utilization phenotypes. Based on the prior data that the differential activities toward FA utilization in C2C12 myotubes was in the serum PL fraction, we focused on the only one PL among the 4 molecules, m/z=788.6, putatively identified as PC(36:1). To determine the physiologic relevance of this PL, we examined the extracted ion chromatogram (EIC) of PC(36:1), m/z=788.6 over time and found this specific PL displayed diurnal rhythmicity peaking at night in serum from wt but not LPPARDKO mice (Figure 3.5E). PC(36:1) was also reduced in LACC1KD serum, while levels of this PL increased in lysates from hepatic PPARδ over-expression livers (Figure 3.5F). Co-elution experiments with authentic PC(18:0/18:1) confirmed the identity of m/z=788.6 as PC(36:1) (Figure 3.5G, left). To define the exact fatty acyl-chain composition of this molecule, we performed tandem mass spectrometry scanning for lithiated adducts of PC(36:1) [16]. Only the PC(18:0/18:1) (1-stearoyl-2-oleoyl-sn-glycero-3-phosphocholine, SOPC) was above the detection limit, whereas PC(18:1/18:0) was virtually undetectable (Figure 3.5G, right). We then quantified SOPC in wt and LPPARDKO serum using tandem mass spectrometry with deuterated d83-PC(18:0/18:0) as the internal standard. The concentrations of SOPC in wt serum fluctuated ranging from ~70 μM during the day (ZT8) to ~130 μM at night (ZT20). While daytime SOPC levels remained similar between wt and LPPARDKO mice, the increase in serum SOPC in the dark cycle was

significantly diminished in PPARDKO mice (Figure 3.5H). Taken together, we have identified a serum lipid enriched in the dark/feeding cycle, whose levels were increased in the liver by PPARδ activation and decreased in serum by loss of function of hepatic PPARδ or the PPARδ target gene ACC1.

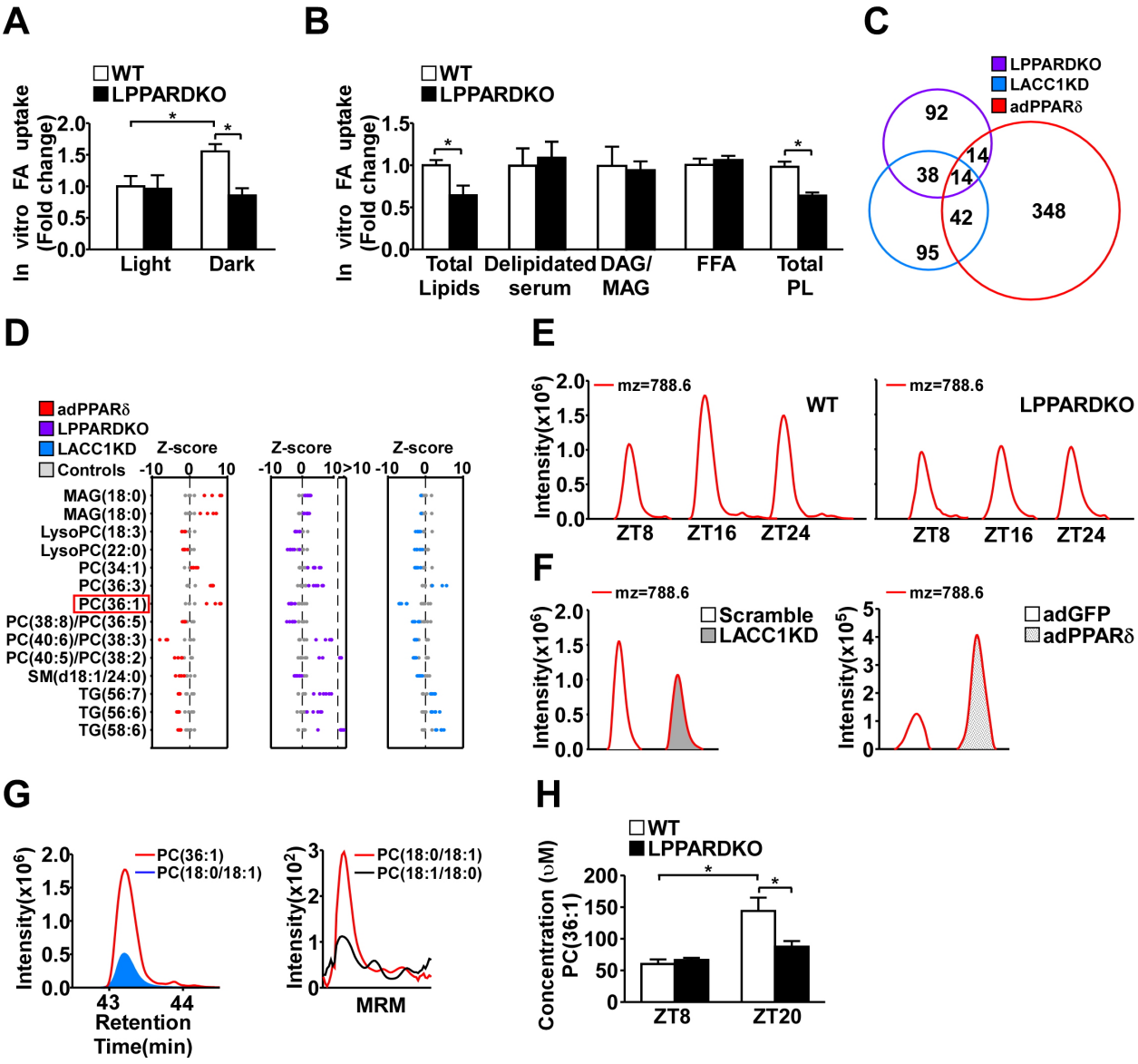

Figure 3.5. Identification of a serum phospholipid associated with hepatic PPARδ-ACC1 activity. **A.** *In vitro* fatty acid uptake in C2C12 myotubes treated with 2% serum pooled from light or dark cycle samples. Myotubes were pre-treated with serum for 48 hours and washed thoroughly with phosphate buffer saline (PBS) before subjecting to FA uptake assay (See methods summary for details). **B.** Fatty acid uptake in C2C12 myotubes treated with 2% serum total lipids, delipidated serum or serum lipid fractions of diacylglycerol/monoacylglycerol (DAG/MAG), free fatty acids (FFA) and phospholipids

(**Figure 3.5. Continued**) (PL) (See Figure 3.4B for lipid fractionation scheme). **C.** Cross-comparison of significantly changed lipids in three models: LPPARDKO vs wt serum, LACC1KD vs Scramble serum and adPPARδ vs adGFP liver lysates. **D.** Z-score plots of commonly changed features in three models using their respective controls as references. The putative identity was defined from database search. Both the H+ and NH_4+ adduct of MAG(18:0) were identified. **E.** Representative Extracted ion chromatogram (EIC) of mz=788.6 in wt and LPPARDKO serum at three time points. **F.** Representative EIC of mz=788.6 in LACC1KD serum (left) and adPPARδ livers (right). **G.** Co-elution of the PC (18:0/18:1) standard with mz=788.6. 100 pmol of PC(18:0/18:1) was injected as a separate sample (left). The acyl-chain composition of PC(36:1) was determined by tandem mass spectrometry running in multiple reaction monitoring (MRM) mode (right). Lithium chloride was added to mobile phases to facilitate adduct formation and fragmentation at sn-1 position of PC(36:1). Detailed MRM parameters were provided in Table. 3.2. **H.** Quantification of PC(36:1) in wt and LPPARDKO mice serum using deuterated d83-PC(18:0/18:0) as the internal standard. *$p<0.05$, two-tailed t-test. Data were presented as mean±SEM.

PC(36:1) facilitates muscle fatty acid utilization

To determine the biological activity of SOPC, we injected wt mice intraperitoneally with SOPC in the dark cycle. A single bolus injection significantly enriched SOPC (~1.4 fold) in serum after 4 hours (Figure 3.7A). SOPC injection coordinately altered lipid metabolism in a concentration-dependent manner, reducing elevated postprandial serum FFA and TG levels (Figure 3.6A), while increasing muscle FA uptake *in vivo* and *ex vivo* (Figure 3.6A, insert and Figure 3.6B), as compared to vehicle controls. Importantly, the reduced muscle FA uptake in LPPARDKO muscle was rescued by SOPC injection (Figure 3.6C). Induction of fatty acid uptake upon SOPC administration was associated with the induction of a panel of fatty acid utilization genes in the muscle, namely CD36, Cidea, FABP4, FATP4, DGAT1 and PPARα (Figure 3.6D). Other FA transporters also exhibited a trend toward increased expression, including FATP1, FABP3 and FABP5, (Figure 3.7B-D). Similarly, the expression of these genes in the muscle was induced in adPPARδ mice and repressed in LPPARDKO and LACC1KD mice. Among those targets, CD36 is a well-established regulator of muscle fatty acid uptake. Interestingly, CD36 expression at mRNA and protein levels also oscillated in wt muscle peaking in the dark cycle (Figure 3.6E). This diurnal pattern was disrupted in LPPARDKO muscle. To assess the direct action of SOPC on muscle fatty acid utilization, we treated myotubes with 1 μM SOPC, its isomer PC(18:1/18:0) (OSPC), a non-specific phosphatidylcholine PC(17:0/17:0) or vehicle alone. Only SOPC was able to induce FA uptake in muscle cells. Furthermore,

the stimulatory effect of SOPC on fatty acid uptake was absent in CD36 knockdown myotubes, compared to controls (Figure 3.6F), supporting the notion that SOPC promotes muscle FA uptake and utilization.

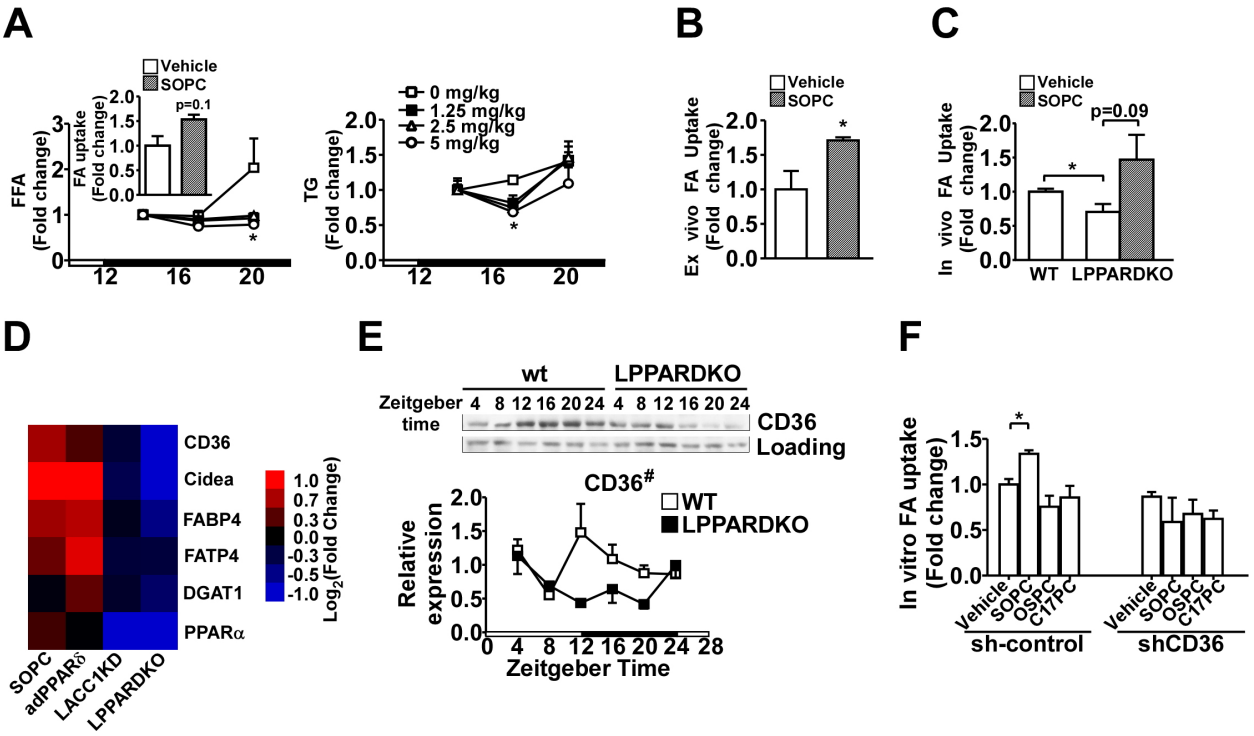

Figure 3.6. PC(36:1) facilitates muscle fatty acid utilization. **A.** Serum FFA (left) and TG (right) levels after i.p. injection of vehicle or PC(36:1) (SOPC) at the beginning of the dark cycle (ZT14). Feeding in the dark cycle led to a steady increase in postprandial serum levels of FFA and TG in vehicle treated mice. SOPC injection reduced postprandial serum FFA and TG in a dose dependent manner. Fold change was calculated using pre-injection FFA and TG values as references (ZT14). Insert: *in vivo* soleus muscle fatty acid uptake 4 hours after SOPC injection (5 mg/kg). **B.** *Ex vivo* FA uptake in isolated soleus muscle 4 hours after vehicle or 5mg/kg SOPC injection. **C.** *In vivo* FA uptake in soleus muscle 4 hours after injection of vehicle or 5mg/kg SOPC in wt or LPPARDKO mice. The injection was carried out at ZT14 and the assay was performed at ZT18. **D**. Transcriptional profiling of fatty acid utilization genes by high throughput RT-qPCR in muscle samples from SOPC vs Vehicle, adPPARδ vs adGFP, LACC1KD vs Scramble, and LPPARDKO vs wt. **E.** CD36 protein (upper) and gene

(**Figure 3.6. Continued**) (lower) expression in wt and LPPARDKO muscles. Statisitical significance was determined by two-way ANOVA. #$p<0.05$ for significance between wt and LPPARDKO. **F.** Fatty acid uptake in control or CD36 Stable knockdown C2C12 myotubes pretreated with respective lipids overnight. FA uptake assay was performed as in Figure 3.5A,B. *$p<0.05$, two-tailed t-test. Data were presented as mean±SEM.

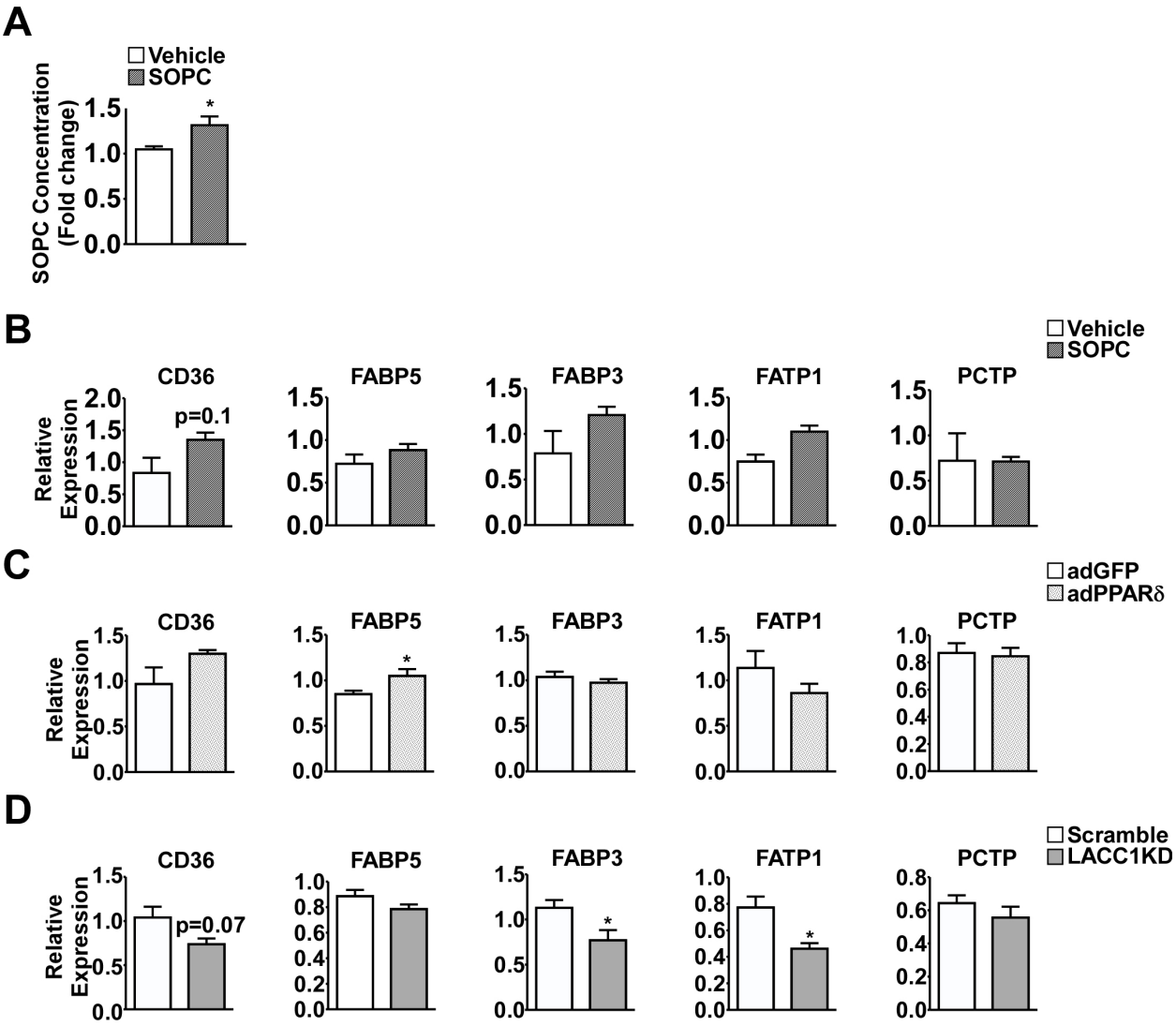

Figure 3.7. A. Increased serum SOPC levels in wt mice 4 hours after a single dose injection of vehicle or 5mg/kg body weight SOPC. **B-D.** RT-qPCR transcriptional profiling of additional fatty acid uptake (FABP5, FABP3, FATP1) and phosphocholine transport (PCTP) genes in muscle from Vehicle and SOPC injected (B), adGFP and adPPARδ (C) and Scramble and LACC1KD mice (D). *$p<0.05$.

Discussion

In summary, we have demonstrated that hepatic PPARδ signaling activates liver FA synthesis and peripheral FA utilization in multiple *in vivo* models. Using an integrated biochemical-cell biology based approach in these models, we identified SOPC as a hepatic PPARδ- and ACC1-dependent serum lipid that can modulate muscle FA utilization. Indeed, exogenous stimulation or administration of SOPC *in vitro* and *in vivo* replicates or rescues the patterns of hepatic lipogenesis on muscle FA oxidation. The peak PPARδ expression in the dark/feeding cycle does not completely overlap with that of lipogenic genes (Figure 3.2A and Figure 3.3A), suggesting that PPARδ activity may be controlled by ligands derived from *de novo* lipogenesis or intake of dietary nutrients. As expression of genes in the phospholipid synthesis pathway were not affected by loss of PPARδ function, the reduction in SOPC in LPPARDKO mice was likely due to decreased production of C18:0 and C18:1, products of *de novo* lipogenesis. The data presented here suggests that diurnal oscillations of the hepatic de novo lipogenesis pathway and lipid metabolite products align metabolic functions between liver and muscle. The integrated lipid synthesis and utilization is facilitated by temporal production of SOPC and muscle FA transporters. Such findings add to the evolving network of systemic signals from one organ to another that can coordinate metabolism in response to specific metabolic cues [12, 17, 18]. It will be of great interest to expand these networks to include the peripheral mechanism for how hepatic PPARδ-derived

SOPC controls levels of muscle CD36 and other FA transporters and the physiological relevance in human populations in future studies.

Material and Methods

Materials

PPARδ or GFP adenovirus was generated as described [9]. The shScrambled and shACC1 adenovirus were provided by Dr. Christopher Newgard [19]. Small hairpin RNA sequences against CD36 [20] or luciferase (control) was cloned in pSIREN-RetroQ vector.

Animals

Mice used in the current study were all on the C57BL6/J background. Liver specific PPARδ knockout mice were generated by crossing albumin-cre transgenic mice to PPARδ f/f mice. Animals were housed in a barrier facility with 12-hour light and dark cycles. For circadian studies, animals were sacrificed every 4 hours starting at 10AM (ZT4) for 24 hours (n=4/genotype/time point) with free access to food and water. For dark cycle time points, animals were sacrificed under safety red light before proceeding to further dissection. Adenoviruses were injected through the tail vein (10^9 pfu/mouse). Subsequent metabolic characterizations were carried out 4 days post injection. 3 cohorts were used for circadian studies (8-12 weeks old, 2 males and 1 female, showing

similar results). AdPPARδ/adGFP was repeated in 3 cohorts (8 weeks old male, n=4-6) and LACCKD was conducted in 2 cohorts (8 weeks old male, n=5). SOPC injection was performed in 2 cohorts (8-12 weeks old male, n=4-6). All animal studies were approved by the Harvard Medical Area Standing Committee on Animals.

Metabolic studies

Metabolic cage studies were performed in a Comprehensive Lab Animal Monitoring System. Data were collected for 48 hours starting at the beginning of the dark cycle. TG and FFA were determined by colorimetric methods. Hepatic TG was determined from chloroform:methanol (2:1 v/v) extracts of vacuum dried liver samples.

Primary hepatocytes and *in vitro* synchronization

Primary hepatocytes were isolated as described [21]. 100 nM of dexamethasone was applied for 1 hour to synchronize cells. After thorough wash, fresh culture media were added and cells were collected at the indicated time after dexamethasone removal.

Generation of stable C2C12 myoblast lines

C2C12 myoblasts were infected with retroviral particles and selected against puromycin. Subsequent populations of puromycin resistant cells were collected as stock. Stable C2C12 CD36 or control knockdown myoblasts were able to differentiate into myotubes with no apparent defects. Differentiation of C2C12 myoblasts was performed in 2% horse serum, DMEM for 8 days.

Gene expression and western blots

Gene expression was determined by SYBR Green based real-time quantitative PCR (RT-qPCR) using 36B4 as an internal standard. A relative standard curve method was used to calculate the relative expression of genes. For high throughput RT-qPCR array, ddCt method was used to measure relative expression. The log2 fold change of the average expression of each probe was calculated. Hierarchical clustering and heatmap were generated by Cluster and Java Treeview. The primers used in this study were listed in table 3.1. Additional primer sequences were obtained from Primer Bank [22]. Protein levels of CD36 were determined by western blotting of muscle lysates using antibody against CD36 (Santa Cruz). For circadian samples, a pooled sample of wt and LPPARDKO (n=4) from each time point was used. For *in vivo* ACC1 knockdown, knockdown efficiency for each individual animal was determined by western blotting (n=5). Two representative animals from each group were shown (Figure 3.1D).

Table 3.1. List of primers used for RT-qPCR

Genes	Forward Sequence	Reverse Sequence
ACC1	CGCTCGTCAGGTTCTTATTG	TTTCTGCAGGTTCTCAATGC
FAS	TCCTGGAACGAGAACACGATCT	GAGACGTGTCACTCCTGGACTTG
SCD1	CTTCTTCTCTCACGTGGGTTG	CGGGCTTGTAGTACCTCCTC
DGAT1	CATGCGTGATTATTGCATCC	ACAGGTTGACATCCCGGTAG
Rev-erbα	TCTCTCCGTTGGCATGTCTAGA	GCAAGCATCCGTTGCTTCTC
CD36	TCATATTGTGCTTGCAAATCCAA	TGTAGATCGGCTTTACCAAAGATG
FABP4	TCACCGCAGACGACAGGAA	CCACCAGCTTGTCACCATCTC
FATP4	CATCAGCGTAAATGGGGATTTGG	CTGTCGTCTGCGGTGATTTCATC
Cidea	TGCTCTTCTGTATCGCCCAGT	GCCGTGTTAAGGAATCTGCTG
PPARα	TGTTTGTGGCTGCTATAATTTGC	GCAACTTCTCAATGTAGCCTATGTTT
FABP3	ACCTGGAAGCTAGTGGACAG	TGATGGTAGTAGGCTTGGTCAT
FATP1	CGCTTTCTGCGTATCGTCTG	GATGCACGGGATCGTGTCT

In vitro fatty acid uptake

C2C12 myotubes were pre-treated with lipids complexed in 0.2% BSA (FA free) overnight. Cells were thoroughly washed with PBS before subjecting to a 5-minute FA loading with 1μCi/ml ^{3}H-oleic acid in Krebs-Ringer Hepes (KRH) buffer, 1% FA free BSA and 100 μM oleic acid. Intracellular ^{3}H radioactivity was determined and normalized to protein concentration.

***Ex vivo* fatty acid oxidation**

Mice were sacrificed and freshly isolated soleus muscles were incubated at 37 °C for 30 minutes with 2% FA free BSA containing KRH buffer supplemented with 0.2 mM palmitic acid, and 4 μCi/ml ^{3}H-palmitic acid. Supernatants were collected and the ^{3}H

radioactivity in the aqueous phase was quantified as described [23].

In vivo fatty acid uptake

We adapted an established protocol from Bartelt et al. [24]. Briefly, mice were anesthetized at different time of the day. 10 μCi of ^{3}H-oleic acid complexed in 3.5% FA free BSA was infused through portal vein. Blood samples were collected at 1, 2, 5, 7 and 10 minutes after infusion. At 10 minutes, soleus and gastrocnemius muscles were isolated. Serum radioactivity levels were determined at each time point. FA uptake was calculated as described [25].

Lipid extraction, fractionation and treatments

Serum lipids were diluted with phosphate buffer saline (PBS) and extracted by chloroform:methanol (2:1:1 v/v). The organic phase (lipids) was evaporated under a constant stream of nitrogen. Lipids were re-dissolved in chloroform. Column purification of serum lipids was carried out as described [26]. Briefly, Aminopropyl column (Sep-Pak Vac NH2 cartridge 3cc/500mg 55-105 μm, Waters) was equilibrated 3 times with acetone/water (7:1). Lipids in chloroform was dried under nitrogen and re-dissolved in hexane/methyl-butyl-tert-ether (MBTE)/acetic acid (100:3:0.3). Lipids were loaded on to the equilibrated column and were eluted sequentially with hexane, hexane/cholorform/ethyl aceate (100:5:5), chloroform/2-propanol (2:1)

(diacylglycerol/monoacylglycerol fraction), chloroform: methanol/acetic acid (100:2:2) (free fatty acid fraction), and methanol/chloroform/water (10:5:4) (phospholipids fraction). Each fraction was dried under nitrogen and re-dissolved in chloroform. For *in vitro* experiments, lipids were dissolved in 0.2% fatty acid (FA) free BSA in DMEM with 2% double stripped FBS (charcoal stripped and lipoprotein deficient). The resulting solution was applied to cells overnight. Cells were washed extensively before subjecting to functional assays. For *in vivo* experiments, SOPC was re-suspended with sonication in 0.5% FA free BSA in PBS [12] to make a stock solution of 0.4 g/L. The solution was made fresh each time. Unless otherwise indicated, 5mg/Kg body weight SOPC was injected i.p.

Liquid-Chromatography Mass-Spectrometry (LC-MS)

A 2:1:1 chloroform:methanol:PBS solution was prepared for lipid extraction to isolate organic soluble metabolites. Following brief vortexing, samples were centrifuged at 2500 x g at 4 °C for 10 minutes. The organic layer (bottom) was transferred to a new vial and solvents were evaporated under a stream of nitrogen. Samples were resuspended in chloroform (120 µl) and stored at -80 °C until LC/MS analysis (within 48 hours of extraction). For both positive and negative ionization mode LC-MS runs, 20 µl of extract was injected. LC-MS analysis was performed using an Agilent 6210 Accurate-Mass time-of-flight LC-MS system as described [10, 11]. For LC analysis in negative mode, a Gemini (Phenomenex) C18 column (5 mm, 4.6 x 50 mm) was used together

with a pre-column (C18, 3.5 mm, 2 x 20 mm). Mobile phase A consisted of 95:5 water:methanol and mobile phase B was composed of 60:35:5 isopropanol:methanol:water. Both A and B were supplemented with 0.1% ammonium hydroxide solution (28% in water). The flow rate for each run was 0.5 ml/min. The gradient started at 0% B for 5 minutes and linearly increased to 100% B over 40 minutes, was then maintained at 100% B for 8 minutes before re-equilibrating for 7 minutes at 0% B. For the LC analysis in positive mode, a Luna (Phenomenex) C5 column (5 mm, 4.6 x 50 mm) was used together with a pre-column (C4, 3.5 mm, 2 x 20 mm). Mobile phase A and B and the gradient were the same as for positive mode, but supplemented with 0.1% formic acid and 5 mM ammonium formate. MS analysis was performed with an electrospray source ionization (ESI) interface. The capillary voltage was set to 3.0 kV and the fragmentor voltage to 100 V. The drying gas temperature was 350 °C, the drying gas flow was 10 L/min, and the nebulizer pressure was 45 psi. Data was collected using a mass range from 100-1500 Da. For wt and LPPARDKO serum samples, all samples of each genotype from different time points were detected in a single consecutive run. To validate the results, samples from ZT8, ZT16 and ZT24 were subject to a second run. For Scramble and LACC1KD serum or GFP and PPARδ liver, the entire sample set was run in a single session.

Targeted analysis of phosphocholine species

Side-chain composition of phosphocholine species. Phosphatidylcholine fatty acyl chain

composition was analyzed separately on an Agilent 6410 triple quadrupole-mass spectrometer (QQQ-MS) by direct injection of 1 µl of serum lipid extracts without chromatography [16]. The QQQ-MS was operated in multiple reaction monitoring mode (MRM), targeting lithium adduct precursors and product ions. The full list of MRM transitions and parameters is detailed in the table 3.2. Mobile phase was comprised of 98:2 methanol:water with 1 mM LiCl to facilitate the formation of lithium adducts for analysis. Samples were run in positive ionization mode with fragmentor voltage of 150 V, collision energy of 35 V and a dwell time of 25 ms.

Quantification of phosphocholine species. 200 pmol of 1,2-distearoyl(d70)-sn-glycero-3-phosphocholine-1,1,2,2-d4-N,N,N-trimethyl-d9 (D83 PC(18:0/18:0)) was spiked into 50 µl of serum as the recovery standard. Serum was extracted as above. LC-MS/MS analysis was performed using an Agilent 6410 QQQ-MS in positive ionization mode equipped with an electrospray source ionization interface and an Agilent 1200 Binary Pump. For LC analysis a Gemini (Phenomenex) C18 column (50 mm x 2.0 mm, 3 µm particle size with 100 angstrom pore) was used with a 50 µm steel mesh filter. Mobile phase A consisted of 95:5 water:methanol and mobile phase B consisted of 80:20 isopropanol:methanol. Both A and B were supplemented with 0.1% formic acid. The flow rate was 0.3 ml/min. The gradient started at 20% B and linearly increased to 100% B over 45 minutes, was maintained at 100% B for 10 minutes before equilibrating for 5 minutes at 20% B. The QQQ-MS was operated in MRM mode and PCs were targeted using the m/z $[M + H]^+$ to m/z 281.2 transition for all PCs. Capillary voltage was set to 3.0 kV, the fragmentor voltage to 200 V with a collision energy of 35 V. The drying gas

temperature was 350 ºC, the drying gas flow was 10 L/min and the nebulizer pressure was 45 psi. The integrated peak area for each species was normalized to the peak area of the recovery standard.

Table 3.2. List of multiple reaction monitoring (MRM) parameters for the identification of acyl-chain composition of PC(36:1).

Phosphatidylcholine	Precursor Ion $[M+Li]^+$	Product Ion
C18:1/C18:0	794.6	453.4
C18:0/C18:1	794.6	451.4

Data analysis (Figure 3.9)

Data preprocessing. Raw data files were converted to mzXML files and subsequently aligned by XCMS [27]. The resulting aligned features derived from wt, LPPARDKO, Scramble and LACC1KD serum were compared to identify common features using metaXCMS [28] with a mass tolerance of 0.01 and retention time tolerance of 60 seconds. Identical procedures were carried out to generate common features from adPPARδ and adGFP liver lysates. Subsequently, these features from serum and liver lysates samples were processed by an automated workflow [29] to identify isotopic peaks and assign putative identity with 3ppm mass tolerance. All isotopic peaks were removed and the remaining data were cutoff for features with median intensity less than $5x10^4$. The reproducibility of the untargeted metabolomics platform was evaluated from

two independent runs of 6 samples. The Spearman's rank correlation coefficient was calculated and the duplicate pair with lowest correlation coefficient was plotted (Figure 3.8A).

Data normalization. We adapted methods from Sreekumar et al [30]. Briefly, each sample was centered by median and scaled by its inter-quartile range (IQR). The normalized distributions of samples were plotted in Figure 3.8B as Box-and-Whisker plot.

Hierarchical clustering. Both positive and negative ionization mode features from wt and LPPARDKO serum around the clock were mean centered and scaled by standard deviation on a per feature basis (auto-scaling). To simplify the visualization, only the mean value of each feature from every time point was used for the construction of heat map. The resulting data sets of each genotype were clustered using Euclidean distance as the similarity metric in Cluster 3.0. Heat maps were generated by Java Treeview. Heat map of LPPARDKO serum was aligned to wt for comparison. Dendrogram of samples was plotted based on Spearman correlation with Ward linkage.

Principal component analysis. Auto-scaling was applied on a per metabolite basis to each biological group (wt vs LPPARDKO and Scramble vs LACC1KD). Principal component analysis was performed in Metaboanalyst [31]. The 3D view of the first 3 principal components was plotted.

Identification of significant features. The empirical p-value for each pair of comparison was calculated by randomly permuting sample labels for 1000 times to obtain the null distribution. The analysis was carried out in Multiple Experiment Viewer [32]. False

discovery rate was determined by Benjamini-Hochberg method. A feature is considered significant for downstream cross-comparison with unadjusted $p<0.05$. Significantly changed features in wt and LPPARDKO mice serum at night (n=6, pooled sample set from ZT16 and ZT20), Scramble and LACC1KD mice serum (n=5), and adGFP and adPPARδ liver lysates (n=4) were compared and visualized in Venn diagram.

Metabolites Set Enrichment Analysis (MESA). Significantly altered features in adPPARδ/adGFP liver lysates comparisons were assigned putative identities based on database search. Their identities were further validated from an internal reference database. Validated lipid species were matched to human metabolites database (HMDB). The mappable species were assigned a HMDB ID for subsequent MESA analysis implemented in the Metaboanalyst [31].

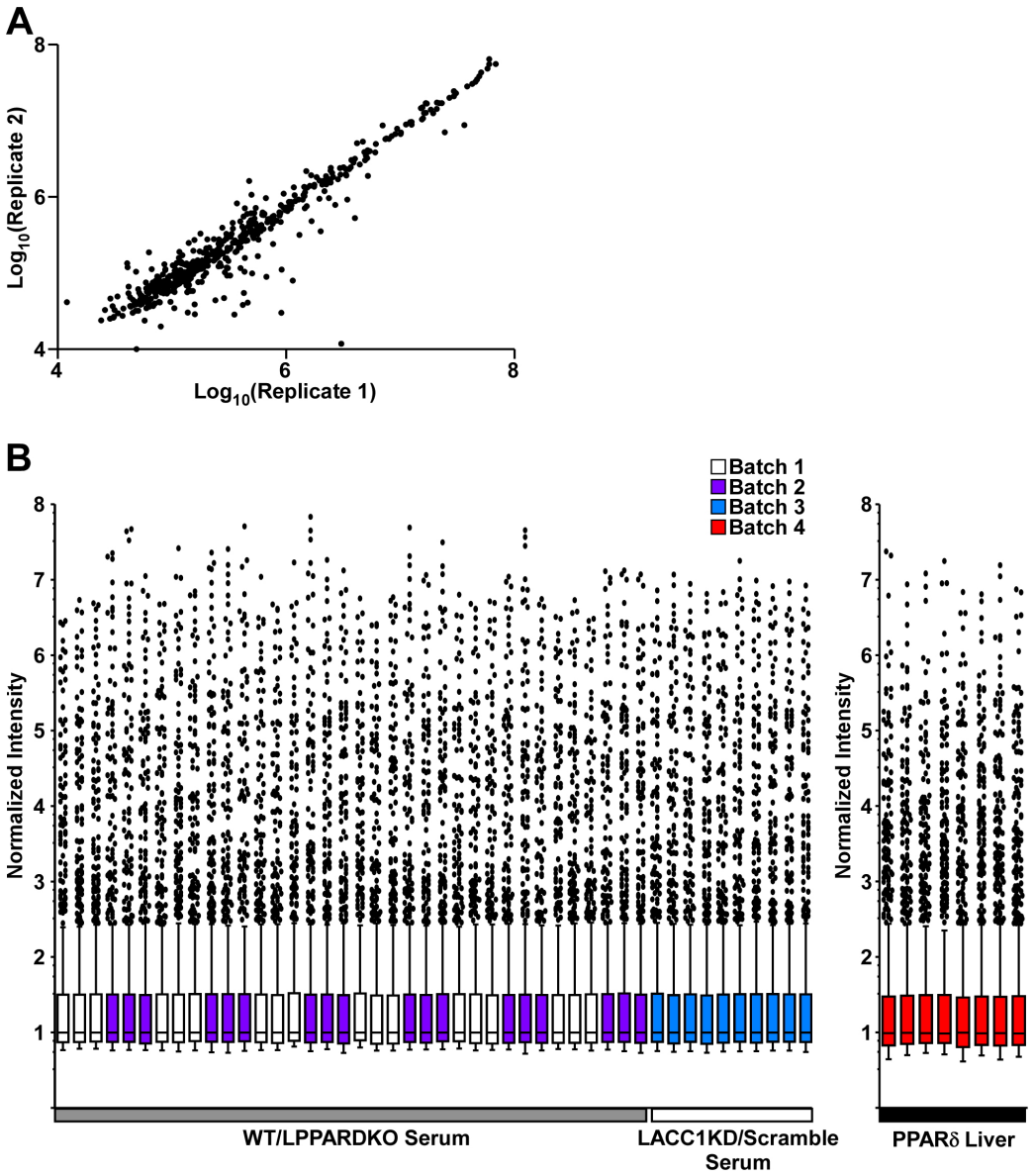

Figure 3.8. A. The reproducibility of the untargeted metabolomics platform was validated from two separate runs of 6 serum samples. The Spearman's rank correlations are between 0.9 and 0.94. The duplicate pair with the lowest correlation (Spearman's r=0.90) is shown. **B.** Raw intensity of samples was subject to normalization with median centering and inter-quartile range (IQR) scaling. The resulting data show equal distribution among different groups of samples. White bar represents samples obtained in the light cycle and black bar for those in the dark cycle.

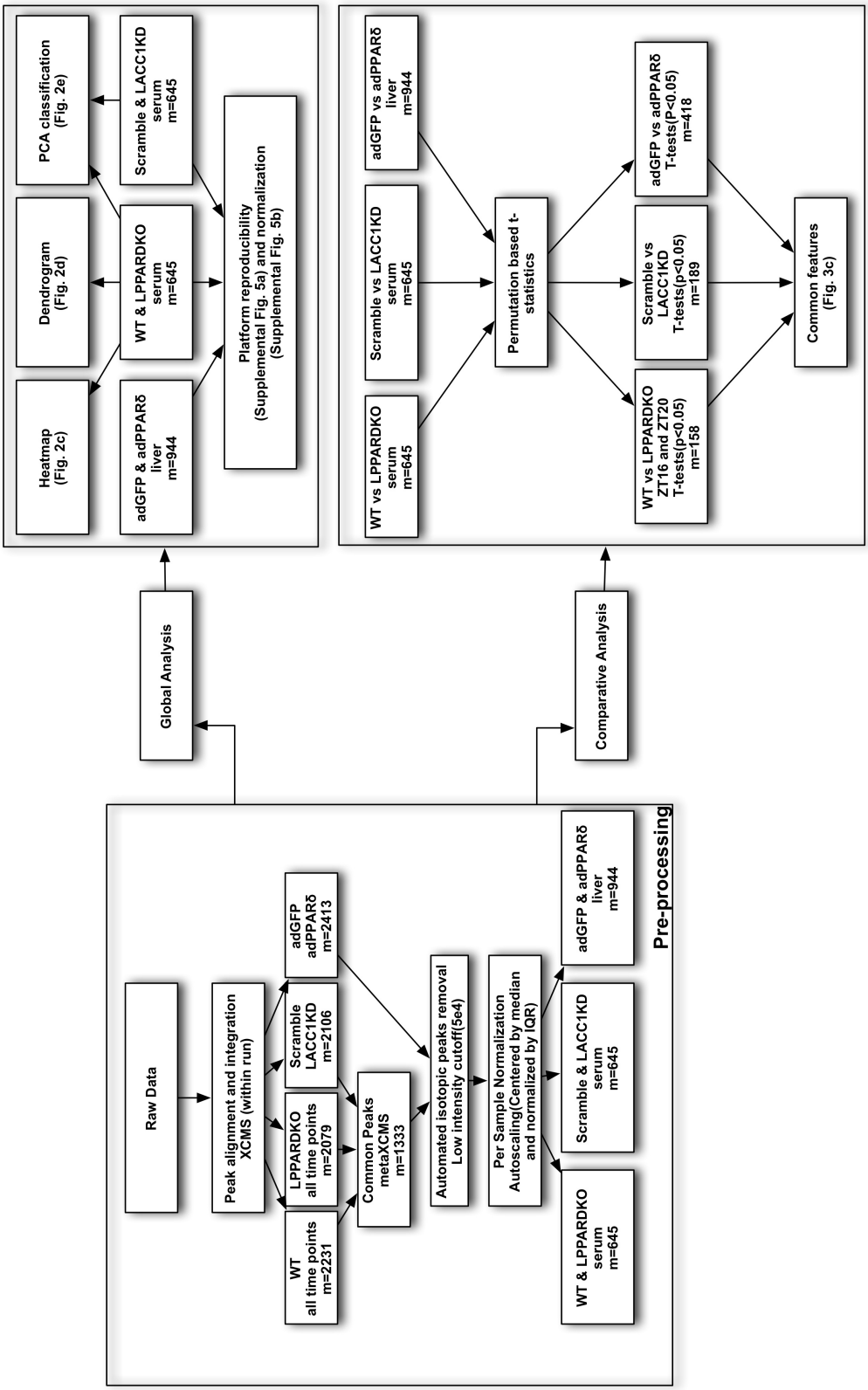
Raw Data
Peak alignment and integration XCMS (within run)
WT all time points m=2231
LPPARDKO all time points m=2079
Scramble LACC1KD m=2106
adGFP adPPARδ m=2413
Common Peaks metaXCMS m=1333
Automated isotopic peaks removal Low intensity cutoff(5e4)
Per Sample Normalization Autoscaling(Centered by median and normalized by IQR)
WT & LPPARDKO serum m=645
Scramble & LACC1KD serum m=645
adGFP & adPPARδ liver m=944
Pre-processing
Global Analysis
Comparative Analysis
Heatmap (Fig. 2c)
Dendrogram (Fig. 2d)
PCA classification (Fig. 2e)
adGFP & adPPARδ liver m=944
WT & LPPARDKO serum m=645
Scramble & LACC1KD serum m=645
Platform reproducibility (Supplemental Fig. 5a) and normalization (Supplemental Fig. 5b)
WT vs LPPARDKO serum m=645
Scramble vs LACC1KD serum m=645
adGFP vs adPPARδ liver m=944
Permutation based t-statistics
WT vs LPPARDKO ZT16 and ZT20 T-tests(p<0.05) m=158
Scramble vs LACC1KD T-tests(p<0.05) m=189
adGFP vs adPPARδ T-tests(P<0.05) m=418
Common features (Fig. 3c)

Figure 3.9

(**Figure 3.9. Continued**) Flow chart of metabolomics data analysis (See methods for detailed description).

Statistical analysis

Unless otherwise noted, statistical significance was calculated by unpaired, two-tailed student's t test. In time series data, two-way ANOVA was performed. Significance was set at $p<0.05$.

References

1. Asher, G. and U. Schibler, *Crosstalk between Components of Circadian and Metabolic Cycles in Mammals.* Cell metabolism, 2011. **13**(2): p. 125-137.

2. Bass, J., et al., *Circadian Integration of Metabolism and Energetics.* Science (New York, N.Y.), 2010. **330**(6009): p. 1349-1354.

3. Feng, D., et al., *A circadian rhythm orchestrated by histone deacetylase 3 controls hepatic lipid metabolism.* Science (New York, N.Y.), 2011. **331**(6022): p. 1315-1319.

4. Miyazaki, M., et al., *Hepatic stearoyl-CoA desaturase-1 deficiency protects mice from carbohydrate-induced adiposity and hepatic steatosis.* Cell metabolism, 2007. **6**(6): p. 484-96.

5. Matsuzaka, T., et al., *Crucial role of a long-chain fatty acid elongase, Elovl6, in obesity-induced insulin resistance.* Nature Medicine, 2007. **13**(10): p. 1193-1202.

6. Biddinger, S.B., et al., *Hepatic Insulin Resistance Is Sufficient to Produce Dyslipidemia and Susceptibility to Atherosclerosis.* Cell metabolism, 2008. **7**(2): p. 125-134.

7. Choi, C.S., et al., *Suppression of diacylglycerol acyltransferase-2 (DGAT2), but not DGAT1, with antisense oligonucleotides reverses diet-induced hepatic steatosis and insulin resistance.* The Journal of biological chemistry, 2007. **282**(31): p. 22678-22688.

8. Savage, D.B., et al., *Reversal of diet-induced hepatic steatosis and hepatic insulin resistance by antisense oligonucleotide inhibitors of acetyl-CoA carboxylases 1 and 2.* The Journal of clinical investigation, 2006. **116**(3): p. 817-24.

9. Liu, S., et al., *Role of peroxisome proliferator-activated receptor {delta}/{beta} in hepatic metabolic regulation.* J Biol Chem, 2011. **286**(2): p. 1237-47.

10. Homan, E.A., et al., *Monoalkylglycerol ether lipids promote adipogenesis.* Journal of the American Chemical Society, 2011. **133**(14): p. 5178-81.

11. Brown, J.D., et al., *VLDL hydrolysis by hepatic lipase regulates PPARdelta transcriptional responses.* PLoS One, 2011. **6**(7): p. e21209.

12. Cao, H., et al., *Identification of a lipokine, a lipid hormone linking adipose tissue to systemic metabolism.* Cell, 2008. **134**(6): p. 933-44.

13. Chakravarthy, M.V., et al., *Identification of a physiologically relevant endogenous ligand for PPARalpha in liver.* Cell, 2009. **138**(3): p. 476-88.

14. Fu, S., et al., *Aberrant lipid metabolism disrupts calcium homeostasis causing liver endoplasmic reticulum stress in obesity.* Nature, 2011. **473**(7348): p. 528-31.

15. Kotronen, A., et al., *Comparison of lipid and fatty acid composition of the liver, subcutaneous and intra-abdominal adipose tissue, and serum.* Obesity, 2010. **18**(5): p. 937-44.

16. Hsu, F.F., A. Bohrer, and J. Turk, *Formation of lithiated adducts of glycerophosphocholine lipids facilitates their identification by electrospray ionization tandem mass spectrometry.* Journal of the American Society for Mass Spectrometry, 1998. **9**(5): p. 516-26.

17. Bostrom, P., et al., *A PGC1-alpha-dependent myokine that drives brown-fat-like development of white fat and thermogenesis.* Nature, 2012. **481**(7382): p. 463-8.

18. Lee, J.M., et al., *A nuclear-receptor-dependent phosphatidylcholine pathway with antidiabetic effects.* Nature, 2011. **474**(7352): p. 506-10.

19. Ronnebaum, S.M., et al., *Chronic suppression of acetyl-CoA carboxylase 1 in beta-cells impairs insulin secretion via inhibition of glucose rather than lipid metabolism.* The Journal of biological chemistry, 2008. **283**(21): p. 14248-56.

20. Lobo, S., B.M. Wiczer, and D.A. Bernlohr, *Functional analysis of long-chain acyl-CoA synthetase 1 in 3T3-L1 adipocytes.* J Biol Chem, 2009. **284**(27): p. 18347-56.

21. Kang, K., et al., *Adipocyte-derived Th2 cytokines and myeloid PPARdelta regulate macrophage polarization and insulin sensitivity.* Cell Metab, 2008. **7**(6): p. 485-95.

22. Spandidos, A., et al., *PrimerBank: a resource of human and mouse PCR primer pairs for gene expression detection and quantification.* Nucleic Acids Res, 2010. **38**(Database issue): p. D792-9.

23. Reilly, S.M., et al., *Nuclear receptor corepressor SMRT regulates mitochondrial oxidative metabolism and mediates aging-related metabolic deterioration.* Cell metabolism, 2010. **12**(6): p. 643-53.

24. Bartelt, A., et al., *Brown adipose tissue activity controls triglyceride clearance.* Nature medicine, 2011. **17**(2): p. 200-5.

25. Shearer, J., et al., *Long chain fatty acid uptake in vivo: comparison of [125I]-BMIPP and [3H]-bromopalmitate.* Lipids, 2008. **43**(8): p. 703-11.

26. Agren, J.J., A. Julkunen, and I. Penttila, *Rapid separation of serum lipids for fatty acid analysis by a single aminopropyl column.* Journal of lipid research, 1992. **33**(12): p. 1871-6.

27. Smith, C.A., et al., *XCMS: processing mass spectrometry data for metabolite profiling using nonlinear peak alignment, matching, and identification.* Analytical chemistry, 2006. **78**(3): p. 779-87.

28. Tautenhahn, R., et al., *metaXCMS: second-order analysis of untargeted metabolomics data.* Analytical chemistry, 2011. **83**(3): p. 696-700.

29. Brown, M., et al., *Automated workflows for accurate mass-based putative metabolite identification in LC/MS-derived metabolomic datasets.* Bioinformatics, 2011. **27**(8): p. 1108-12.

30. Sreekumar, A., et al., *Metabolomic profiles delineate potential role for sarcosine in prostate cancer progression.* Nature, 2009. **457**(7231): p. 910-914.

31. Xia, J. and D.S. Wishart, *Web-based inference of biological patterns, functions and pathways from metabolomic data using MetaboAnalyst.* Nature protocols, 2011. **6**(6): p. 743-60.

32. Saeed, A.I., et al., *TM4 microarray software suite.* Methods Enzymol, 2006. **411**: p. 134-93.

Chapter 4:

DISCUSSION

Summary and Significance of Thesis Work

The main focus of this thesis work is to understand the role of hepatic *de novo* lipogenesis in controlling systemic metabolic homeostasis. In chapter 2, we identified the nuclear receptor PPARδ as a transcription factor regulating *de novo* lipogenesis in the liver. Activation of hepatic PPARδ induces key genes involved in *de novo* lipogenesis such as ACC1/2 and SCD1. We characterized the molecular mechanism for PPARδ mediated activation on these genes using promoter reporter assays. We demonstrated direct transcriptional activation by PPARδ on these genes. In addition, we demonstrated that the activity of PPARδ in the liver is controlled via two mechanisms: (1) the initial activity of PPARδ generates endogenous ligands of PPARδ, thereby creating a feed forward mechanism of activation; (2) the nuclear receptor co-activator PGC-1β, previously implicated in mediating the lipogenic effects of fructose [1] and saturated fatty acids [2], was shown to co-activate PPARδ. We further addressed the effects of acute PPARδ activation on global glucose homeostasis and insulin sensitivity under pathophysiological conditions. High fat diet (HFD) fed mice had significantly improved glucose tolerance, reduced hepatic glucose production and improved insulin sensitivity upon PPARδ overexpression in the liver. These metabolic improvements were associated with reduced hepatic inflammation and enhanced AMPK activation.

During the course of the study, we unexpectedly observed significantly reduced serum lipid concentrations, despite increased hepatic lipid synthesis and normal triglyceride output in PPARδ overexpression (adPPARδ) mice. This prompted us to

hypothesize that extra-hepatic tissues had enhanced lipid clearance. This was indeed the case. We demonstrated a link between hepatic *de novo* lipogenesis and muscle fatty acid utilization *in vivo*. Treatment of fully differentiated C2C12 myotubes with serum obtained from wild type (WT) or liver specific PPARδ knockout (LPPARDKO) mice recapitulated the effects seen *in vivo*, suggesting that serum factor(s) might be responsible for this inter-organ communication. Using the untargeted metabolomics approach, we compared the serum lipid profile from multiple genetic models that display differential muscle fatty acid utilization. This comparison yielded a PC species, PC(18:0/18:1) or SOPC, as the likely candidate. Administration of SOPC promoted fatty acid utilization in the muscle, thereby confirming the role of SOPC as a lipid mediator linking lipogenic activity in the liver with fatty acid utilization in the muscle.

Although these findings provide a glance into inter-organ communication through biosynthetic pathways, several questions remain to be answered. The impact of reduced fatty acid uptake in the muscle under normal physiological and pathophysiological conditions warrants further study. With regard to the circadian regulation of PPARδ activity and SOPC levels, whether it is driven by the acute response to feeding, systemic signal from the central clock or the endogenous clock in the liver is not fully understood. The specificity, potency and mechanism of action of SOPC on muscle fatty acid uptake are also not clear. These aspects will be discussed below.

PPARδ Signaling and Metabolic Flexibility

I. Hepatic PPARδ Activation and Metabolic Flexibility

Although the improved glucose homeostasis in PPARδ overexpression animals under HFD can be attributable to the removal or sequestration of deleterious intermediate metabolites that impair insulin actions, in chapter 2, we demonstrated a direct transcriptional regulation of PPARδ on hepatic glucokinase, a rate-limiting enzyme in glycolysis. Furthermore, acute activation of PPARδ elevates AMPK activity in primary hepatocytes, leading to decreased glucose production. These data suggested a direct regulatory role of PPARδ in both glucose and lipid metabolism. Therefore, the unique action of hepatic PPARδ suggests a potential therapeutic strategy to combat the metabolic inflexibility associated with the insulin resistantance. By channeling glucose into lipids for storage and reducing glucose output, acute activation of hepatic PPARδ may be an alternative route to restore metabolic flexibility. This idea is akin to the beneficial effects seen in several animal models with enhanced adipose tissue lipogenesis [3-5]. However, liver is not the major site for lipid storage. The accumulation of lipid droplets may eventually exceed the capacity of hepatocytes, causing cellular dysfunction and eventually insulin resistance, as seen in liver specific SREBP1c transgenic mice. Therefore, the extent of benefits upon hepatic PPARδ activation over long term remains to be evaluated.

II. The Role of PPARδ Signaling in Normal Physiology

In chapter 3, we established a liver-muscle crosstalk coupling fatty acid synthesis to fatty acid utilization. How this crosstalk might impact overall metabolic homeostasis has not been examined. The ability to utilize fatty acids is central to maintaining metabolic flexibility. We hypothesize that a lack of fatty acid utilization promotes glucose utilization to compensate for the energy needs in the muscle. To test this hypothesis, we measured blood glucose levels in both LPPARDKO and ACC1 knockdown (LACC1KD) mice. These two models had reduced fatty acid uptake in the muscle, but lowered blood glucose level specifically in the dark cycle, suggesting an increase in glucose utilization (Figure 4.1A). Consistent with these observations, adPPARδ mice and mice injected with SOPC had reduced glucose utilization in the muscle (Figure 4.1B). In *ad libitum* conditions, these changes may have little impact to the overall metabolic fitness. However, we reason that in the wild, where food access is periodical, this mechanism may play a key role in metabolic adaptation. To test this idea, we performed a preliminary experiment using daily restricted feeding as a model to mimic wild condition. We sampled blood glucose and TG levels every 8 hours for 3 consecutive days starting at the first day of restricted feeding in WT and LPPARDKO mice. Indeed, after the initial acute response to fasting and feeding, WT mice quickly adapted to this new feeding scheme and their blood glucose levels were stabilized. In contrast, LPPARDKO continued to have a large fluctuation of blood glucose levels following fasting and feeding cycle, indicating an impaired mechanism to switch from glucose to fatty acid

utilization during the fasting state (Figure 4.1C). To further support this notion, we looked at their serum TG levels over the course of the experiment. LPPARDKO mice had higher serum TG levels compared to WT counterparts, suggesting the lack of fatty acids utilization in these animals (Figure 4.1C). As such, the fluctuation of blood glucose may hinder the metabolic adaptation of LPPARDKO mice in the wild.

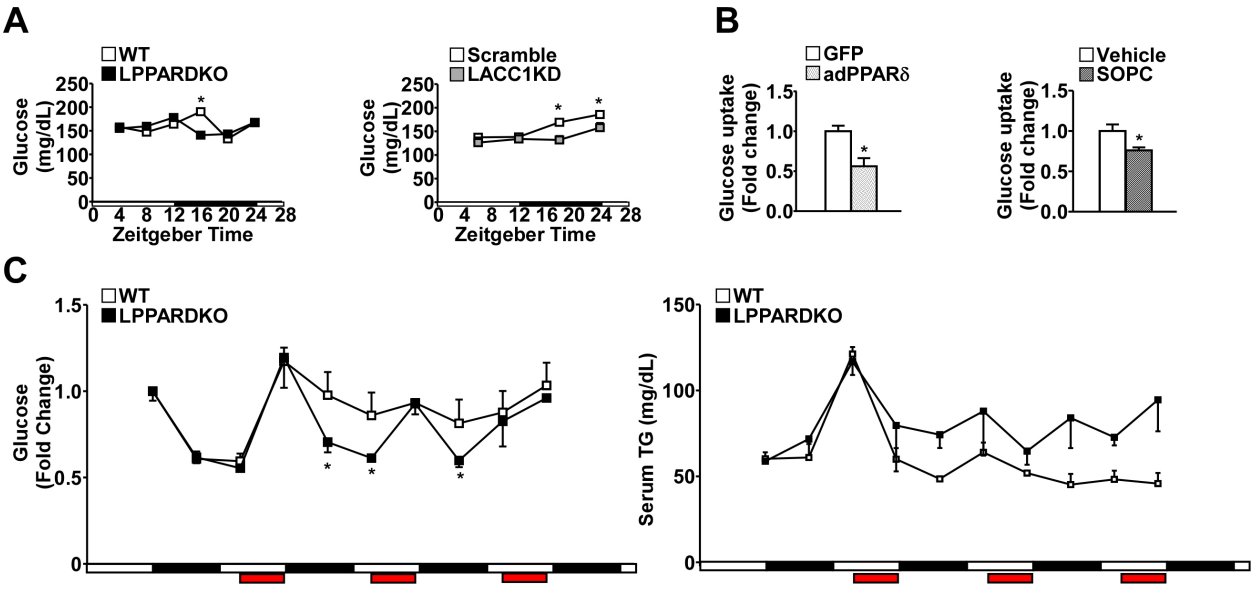

Figure 4.1. The role of PPARδ signaling in normal physiology. **A.** Blood glucose levels in LPPARDKO or LACC1KD mice and their controls around the clock. For WT and LPPARDKO mice, blood glucose was measured every 4 hours starting at ZT4 (left). For LACC1KD and Scramble mice, blood glucose was measured every 6 hours starting at ZT6. (ZT, Zeitgeber time. ZT0: 6AM and ZT12: 6PM). White bar: light cycle, black bar: dark cycle. **B.** *Ex vivo* muscle glucose uptake. Soleus muscle was isolated from mice with respective treatments. ^{3}H labeled 2-deoxy-glucose was used to measure glucose uptake. Normalized radioactivity accumulation in the muscle was determined as the glucose uptake capacity. **C.** WT and LPPARDKO mice were fasted from ZT12 to ZT4 the ensuing day for 3 consecutive days. Red bar: time when food was presented. Blood glucose (left) and serum TG levels (right) were measured every 8 hours for the experimental period. Blood glucose levels were expressed as the fold change of the initial concentration. *$p<0.05$, two-tailed student's t-test. Value was expressed as mean±SEM.

III. The Role of PPARδ Signaling in Pathophysiology

While *de novo* lipogenesis is important in normal physiology, current western diet has pushed the metabolic balance toward excessive hepatic lipogenesis. Therefore, limiting fatty acid uptake in the muscle may relieve the metabolic stress caused by lipotoxicity. HFD induced hepatic lipogenesis and increased serum SOPC concentrations compared to chow fed controls (Figure 4.2A). Elimination of hepatic PPARδ reduced *de novo* lipogenesis *in vivo*, suppressed serum PC(36:1) (SOPC) concentrations and lowered muscle fatty acid uptake (Figure 4.2B). Consistent with these data, a euglycemic-hyperinsulinemic clamp study indicated improved glucose utilization in LPPARDKO mice as measured by glucose infusion rate. This improvement was contributed by both the reduced hepatic glucose production under clamp and increased muscle glucose uptake (Figure 4.2C).

Does SOPC cause glucose intolerance and insulin resistance? In the case of prolonged activation of this pathway, such as under HFD, the muscle is unable to switch from fatty acid utilization to glucose oxidation and is overloaded with deleterious lipid intermediates, thereby causing insulin resistance. However, although not directly addressed in this thesis work, acute increase in serum SOPC levels may provide beneficial effects by reducing the circulating lipid levels and alleviating lipotoxicity. The seemingly contradicting role of SOPC mediated muscle fatty acid utilization resembles the opposing metabolic effects of prolonged versus acute activation of hepatic *de novo* lipogenesis discussed in the previous section. Thus it is necessary to emphasize that

the metabolic flexibility is maintained through balanced actions of multiple physiological processes. The eventual outcome of the PPARδ-SOPC mediated fatty acid utilization program is dependent upon the duration and perhaps the timing of its activation. Future experiments will be needed to elucidate whether SOPC alone is sufficient to cause insulin resistance upon prolonged administration, and to determine the timing of its induction with respect to other HFD induced signaling pathways.

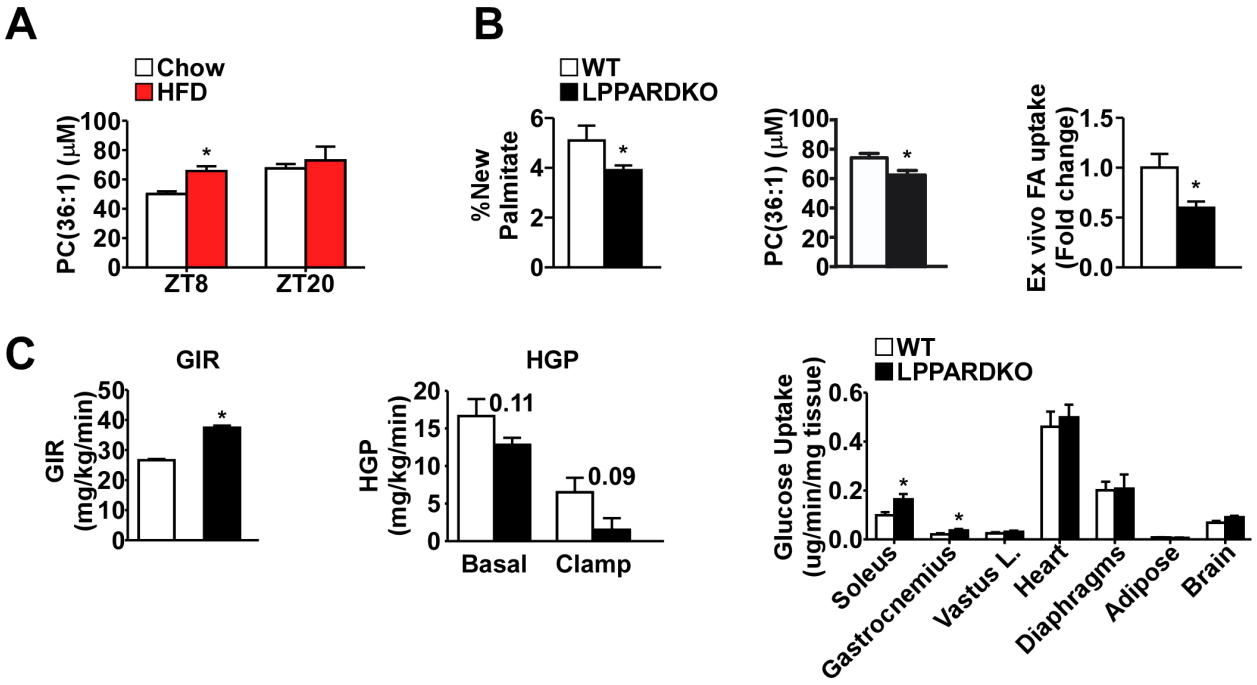

Figure 4.2. The role of PPARδ signaling in pathophysiology. **A.** Serum concentrations of PC(36:1) or SOPC determined by targeted metabolomics. WT mice were fed on HFD or chow for 4 months before being sacrificed at two time points of the day (ZT8, 2PM and ZT20, 2AM). **B.** WT and LPPARDKO mice were put on HFD for 2 months. Hepatic *de novo* lipogenesis was measured by stable tracer D_2O (left), serum PC(36:1) or SOPC concentrations were determined by targeted metabolomics (middle) and *ex vivo* fatty acid uptake in the soleus muscle was determined by ^3H labeled oleic acid (right) (See chapter 3 methods for details). **C.** WT and LPPARDKO mice were subject to a euglycemic-hyperinsulinemic clamp after 2 months on HFD. The exogenous glucose infusion rate (GIR), hepatic glucose production (HGP) under basal or clamped conditions, and tissue specific glucose uptake at the end of the clamp were determined. *p<0.05, two-tailed student's t-test. Value was expressed as mean±SEM.

PPARδ, a New Player in the Circadian Regulatory Network

In chapter 3, we attempted to evaluate the possibility that hepatic PPARδ is directly under the control of endogenous clock by using synchronized primary hepatocytes. We observed persistent PPARδ expression cycle similar to other core clock genes in the primary hepatocytes without external stimuli. Although the expression of PPARδ can be regulated by the liver endogenous clock, the expression of lipogenic targets of PPARδ, SOPC levels and muscle CD36 expressions cannot be addressed using this minimal system. The benchmark assay to determine whether a biological process is controlled by endogenous clock in the liver is to perform reverse feeding. Peripheral clock, especially in the liver is subject to the regulation from food derived cues. Restricted feeding during the day sets the peripheral clock independent of the central clock. After 7 days of restricted feeding with WT and LPPARDKO mice, we observed a complete switch of the liver clock with the peak expression of Rev-erbα, the daytime marker, shifting to the dark cycle (Figure 4.3A). The hepatic expression of PPARδ target ACC1 was opposite to what was seen under *ad libitum* feeding conditions in the WT mice, whereas in LPPARDKO mice, the expression of ACC1 did not exhibit strong reversed rhythm and the overall expression level was lower (Figure 4.3A). Consistent with these findings, CD36 expression in the LPPARDKO muscle did not have reversed expression profile as seen in WT muscles (Figure 4.3A). Taken together, these experiments suggest that the PPARδ-SOPC-CD36 axis is directly under the control of endogenous liver clock instead of signals from the central clock, as this would

not result in reversed expression profile, given the identical lighting condition.

Although these experiments would differentiate light versus food derived cues, they are not sufficient to distinguish whether the PPARδ-SOPC-CD36 program is associated with mere acute response to feeding, as opposed to the food entrainable clock regulated program. In fact, we provided evidence that fatty acids or PGC1β binding are capable of activating PPARδ associated lipogenic program in chapter 2. Thus the relative importance of clock regulated versus acute substrate or co-factor binding driven PPARδ activity needs to be clarified.

The distinction between these two is minor: the food entrainable clock still requires food cues to exert its downstream physiological output. However, the idea of a clock system is to proactively regulate biological processes. One would predict that certain biological processes in response to food would be maximized or minimized as the endogenous clock is set to a new time by restricted feeding. In other words, if a process is controlled by local clock, the response of this process to feeding will be different as restricted feeding continues, whereas a pure acute response will have the same degree of response each day. By examining the expression profile of hepatic PPARδ and muscle CD36 as well as serum concentrations of SOPC over the course of a consecutive reverse feeding experiment as described earlier, the change of these readouts therefore is able to discern whether the hepatic PPARδ controlled program is regulated by the food entrainable clock.

We intend to determine the core clock protein that is directly responsible for the circadian expression of PPARδ. Given that large scale ChIP-seq experiments have

been performed on each core clock genes in the liver, a bioinformatics search for core clock genes bound to the PPARδ upstream regulatory region is possible [6-8]. Publicly available data show several binding peaks of the core clock gene Rev-erbα and β on PPARδ 5'-UTR region, suggesting a regulatory role (Figure 4.3B). Rev-erbα and β have already been identified as the master repressor for hepatic *de novo* lipogenic program [7, 9]. Yet combined knockout or pharmacological inhibition of these genes in the liver does not lead to constitutively elevated lipogenic gene expression [7, 10]. Rather, those mouse livers show shifted expression pattern, suggesting the involvement of additional transcription factors, such as PPARδ. We preliminarily explored this possibility. Overexpression of Rev-erbα in primary hepatocytes led to reduced expression of PPARδ (Figure 4.3C). Further studies are warranted to examine whether Rev-erbα and β are able to control PPARδ and its associated program *in vivo*.

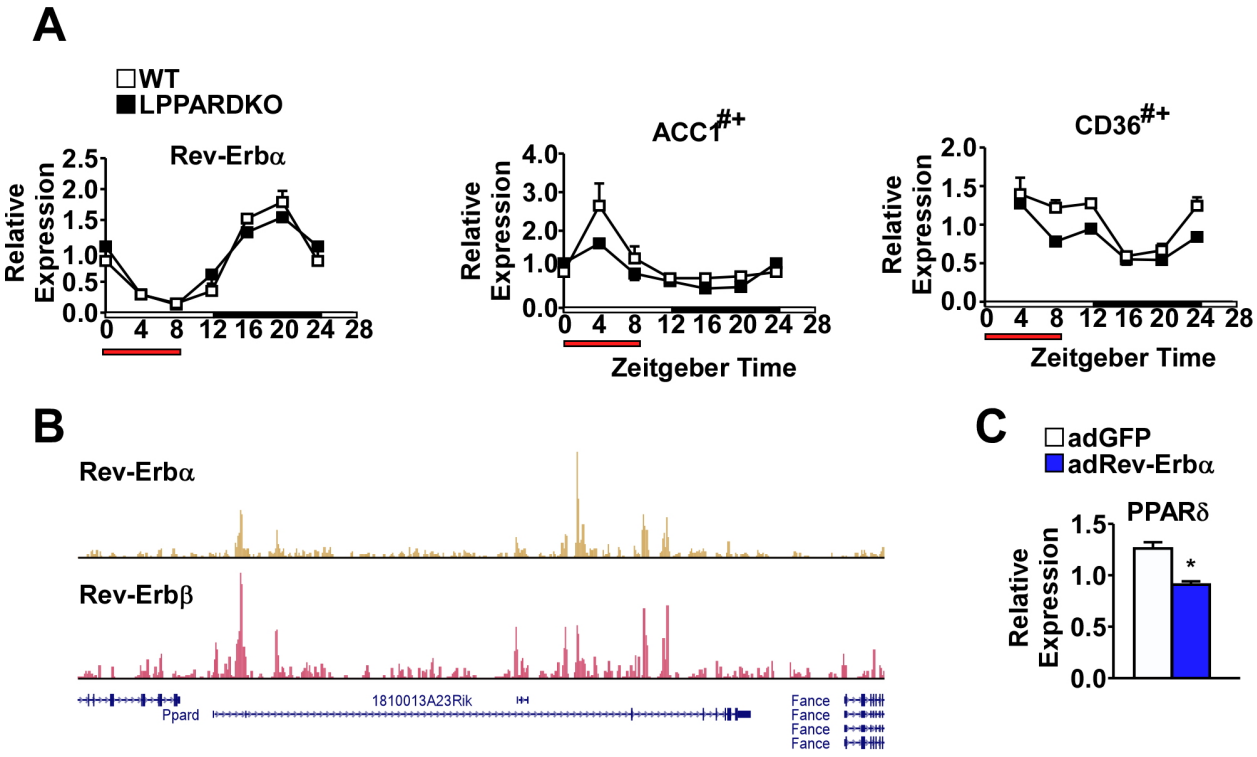

Figure 4.3. PPARδ, a new player in the circadian regulatory network. **A.** WT and LPPARDKO mice were subject to 7 days of restricted feeding with the feeding time restricted between ZT0 and ZT8 (red bar). Mice were sacrificed every 4 hours starting at ZT0 for 24 hours. Liver (Rev-erbα and ACC1) and muscle (CD36) gene expression was measured by real-time PCR. **B.** Chip-Seq signals of Rev-Erbα/β around PPARδ genomic location in the liver. The data was obtained from Cho et al. [7]. **C.** Primary hepatocytes were transduced with either GFP or Rev-Erbα adenovirus for 48 hours. PPARδ gene expression was determined by real-time PCR. *p<0.05, two-tailed student's t-test. Circadian gene expression data were tested by Two-way ANOVA. #p<0.05 for genotype significance and +p<0.05 for genotype-time interaction significance. Value was expressed as mean±SEM.

The Biology of SOPC

I. SOPC Synthesis, Output and Delivery

To fully understand the physiological relevance of the liver and muscle crosstalk, it will be critical to determine how SOPC is produced, transported out from the liver and delivered to the muscle. We have so far linked the changes in hepatic *de novo* lipogenesis to serum SOPC levels. As discussed previously, Hepatic *de novo* lipogenesis provides fatty acyl-CoAs for the synthesis of phospholipids. There is very little information regarding how specific side chain composition is determined. PCs can be synthesized *de novo* through the Kennedy pathway [11]. In this pathway, the final enzyme catalyzing the addition of choline head group to DAG, CEPT1 has limited substrates specificity. It was shown that DAG(16:1/16:1), DAG(18:1/18:1) and DAG(16:0/18:1) are the major substrates [12]. The diversity of PC species is mainly generated from the remodeling process. Almost 50% of all PCs are derived from this pathway, termed Lands cycle [13, 14]. In this remodeling process, the sn-2 position is removed by phospholipases and a new acyl chain is added by lysophosphocholine acyltransferases (LPCATs). In the liver, the newly discovered LPCAT3 is perhaps responsible for the majority of the LPCATs activity in the liver [15]. It prefers unsaturated fatty acyl-CoAs with high activity toward arachidonic acid, linoleic acid and oleic acid as the substrates. Its expression is regulated by the PPARα ligands, suggesting a role of PPAR family nuclear receptors in the control of phospholipid remodeling. In chapter 2,

we showed significantly increased oleic acid and decreased palmitic acid levels in the liver of adPPARδ mice with no difference in linoleic acid and slightly reduced stearic acid levels. This lipid profile therefore may facilitate the synthesis of PC species containing stearic acid at the sn-1 and oleic acid at the sn-2 position. In a recent human genome-wide association study (GWAS), a single nucleotide polymorphism (SNP) within the coding region of the phospholipase PLRP2 that causes a non-synonymous mutation is associated with the percentage of serum PC(36:1) levels [16]. Given the minimal quantity of PC(18:1/18:0), it is likely that this mutation is associated with the serum level of PC(18:0/18:1) (SOPC). Therefore, it may provide the molecular mechanism that accounts for the SOPC production.

PCs are highly water insoluble and therefore they seldom spontaneously dissociate from the membrane structures [17]. Lipoproteins and cellular membranes are the main site of PC localization. Approximately 25% of the total ER membrane PCs is SOPC in the bovine liver [18]. In the postprandial state, hepatic *de novo* lipogenic activity is coupled with lipoprotein production and output through the ER-Golgi route [19]. Therefore it is likely that SOPC is attached to VLDL particles to be exported together with TG. This notion is tempting as it couples signaling molecules with energy substrates. However, future experiments are needed to profile the PC composition from all lipoprotein fractions in WT and LPPARDKO mice serum to test this hypothesis.

Once delivered into the circulation, SOPC, a charged lipid needs to cross the plasma membrane and exert its action in the muscle. How SOPC is recognized on the cell surface and enriched inside of the cell remain a question. Although we hypothesize

that SOPC is co-transported with lipoproteins, it does not appear that the action of SOPC is dependent on lipoproteins. In C2C12 cells, treatment of SOPC coupled with lipoprotein deficient FBS is sufficient to elevate fatty acid uptake. Therefore, the route of transport may be independent of lipoprotein particles. However, this does not rule out the ability of lipoprotein particles to facilitate its action. Three classes of proteins are known to transfer PCs intracellularly: (1) Phosphatidylcholine transfer protein (PCTP); (2) Phosphatidylinositol transfer protein (PITP); (3) Sterol carrier protein 2 (SCP2). PCTP has been demonstrated to be unable to bind to SOPC, while the PC substrate preference of PITP and SCP2 has not been extensively studied [20]. To this end, we have not been able to identify a potential mechanism through which SOPC is taken up and transported. To address this issue, new tools and techniques are likely required. We plan to collaborate with chemists to synthesize chemical probes including ether linked, isotope tagged, fluorophore tagged, and biotin tagged SOPC. These tools will facilitate the identification of its metabolic fate, cellular location and protein partners.

II. SOPC as a Signaling Molecule?

Although our initial cross-comparison yielded SOPC as the only likely candidate, later targeted metabolomics profiling focusing on PC species has identified additional species that are down-regulated in LPPARDKO mice serum. This raised the concern on the specificity of SOPC action in the muscle. We set out to address these issues by choosing several related phospholipid species and testing their activities on muscle fatty

acid uptake *in vitro* and *in vivo*. We chose PC(18:1/18:0), PC(16:0/18:1), PC(18:1/18:1), PE(18:0/18:1), and PA(18:0/18:1) as control lipids. Some of these lipids have reduced levels in LPPARDKO serum. We reason that these lipids would be able to address whether the activity is derived from the sn-2 fatty acids, DAG, or head group. *In vitro* fatty acid uptake assay in C2C12 myotubes using these lipids demonstrated no significant stimulatory activity on fatty acid uptake (Figure 4.4A). For further validation, we injected SOPC, PC(16:0/18:1) or PC(18:1/18:1) into FVB/NJ mice and showed significant reduction in serum TG concentration only in SOPC treated group (Figure 4.4B).

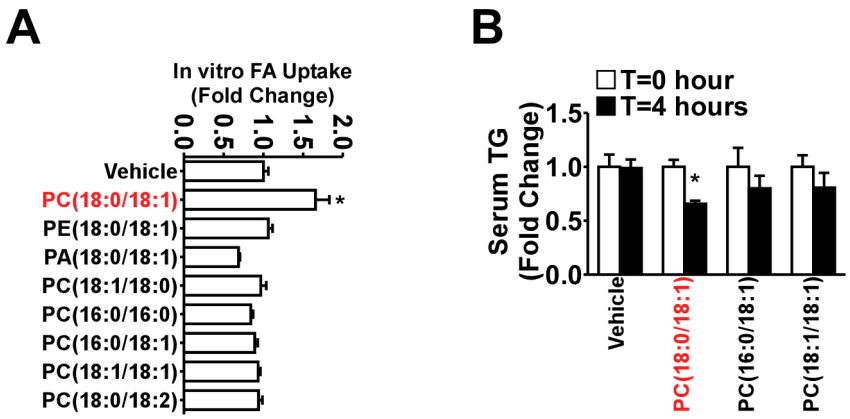

Figure 4.4. The specificity of SOPC. **A.** *In vitro* fatty acid uptake in C2C12 myotubes treated with PCs. 50 μM of the indicated PC species were applied to fully differentiated C2C12 myotubes overnight. Fatty acid uptake capacity was determined by ^{3}H labeled oleic acid (See chapter 3 methods for details). **B.** Changes in serum TG contents after PCs injection. FVB/NJ mice were injected with indicated PCs via tail vein. Baseline and 4 hours post-injection serum TG levels were determined. Food was removed during the experiment. SOPC was highlighted in red. Data were expressed as fold change of the baseline values. *$p<0.05$, two-tailed student's t-test. Value was expressed as mean±SEM.

While these experiments confirmed that SOPC has specific activity on muscle fatty acid uptake, it is possible that additional tissues are targets of SOPC and the specific activity in those tissues contribute to the overall reduction in serum TG. Adipose tissue and liver are the additional sites of consideration.

Our *in vivo* radiolabelled tracer experiments showed no difference in fatty acid uptake capability of the adipose tissue between WT and LPPARDKO mice or between vehicle and SOPC injected mice (data not shown). However, we have not examined in detail the molecular events in LPPARDKO or SOPC treated adipose tissue. Preliminary radiolabelled tracer study of WT mice *in vivo* showed diurnal difference in fatty acid uptake between adipose tissue and muscle (data not shown). The adipose tissue uptake peaks at early dark cycle, whereas the muscle uptake peaks late in the dark cycle. Serum SOPC concentration peaks late in the dark cycle, suggesting its role in mediating muscle fatty acid uptake. However, understanding the molecular targets of SOPC will also be helpful to delineate its tissue specificity, as the target protein may have limited expression profile among tissues.

Phospholipids are important constituents of VLDL particles [19]. Disrupted VLDL secretion can contribute to overall reduced serum TG levels. Adenovirus mediated overexpression of PPARδ in the liver did not alter TG production. Moreover, LPPARDKO mice did not have more TG accumulation in their livers, suggesting the lipid lowering effects of SOPC are unlikely contributed by impaired TG production (data not shown). Nevertheless, we have not directly addressed the effects of SOPC on liver metabolism. Future work using primary hepatocytes will be instrumental to examine the

role of SOPC on liver metabolism, if any.

A typical hormone has a large dynamic range, producing several fold higher concentration when induced, such as insulin and leptin [21]. However, serum SOPC concentrations increase only by two fold from day to night. Such a modest change challenges the idea that SOPC is a hormonal signal. Since PCs are likely partitioned into lipoprotein fractions, the biological activity may only be accessible in certain fractions. Lipidomics analysis of fasted human lipoprotein composition revealed that, of the approximately 2 mM of PCs, 62% are located in HDL, 30% in LDL and 8% in VLDL. In the same study, PC(36:1) was measured to account for about 2.5% of total PCs within each lipoprotein classes [22]. Therefore, the quantity of PC(36:1) is calculated to be 4 μM in VLDL, 14.8μM in LDL and 30.8 μM in HDL. If in the postprandial state, as discussed in the last section, SOPC is mainly enriched in the VLDL fraction due to its ER origin, a modest 20 μM increase would lead to a 1.4 fold increase in total SOPC, but a dramatic 5 fold increase in the VLDL fraction. Such a dynamic range would fit with its role as a regulatory molecule. Of course, this hypothesis needs to be rigorously tested using the targeted metabolomics profiling of ER and lipoprotein PCs with our genetic models.

We are also keenly aware that most of the changes elicited by SOPC *in vivo* are within two fold. As discussed in chapter 1, lipid metabolism and metabolism in general are tightly regulated by multiple pathways to achieve metabolic homeostasis. In fact, many physiological metabolic changes are of small magnitude. For example, many circulating metabolites have been found to fluctuate within two fold diurnally [21].

Genome-wide expression profiling studies also demonstrated that alteration in metabolic gene expression between normal and metabolic disease states is less than 2 fold [23-26]. It is because of this tight control, a 1.5 fold change in lipid concentration can be consequential. The impact of reduced fatty acid uptake under normal physiology and pathophysiological conditions has been discussed in earlier sections.

III. Molecular Mechanism of Action

The molecular nature of SOPC's action in the muscle remains a critical question to be addressed. A common consequence of lipid loading containing saturated fatty acids is the development of cellular insulin resistance, which exacerbates fatty acid uptake in the muscle. To determine whether the mechanism of SOPC's action is due to cellular insulin resistance, we pretreated C2C12 myotubes with SOPC or vehicle and stimulated with insulin. The results did not suggest an impairment of insulin signaling judged by equal levels of Akt phosphorylation in both groups (Figure 4.5A). Furthermore, under chow diet condition, LPPARDKO mice did not show enhanced insulin sensitivity measured by glucose and insulin tolerance test compared to their WT counterparts, nor did they display differences in muscle Akt phosphorylation levels (Figure 4.5B-D). These data suggest that insulin resistance is not the cause of muscle fatty acid uptake phenotype. However, it is possible that under HFD challenge, the reduced fatty acid uptake in LPPARDKO mice may exert protective effects and improve insulin sensitivity as a secondary effect (Discussed earlier).

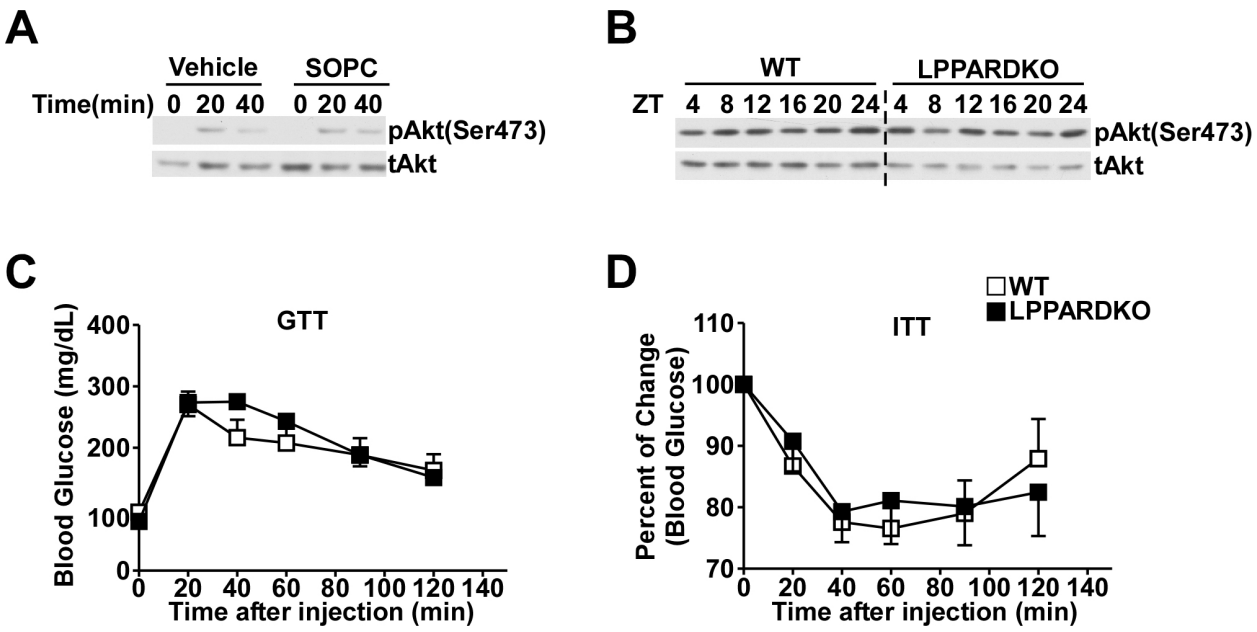

Figure 4.5. The effects of hepatic PPARδ activity on muscle insulin sensitivity. **A.** C2C12 myotube phospho-Akt levels after insulin stimulation for the indicated time. Myotubes were pretreated with vehicle or 50μM of SOPC overnight before being subject to 1 hour serum starvation followed by 10nM insulin stimulation. Total Akt levels were used as loading control. **B.** Muscle phospho- and total Akt levels in two month old WT and LPPARDKO mice muscle on chow diet around the clock. 3-4 samples were pooled for each genotype at each time point. **C. and D.** Glucose (GTT) (C) and insulin (ITT) (D) tolerance test on overnight fasted WT and LPPARDKO mice at 2 month age. 1.5mg/kg body weight of glucose and 1U/kg body weight of insulin were used for GTT and ITT, respectively. *$p<0.05$, two-tailed student's t-test. Value was expressed as mean±SEM.

In light of recent discoveries that intact PCs can act as nuclear receptor ligands, we took a candidate approach to hypothesize that SOPC exerts its action through the nuclear receptor PPARα. PPARα muscle specific transgenic mice have increased fatty acid uptake with elevated muscle CD36 expressions [27], similar to what we saw in SOPC treated muscles. In addition, a similar PC species PC(16:0/18:1) was recently identified as an endogenous ligand of PPARα in the liver [28]. Gavage of SOPC increased muscle fatty acid uptake in WT animals but not in PPARα knockout (PPARα KO) mice (Figure 4.6A). Overexpression of PPARδ in WT mice liver induced fatty acid uptake in the muscle but not in PPARα KO mice (Figure 4.6B). Stable knockdown of PPARα in C2C12 myotubes eliminated the effect of SOPC on fatty acid uptake (Figure 4.6C). These three lines of evidence strongly support a role of PPARα in mediating the effects of SOPC in the muscle.

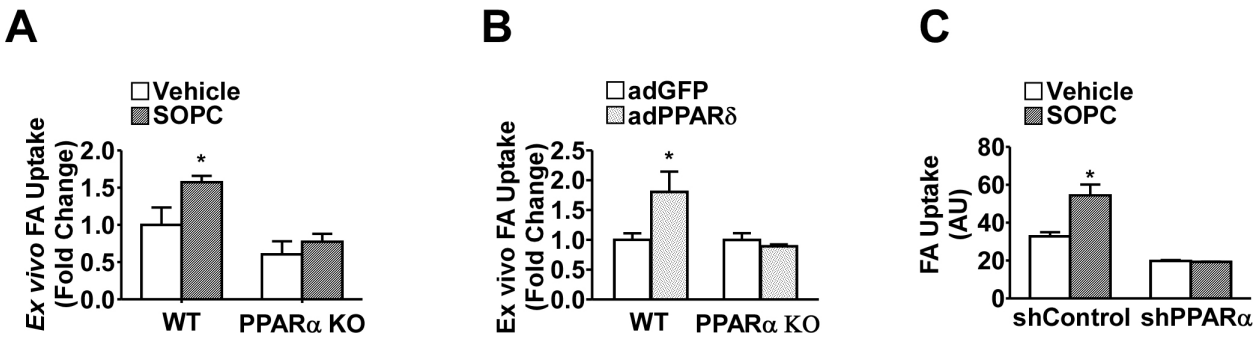

Figure 4.6. SOPC promotes muscle fatty acid uptake through PPARα. **A.** Soleus muscle fatty acid uptake in WT and PPARα KO mice 4 hours after gavage of 40mg/kg body weight of SOPC with 150 µl of olive oil. Food was removed during the experiment. **B.** Soleus muscle fatty acid uptake in WT and PPARα KO mice 4 days after the tail vein injection of GFP or PPARδ adenovirus. **C.** *Ex vivo* fatty acid uptake in C2C12 myotubes with stable knockdown of PPARα or control. There was no difference in C2C12 myotubes differentiation between knockdown groups. 50 µM of SOPC or vehicle was pretreated to cells overnight before the assay. *$p<0.05$, two-tailed student's t-test. Value was expressed as mean±SEM.

Is SOPC a ligand of PPARα? Despite strong genetic evidence, we could only demonstrate a very modest induction of PPARα activity using the PPARα ligand binding domain Gal4 fusion protein (Gal4-PPARα-LBD) in 293 cells. We also could not show a strong recruitment of co-activator peptides (data not shown). This perhaps is not surprising. As discussed in the previous section, we failed to show the ability of PC(16:0/18:1), the putative ligand of PPARα to induce muscle fatty acid uptake, whereas the synthetic PPARα ligand Wy14643 is able to induce CD36 expression similar to SOPC in C2C12 myotubes (data not shown). These data suggest that the synthetic ligand likely does not discriminate the cellular context, while endogenous ligands have tissue specific activities. Therefore, 293 cells likely do not share the same cellular environment as C2C12 myotubes and are unable to demonstrate the effects of SOPC on PPARα activity. To circumvent this issue, we plan to generate stable C2C12 lines with integrated PPAR response element luciferase (PPRE-luc). Using stable C2C12 lines overexpressing an intact or a truncated form of PPARα that is not responsive to ligands, we can further evaluate whether the effects on fatty acid uptake is dependent on a functional ligand binding domain.

Phospholipids undergo extensive modifications *in vivo*. The presence of phospholipases can release fatty acids, lysophosphocholines (LPC), phosphatic acid (PA), lysophosphatic acid (LPA) and diacylglycerols (DAG) from PC substrates [14]. Each of these breakdown products can act as a signaling molecule. Cellular assays mentioned above will not be sufficient to evaluate whether intact SOPC is able to activate PPARα. We plan to determine the binding of SOPC to PPARα biochemically.

Using a fluorescent or radiolabelled PPARα liand bound to PPARα-LBD, the displacement of fluorescence or radioactivity by cold SOPC will be examined. These biochemical assays in cell free environment should address whether SOPC is a PPARα ligand. A second possibility is that SOPC acts on upstream signaling pathways that converge at PPARα. These effects can be initiated either by intact SOPC via yet unknown mechanisms or through its breakdown products, such as DAG, PA, LPA, and fatty acids. These products have been linked with Insulin signaling, Src family kinase, AMPK, and MAPK pathways. Each of these pathways is capable of modulating PPARα activity via direct or indirect mechanisms [29]. We plan to use pathway specific inhibitors or activators in C2C12 myotubes to identify candidates for further study.

In addition to the candidate approach, unbiased whole transcriptome profiling will be helpful not only to elucidate signaling pathways leading to the increased fatty acid uptake, but also to identify the full spectrum of actions mediated by SOPC. These goals may be achieved by performing *in silico* analysis of pathway enrichment as well as virtual chemical/genetic screen.

Working Model

Based on the evidence provided in this thesis, we would like to propose a working model for the role of hepatic *de novo* lipogenesis in the regulation of systemic metabolic homeostasis (Figure 4.7). The diurnal and/or circadian regulation of hepatic lipogenesis in mice is controlled through transcriptional repression via a Rev-erbα/β-

HDAC3 complex in the daytime and transcriptional activation by PPARδ at night. Elevated PPARδ activity at night is a result of increased gene expression modulated by circadian clock machinery and the influx of endogenous ligands that are coupled with the feeding cycle. Activation of PPARδ promotes fatty acid synthesis from carbohydrates and output of TG/FA and SOPC. Elevated SOPC levels at night facilitate TG/fatty acids utilization in the peripheral tissues (e.g. muscle) by activating fatty acids utilization genes such as CD36 potentially through nuclear receptor PPARα, therefore linking lipid production in the liver to utilization in the muscle. In the absence of hepatic PPARδ, the reduced serum SOPC concentration dampens the fatty acid uptake in the muscle at the postprandial state. Such reduction under the periodic fasting-feeding cycle facilitates excessive glucose utilization and may pose a risk for animals due to hypoglycemia. On the contrary, chronic over-nutrition leads to persistent hepatic PPARδ activation that eventually exceeds the fatty acid handling capacity of the muscle, causing metabolic dysfunction. However, acute induction of hepatic PPARδ activity in the insulin resistant state may restore metabolic flexibility by promoting glucose to fatty acids conversion and preventing lipotoxicity in the liver.

Our study emphasizes a central role of hepatic *de novo* lipogenesis in modulating the fuel selection in peripheral tissues such as the muscle, therefore providing a molecular mechanism through which systemic metabolic flexibility is established.

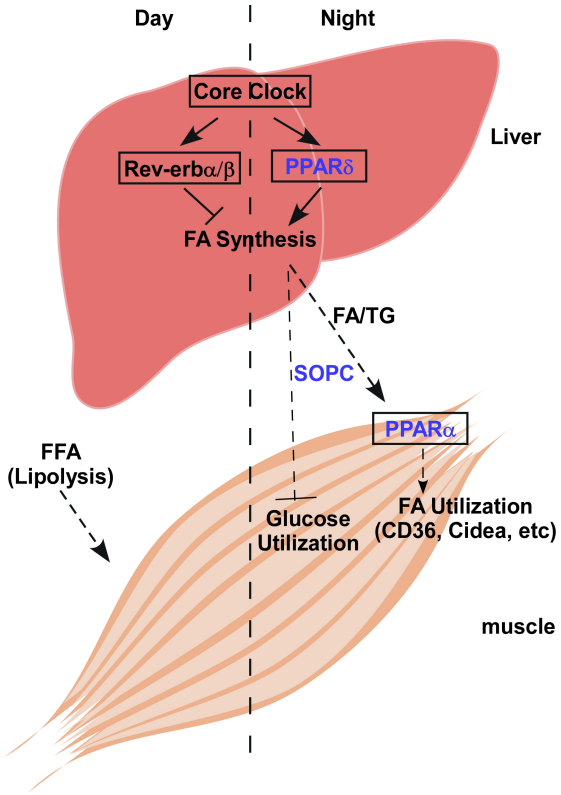

Figure 4.7. Working model.

References

1. Nagai, Y., et al., *The role of peroxisome proliferator-activated receptor gamma coactivator-1 beta in the pathogenesis of fructose-induced insulin resistance.* Cell Metab, 2009. **9**(3): p. 252-64.

2. Lin, J., et al., *Hyperlipidemic effects of dietary saturated fats mediated through PGC-1beta coactivation of SREBP.* Cell, 2005. **120**(2): p. 261-73.

3. Herman, M.A., et al., *A novel ChREBP isoform in adipose tissue regulates systemic glucose metabolism.* Nature, 2012. **484**(7394): p. 333-8.

4. Cao, H., et al., *Regulation of metabolic responses by adipocyte/macrophage Fatty Acid-binding proteins in leptin-deficient mice.* Diabetes, 2006. **55**(7): p. 1915-22.

5. Maeda, K., et al., *Adipocyte/macrophage fatty acid binding proteins control integrated metabolic responses in obesity and diabetes.* Cell Metab, 2005. **1**(2): p. 107-19.

6. Koike, N., et al., *Transcriptional architecture and chromatin landscape of the core circadian clock in mammals.* Science, 2012. **338**(6105): p. 349-54.

7. Cho, H., et al., *Regulation of circadian behaviour and metabolism by REV-ERB-alpha and REV-ERB-beta.* Nature, 2012. **485**(7396): p. 123-7.

8. Feng, D., et al., *A circadian rhythm orchestrated by histone deacetylase 3 controls hepatic lipid metabolism.* Science, 2011. **331**(6022): p. 1315-9.

9. Bugge, A., et al., *Rev-erbalpha and Rev-erbbeta coordinately protect the circadian clock and normal metabolic function.* Genes Dev, 2012. **26**(7): p. 657-67.

10. Solt, L.A., et al., *Regulation of circadian behaviour and metabolism by synthetic REV-ERB agonists.* Nature, 2012. **485**(7396): p. 62-8.

11. Kennedy, E.P. and S.B. Weiss, *The function of cytidine coenzymes in the biosynthesis of phospholipides.* J Biol Chem, 1956. **222**(1): p. 193-214.

12. Wright, M.M. and C.R. McMaster, *PC and PE synthesis: mixed micellar analysis of the cholinephosphotransferase and ethanolaminephosphotransferase activities of human choline/ethanolamine phosphotransferase 1 (CEPT1).* Lipids, 2002. **37**(7): p. 663-72.

13. Lands, W.E., *Metabolism of glycerolipids. 2. The enzymatic acylation of lysolecithin.* J Biol Chem, 1960. **235**: p. 2233-7.

14. MacDonald, J.I. and H. Sprecher, *Phospholipid fatty acid remodeling in mammalian cells.* Biochim Biophys Acta, 1991. **1084**(2): p. 105-21.

15. Zhao, Y., et al., *Identification and characterization of a major liver lysophosphatidylcholine acyltransferase.* J Biol Chem, 2008. **283**(13): p. 8258-65.

16. Demirkan, A., et al., *Genome-wide association study identifies novel loci associated with circulating phospho- and sphingolipid concentrations.* PLoS Genet, 2012. **8**(2): p. e1002490.

17. Smith, R. and C. Tanford, *The critical micelle concentration of L- -dipalmitoylphosphatidylcholine in water and water-methanol solutions.* J Mol Biol, 1972. **67**(1): p. 75-83.

18. de Brouwer, A.P., et al., *The binding of phosphatidylcholine to the phosphatidylcholine transfer protein: affinity and role in folding.* Chem Phys Lipids, 2001. **112**(2): p. 109-19.

19. Yao, Z.M. and D.E. Vance, *The active synthesis of phosphatidylcholine is required for very low density lipoprotein secretion from rat hepatocytes.* J Biol Chem, 1988. **263**(6): p. 2998-3004.

20. Kang, H.W., J. Wei, and D.E. Cohen, *PC-TP/StARD2: Of membranes and metabolism.* Trends Endocrinol Metab, 2010. **21**(7): p. 449-56.

21. Hatori, M., et al., *Time-Restricted Feeding without Reducing Caloric Intake Prevents Metabolic Diseases in Mice Fed a High-Fat Diet.* Cell Metab, 2012. **15**(6): p. 848-60.

22. Wiesner, P., et al., *Lipid profiling of FPLC-separated lipoprotein fractions by electrospray ionization tandem mass spectrometry.* J Lipid Res, 2009. **50**(3): p. 574-85.

23. Recinos, A., 3rd, et al., *Liver gene expression associated with diet and lesion development in atherosclerosis-prone mice: induction of components of alternative complement pathway.* Physiol Genomics, 2004. **19**(1): p. 131-42.

24. de Wilde, J., et al., *An 8-week high-fat diet induces obesity and insulin resistance with small changes in the muscle transcriptome of C57BL/6J mice.* J Nutrigenet Nutrigenomics, 2009. **2**(6): p. 280-91.

25. Elbein, S.C., et al., *Global gene expression profiles of subcutaneous adipose and muscle from glucose-tolerant, insulin-sensitive, and insulin-resistant individuals matched for BMI.* Diabetes, 2011. **60**(3): p. 1019-29.

26. Rome, S., et al., *Microarray analysis of genes with impaired insulin regulation in the skeletal muscle of type 2 diabetic patients indicates the involvement of basic helix-loop-helix domain-containing, class B, 2 protein (BHLHB2).* Diabetologia, 2009. **52**(9): p. 1899-912.

27. Finck, B.N., et al., *A potential link between muscle peroxisome proliferator-activated receptor-alpha signaling and obesity-related diabetes.* Cell Metab, 2005. **1**(2): p. 133-44.

28. Chakravarthy, M.V., et al., *Identification of a physiologically relevant endogenous ligand for PPARalpha in liver.* Cell, 2009. **138**(3): p. 476-88.

29. Burns, K.A. and J.P. Vanden Heuvel, *Modulation of PPAR activity via phosphorylation.* Biochim Biophys Acta, 2007. **1771**(8): p. 952-60.